Spatio-temporal analysis of extracellular DNA in bacterial colonies

Dynamics of penetration, uptake and transformation

- Inaugural-Dissertation -

zur

Erlangung des Doktorgrades

der Mathematisch-Naturwissenschaftlichen Fakultät

der Universität zu Köln

vorgelegt von

Niklas Bender

aus Köln

Köln

2021

Berichterstatter:	Prof. Dr. Berenike Maier
(Gutachter)	Prof. Dr. Tobias Bollenbach

Tag der mündlichen Prüfung: 20.01.2022

Abbreviations

ATP	Adenosine triphosphate
A.U.	arbitrary units
COM	Center of mass
DNA	Deoxyribonucleic acid
dsDNA	double stranded DNA
DUS	DNA uptake sequence
DUS^{+}	DNA containing DUS sequences
DUS^{-}	DNA lacking DUS sequences
ECM	Extracellular matrix
eDNA	Extracellular DNA
gDNA	genomic DNA
GGI	Gonococcal genetic island
HGT	Horizontal gene transfer
OD_{600}	Optical density measured at a wavelength of 600 nm
ORF	Open reading frame
PBS	Phosphate-buffered saline (buffer)
PCR	Polymerase chain reaction
RNA	Ribonucleic acid
ssDNA	single stranded DNA
TAE	TRIS-Acetic acid-EDTA (buffer)
T4P	Type IV pilus
T4PM	Type IV pilus machinery
T4SS	Type IV secretion system
VGT	Vertical gene transfer

Abstract

Bacteria spend most of their life in surface-associated, multicellular communities called biofilms. Within biofilms, bacteria embed themselves in a matrix of self-produced extracellular components, which protects them from deleterious components like antibiotics and provides a scaffold for extensive cell-to-cell interactions. One of the key components of the biofilm matrix is extracellular DNA, which is a critical structural element, as well as a connective linker between individual cells. There is a common consensus that abundant DNA, coupled with extensive cell-to-cell interactions within biofilms, facilitates horizontal gene transfer, the exchange of mobile genetic material between genetically distinct organisms. However, this assumption is not always critically questioned and many of the biological roles of extracellular DNA, as well as horizontal gene transfer within bacterial biofilms, are still poorly understood.

In this thesis we characterized the dynamics of penetration, uptake, and transformation of external DNA in microcolonies of the naturally competent human pathogen *Neisseria gonorrhoeae* with spatial and temporal resolution. Utilizing fluorescently labelled DNA probes, we found that penetration and retention of extracellular DNA within bacterial colonies depends on the length of the penetrating nucleotide and on specific binding of DNA to bacteria by the DNA uptake sequence (DUS). In particular, we find that the speed of penetration decreases as a function of DNA length. Yet, even genomic DNA of other species lacking the DUS reach the center of the colonies within few hours. Gonococcal genomic DNA, in which DUS are abundant, binds efficiently to the periphery of the colony but does not enter the colony center.

We relate our understanding of the penetration dynamics to DNA uptake and transformation. To this end, we devised experimental assays that allowed the detection of both processes in the presence of external DNA. We show that transformation efficiencies depend on the length of transforming DNA and on the position of transforming cells within the cell aggregate. Specifically, we find that uptake and transformation are both limited to the outer periphery of colonies, which suggests that cells in the colony center feature restricted or limited competence.

Finally, we investigate DNAs putative role as a structural element of the biofilms matrix by staining free DNA with a cell impermeable DNA-stain. In doing so, we find that DNA forms a mesh, or network, of DNA filaments in gonococcal cell aggregates. Dissolution of the DNA mesh affects colony architecture and morphology, suggesting that DNA is, indeed, an important connective linker in bacterial colonies.

Combined, our findings show that extracellular DNA is abundant even in young colonies and that gonococcal DNA rapidly forms a network spanning large parts of the colonies. Moreover, external DNA readily penetrates the bacterial cell aggregates. Yet, transformation remains limited to the outer periphery of colonies, which raises doubts about the idea of biofilms as hot spots for gene transfer. It will be important to find out, by which mechanism competence for transformation is inhibited within colonies and bacterial biofilms.

Zusammenfassung

Bakterien verbringen die meiste Zeit ihres Lebens in oberflächenassoziierten, mehrzelligen Gemeinschaften die als Biofilme bezeichnet werden. Innerhalb von Biofilmen betten sie sich in eine Matrix aus selbst produzierten extrazellulären Komponenten ein, die sie vor schädlichen Komponenten wie Antibiotika schützt und ein Gerüst für umfangreiche Zell-Zell-Interaktionen bietet. Eine der Schlüsselkomponenten der Biofilmmatrix ist extrazelluläre DNA, die ein wichtiges Strukturelement und Bindeglied zwischen einzelnen Zellen darstellt. Es herrscht ein allgemeiner Konsens darüber, dass große Mengen an verfügbarer DNA in Verbindung mit umfangreichen Zell-Zell-Interaktionen in Biofilmen den horizontalen Gentransfer, den Austausch von mobilem genetischem Material, zwischen genetisch unterschiedlichen Organismen, fördert. Diese Annahme wird jedoch nicht immer kritisch hinterfragt und viele der biologischen Zusammenhänge von extrazellulärer DNA sowie des horizontalen Gentransfers innerhalb bakterieller Biofilme sind noch immer unzureichend aufgeklärt.

In dieser Arbeit haben wir die Dynamik der Penetration, Aufnahme sowie Transformation externer DNA in Mikrokolonien des natürlich kompetenten Humanpathogens *Neisseria gonorrhoeae* mit räumlicher und zeitlicher Auflösung charakterisiert. Unter Verwendung fluoreszenzmarkierter DNA-Sonden konnten wir herausfinden, dass die Penetration und Retention extrazellulärer DNA in Bakterienkolonien von der Länge des eindringenden Nukleotids und von der spezifischen Bindung der DNA an Bakterien durch die DNA-Aufnahmesequenz (DUS) abhängt. Wir stellen dabei insbesondere fest, dass die Penetrationsgeschwindigkeit als Funktion der DNA-Länge abnimmt. Jedoch erreicht auch genomische DNA anderer Spezies, in denen die DUS nicht vorkommt, innerhalb weniger Stunden das Zentrum der Kolonien. Genomische DNA von Gonokokken, in der die DUS in großer Zahl vorhanden ist, bindet hingegen effizient an die Peripherie der Kolonie, dringt jedoch nicht in deren Zentrum ein.

Wir wenden unser Verständnis der Penetrationsdynamik zudem auf die Aufnahme und Transformation von DNA an. Zu diesem Zweck haben wir experimentelle Assays entwickelt, die den Nachweis beider Prozesse in Gegenwart externer DNA ermöglichen. Wir zeigen, dass die Transformationseffizienzen von der Länge der transformierenden DNA sowie von der Position der transformierenden Zellen innerhalb des Zellaggregates abhängen. Insbesondere stellen wir fest, dass sowohl die Aufnahme als auch die Transformation auf die äußere

Peripherie von Kolonien beschränkt ist, was darauf hindeutet, dass Zellen im Koloniezentrum eine eingeschränkte oder begrenzte Kompetenz aufweisen.

Schließlich untersuchen wir die Rolle der DNA als strukturelles Element der Biofilmmatrix, indem wir freie DNA mit einem zellundurchlässigen DNA-Farbstoff visualisieren. Dabei stellten wir fest, dass DNA ein Netzwerk von Filamenten in Zellaggregaten von Gonokokken bildet. Das Auflösen dieses Netzwerks beeinflusst die Koloniearchitektur und -morphologie, was darauf hindeutet, dass DNA tatsächlich ein wichtiger Bestandteil in Bakterienkolonien darstellt.

Zusammenfassend lässt sich sagen, dass extrazelluläre DNA selbst in jungen Kolonien in großen Mengen vorhanden ist, sowie, dass Gonokokken in kürzester Zeit ein Netzwerk aus DNA bilden, das große Teile der Kolonien umfasst. Darüber hinaus dringt externe DNA leicht in die Bakterienaggregate ein. Die Transformation von DNA bleibt jedoch auf die äußere Peripherie von Kolonien beschränkt, was Zweifel an der Vorstellung von Biofilmen als „Hot Spots“ für Gentransfer aufkommen lässt. Im Hinblick darauf, wird es von besonderer Bedeutung sein herauszufinden, durch welchen Mechanismus die Kompetenz zur Transformation innerhalb von Kolonien und bakteriellen Biofilmen gehemmt wird.

Contents

1. Introduction

Bacteria are ubiquitous, free-living organisms which usually consist of a single cell body. In nature, however, bacteria are predominantly associated to surfaces, where they form architecturally complex, multicellular communities called biofilms [López *et al*., 2010]. This alternate mode of existence, which is characterized by an elaborate "group behavior", facilitates growth under various deleterious and adverse conditions [Kostakioti *et al*., 2013]. As such, biofilm formation allows survival in hostile environments and enables colonization of nearly all biotic and abiotic surfaces, rendering biofilms as one of the defining hallmarks in the life cycle of bacterial species [Hall-Stoodley *et al*., 2004]. However, biofilms can be hugely problematic in several different scenarios. For instance, they can cause corrosion or otherwise affect mass or heat transfer in pipes and tubes and, thus, influence and affect many industrial processes [de Carvalho, 2007]. Biofilms are even more problematic is in a medical scenario, as they regularly form on medical devices like catheters and, thereby, cause chronic inflammation [Donlan, 2008; López *et al*., 2010]. Consequently, an increasing effort is undertaken to gain a deeper understanding of the intrinsic processes of biofilm communities; however, many of these processes remain poorly understood.

Another defining hallmark of bacterial life is movement of genetic information between different organisms independent of inheritance. This process, which is referred to as horizontal gene transfer (HGT), describes a mechanism by which bacteria obtain new genes and, thus, traits from distantly related organisms by incorporating foreign DNA into their own genome [Dutta & Pan, 2002; Gyles & Boerlin, 2014; Sevillya *et al*., 2020]. As such, HGT contributed greatly to the evolution, adaptation and diversity of bacterial and microbial species [Wiedenbeck & Cohan, 2011; Oliveira *et al*., 2017]. At the same time, however, it causes undesirable spread of pathogenicity and antibiotic resistance within bacterial populations and, thus, facilitates emergence of many human-related diseases. Consequently, a better understanding of HGT may, therefore, pave the way for the development of more effective diagnostic and therapeutic approaches [Hasegawa *et al*., 2018; Emamalipour *et al*., 2020].

While it may not be immediately obvious, there is increasing evidence that both HGT and biofilm formation are two distinct, yet closely related processes; with extracellular DNA (eDNA) been the connective linker between the two. Biofilms provide and maintain a large reservoir of eDNA, which has previously been shown to be essential for biofilm stability, but may also enhance gene transfer and, thus, HGT within the cellular aggregates [Steinberger &

Holden, 2005]. Consequently, bacterial biofilms and multicellular communities have previously been conceptualized as hot spots for gene transfer processes [Abe *et al*., 2020].

1.1. Bacterial biofilms and multicellular communities

Most bacteria do not live as single cell organisms but rather in complex single- or multispecies communities, known as biofilms [Davey & O'Toole, 2000]. In biofilms, planktonic microbials adhere to surfaces and develop into structurally complex aggregates that are cocooned in an extracellular matrix (ECM) of extracellular polymeric substances produced by the microbials themselves [López et al., 2010; Percival *et al*., 2011a; Flemming *et al*., 2016; Dragoš & Kovács, 2017]. The matrix cross-links individual cells and, thus, acts as a scaffold for the growing community [Wilking *et al*., 2011]. Moreover, immobilization of cells by the biofilm matrix keeps them in close proximity to one another and promotes cell-to-cell interactions, including cellular communication and horizontal gene transfer [Flemming & Wingender, 2010].

The transition from planktonic single cells to biofilm formation is a complex process resembling an alternate lifestyle in which bacteria adopt a multicellular behavior that, ultimately, forms macroscopic objects to facilitate survival in adverse environments [Donlan, 2002; Kostakioti *et al*., 2013; Maier, 2021]. Cells within a biofilm show numerous phenotypic differences compared to their planktonic counterparts, like modified gene expression or altered growth rates [Sharma *et al*., 2019]. Furthermore, cells that form a biofilm can reorganize and adjust the biofilm structure according to the presence or absence of deleterious factors like antibiotics, predators, or nutrient limitations [Kim *et al*., 2014; Müller *et al*., 2015; Wang *et al*., 2017; Maier, 2021]. Consequently, individual cells within a biofilm cooperate to allow the formation of highly complex and dynamic structures which create protected environments against adverse conditions or stresses and, additionally, allow widespread colonization of a wide variety of biological niches and biotopes [Hall-Stoodley *et al*., 2004; Paraje, 2011]. Decreased susceptibility to deleterious stresses may be intrinsic, as a natural outcome of growth in the biofilm, or might be acquired due to horizontal gene transfer [Donlan, 2001]. For example, biofilm-associated bacteria were shown to have drastically reduced susceptibility to antimicrobial agents, which is only one example for why the multicellular lifestyle in biofilms is absolutely essential to bacterial survival [Ceri *et al*., 1999; Letham & Bharat, 2020].

However, while some bacterial biofilms are beneficial to human health, for example in gut microbiota or wastewater treatment, biofilm development is primarily seen as a significant

problem in healthcare, drinking water distribution, and food and marine industries, where they can be difficult to manage due to their resilience to mechanical and chemical stresses [Donlan & Costerton, 2002; Høiby *et al*., 2014; Muhammad *et al*., 2020; Motta *et al*., 2021]. Many studies have, therefore, focused on preventing biofilm development and formation, particularly on medical devices; yet, until recently, the details of biofilm formation have been poorly understood [Hazan *et al*., 2006; Rabin *et al*., 2015]. However, current studies offer new insights into the complex transition from a planktonic-, to a multicellular lifestyle.

1.1.1. Biofilm formation and development

Biofilm formation and maturation consists of various reversible and irreversible stages [Kostakioti *et al*., 2013]. The first step in biofilm development (Fig. 1.1) is attachment to the surface or substratum. Cellular attachment to the surface is a stochastic process, that is driven by Brownian motion and gravitational-, as well as hydrodynamic forces [Beloin *et al*., 2010]. The properties of the substratum, like pH or temperature, combined with the properties of the bacterial cell surface, have a significant effect on the rate and efficiency with which cells can contact the surface [Donlan, 2002]. Initial adhesion to the surface is often weak and resembles a dynamic, reversible process in which single bacteria can, if challenged by hydrodynamic or repulsive forces, detach at any time to rejoin the planktonic population [Dunne, 2002; Monds & O'Toole, 2009]. Cellular appendages provide a competitive advantage in overcoming the repulsive and hydrodynamic forces of the substratum and aid in attaining an irreversible, or secondary, attachment to the substratum [Donlan, 2001; Kostakioti *et al*., 2013]. For instance, *Pseudomonas aeruginosa* utilizes both flagella and type IV pili to initiate surface contact and adherence [O'Toole & Kolter, 1998].

Once cells settle at the surface and start dividing, changes in gene expression and regulation of quorum signaling pathways are triggered in unison to favor the sessile lifestyle of the colonizers [Donlan, 2001; Otto & Silhavy, 2002; Morici *et al*., 2007]. Microcolonies can be motile and potentially fuse with other colonies to reorganize into much larger structures, which contributes to the overall growth into a mature, macroscopic biofilm [Higashi *et al*., 2007]. Aside from translocation-associated growth, biofilm formation is also affected by (clonal) cell division. As cells divide, they grow into the periphery of the colony but remain encased by the biofilm matrix [Monds & O'Toole, 2009]. In addition, biofilms can grow by recruiting planktonic cells from the surrounding medium to join the cell aggregate, which might also

spawn spatial heterogeneity between recruited and sessile cells within the aggregate [El-Khoury *et al*., 2021].

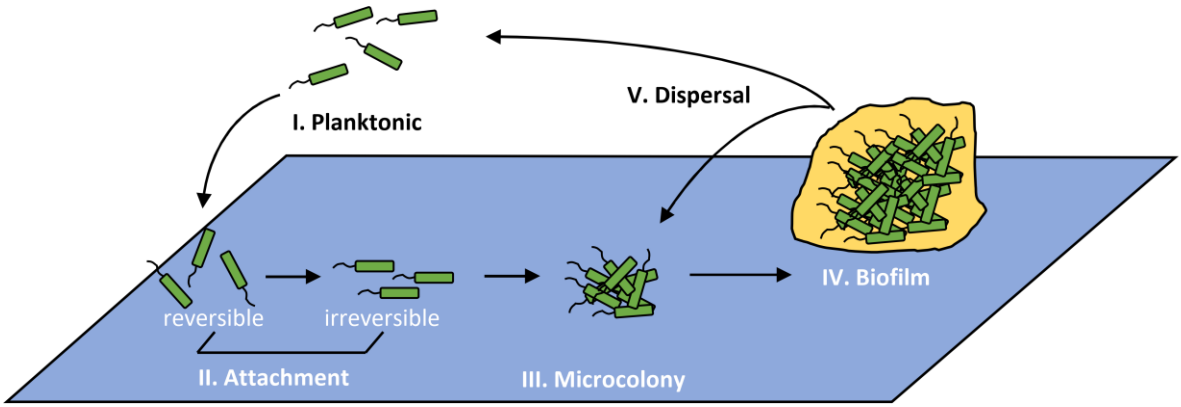

Figure 1.1: Stages of biofilm formation and development.
Planktonic single cells **(I.)**, first, attach to the substratum in a rather unstable manner. Attachment **(II.)** at this early stage may be reversible. Eventually, cells will adhere irreversibly using active attachment mechanisms. Attached cells then begin to form cellular clusters and aggregate into microcolonies **(III.)**. Microcolony formation is facilitated by translocation across the substratum, via cell division and by recruiting additional planktonic cells. Colonies then initiate differentiation into mature biofilms **(IV.)**. The growing biofilm is encaged within an extracellular matrix (ECM, yellow), that stabilizes the cellular aggregate. It consists of macromolecules, cell debris, enzymes, and extracellular DNA. Finally, single cells can be released from the biofilm **(V.)**. They join the planktonic population and restart the cycle of biofilm formation or join other bacterial communities and microcolonies. Image is based on Monds & O'Toole, 2009.

The presence of gradients for nutrients, oxygen, and various other components, leads to the formation of microenvironments and subpopulations of bacteria with differential gene expression patterns [Domka *et al*., 2007; Spormann, 2008; Stewart & Franklin, 2008; López *et al*., 2010; Kostakioti *et al*., 2013]. Simultaneously, depleted oxygen and nutrient levels impair the metabolic-, division-, and growth rates of biofilm-associated cells compared to their planktonic counterparts [Rabin *et al*., 2015]. These and other effects of growing biofilms, like strong sheer forces at the periphery, might trigger dispersal strategies of single cells within the biofilm [Stoodley *et al*., 2002; Sauer *et al*., 2004]. Cells that leave the aggregate and join the planktonic population can colonize other surfaces or might join different, already existing bacterial communities. Dispersal can, however, also be triggered actively, by internal biofilm processes that activate enzymatic digestion and release of ECM-, or surface-binding components [Lee *et al*., 1996; Sauer *et al*., 2002; Kaplan *et al*., 2003]. Dispersion of single cells is, thus, usually considered as the final stage in biofilm growth, since it marks the departure

from the bacterial community and allows colonization of new surfaces, which, in turn, begin new cycles of biofilm formation and development [Rumbaugh & Sauer, 2020].
Throughout the whole biofilm development process extracellular polymeric substances are released by the cells within the community. The production of these substances eventually forms the biofilm matrix, which, once fully developed, defines the structure and many of the unique properties of the cellular aggregate [Donlan, 2001; Hobley *et al*., 2015]. This extracellular matrix is, therefore, of critical importance to the establishment and maintenance of bacterial biofilms [Di Martino, 2018].

1.1.2. The extracellular biofilm matrix (ECM)

Extracellular polymeric substances within a mature biofilm form a complex mesh that is referred to as the extracellular matrix, or ECM, and crosslinks bacteria so that they reside in close proximity to one another. This polymer mesh, eventually, defines the structure of the biofilm (Fig. 1.2) [Donlan, 2001; Dragoš *et al*., 2018; Chew *et al*., 2014].

The composition, structure, and organization of the ECM can vary greatly, and depends on the organisms, local stresses, and the general biofilm environment [Flemming *et al*., 2016]. While a diverse array of ECM components has already been identified, a full characterization of the biofilm matrix and its components remains challenging [Nielsen & Jahn, 1999; Flemming *et al*., 2007]. However, it is well accepted by now that the ECM makes up most of the mass of biofilms and microcolonies, with contents ranging from 79 % to 90 % [Costerton, 1995]. Most of the matrix itself is composed of water, which represents up to 97 % of the matrix [Zhang *et al*., 1998]. Aside from water, the matrix consists mostly of components which are, generally, grouped into two major categories. The first category represents cell-surface-associated components, which include flagella, type IV pili or other cellular appendages, while the second category comprises a more general collection of components, including DNA, RNA, proteins, and polysaccharides [Flemming *et al*., 2016; Bowen *et al*., 2018; Karygianni *et al*., 2020]. While most focus is given to components secreted by bacteria within the biofilm, biomolecules of the surrounding environment, like host proteins for example, could also be considered a part of the matrix [Marsh *et al*., 2000; Karygianni *et al*., 2020]. Thus, the ECM shows great microheterogeneity and establishes various gradients for oxygen, nutrients, or other biomolecules, which create a wide array of different microenvironments and provide a high degree of cell differentiation in biofilms [Sutherland, 2001; Flemming & Wingender, 2010].

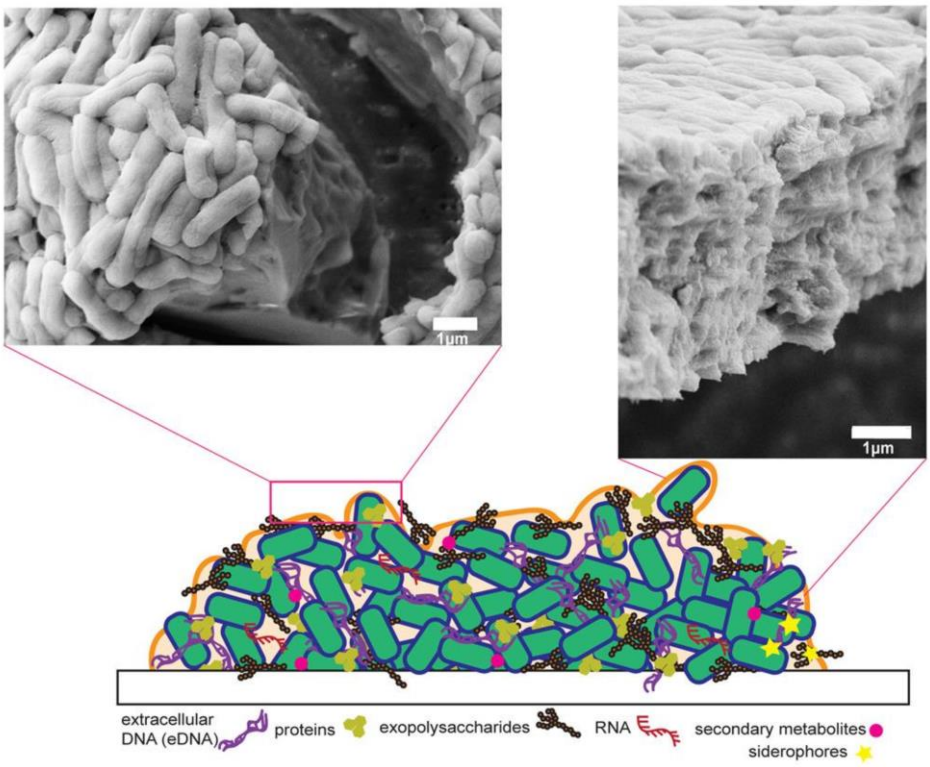

Figure 1.2: Illustration of the extracellular biofilm matrix (ECM).

Shown are some of the major components of the ECM in biofilms: nucleotides (eDNA and RNA), proteins and polysaccharides, as well as secondary components and metabolites. Scanning electron microscopy images of *Escherichia coli* biofilms (top row) highlight the density and layering of the matrix and the cells embedded within. Image adapted from Panlilio & Rice, 2021 and reproduced with permission.

The formation of the ECM comes at great energetic cost but is evolutionary justified given that it provides most of the crucially beneficial properties and functions of biofilms in regard to bacterial growth and survival [Flemming *et al*., 2016]. For instance, biofilm porosity, density, water content or hydrophobicity are affected by components of the ECM [Flemming *et al*., 2007; Percival *et al*., 2011b; Nazir *et al*., 2019; Karygianni *et al*., 2020].

The main functions of the matrix, however, are mechanical stability, scaffolding, adhesion-cohesion, and protection. For example, ECM components promote and enhance adhesion to the substratum during the initial cell attachment phase [Davies *et al*., 1993; Wang *et al*., 2004]. Here, initial polymeric matrix components promote cellular cohesion and microcolony formation by maintaining a diverse network of intermolecular interactions, like hydrogen bonds or electrostatic interactions; thus, initiating the growth phase of the biofilm [Mayer *et al*., 1999; Bowen *et al*., 2018]. Continuous production of ECM polymers throughout biofilm development expands the matrix three-dimensionally, while forming a core of matrix-enclosed bacterial

cells, which act as a scaffold for the development of three-dimensional cell clusters and aggregates [Karygianni *et al*., 2020].

Once the ECM is established, it provides physical resistance to mechanical removal and antimicrobials. For instance, ECM components of mature biofilms establish viscoelastic properties within the cell aggregate, which decrease the likelihood of detachment from the substratum under high mechanical pressure and sheer stresses [Peterson *et al*., 2015]. Furthermore, the ECM also acts as a diffusion-limiting barrier against antibiotics and antimicrobials, which results in retarded drug penetration of the deeper layers of the biofilm [Karygianni *et al*., 2014]. This is further enhanced by the fact that malign molecules can interact with ECM components of the matrix: a cationic molecule could, for example, be bound by an anionic one, which diminishes its diffusion into the biofilm or impacts its activity [Jones *et al*., 2013].

Another important function of the biofilm matrix is its role as a nutrient reservoir. Nutrients surrounding the growing biofilm are depleted by cells at the periphery, which reduces the nutrient availability for cells in the biofilm center [Cugini *et al*., 2019]. Thus, most cells in a biofilm passively wait for nutrients to diffuse to them [Zhang *et al*., 2014]. It is therefore conceivable that more effective, alternative mechanisms of nutrient acquisition do exist. One study, for instance, highlights that *Vibrio cholerae* biofilms initiates matrix-mediated swelling due to osmotic pressure differences, which maximizes biofilm expansion on nutritious surfaces and, thus, nutrient uptake [Yan *et al*., 2017]. In some cases, enzymes directly degrade components of the matrix to produce fermentable polysaccharides during starvation [Karygianni *et al*., 2020]. Extracellular DNA (eDNA) is one such example, since it is actively degraded by nucleases to allow its utilization as a carbon, nitrogen, and phosphate source [Vorkapic *et al*., 2016].

However, eDNA is far more than just a simple nutrient source. As a matter of fact, eDNA is now often conceptualized as one of the most important components of biofilms and the ECM matrix. The biological role of eDNA in the context of bacterial biofilms will be discussed in the following section.

1.1.3. Extracellular DNA (eDNA) as part of the biofilm matrix

The importance of eDNA in bacterial biofilms was mostly ignored, until researchers observed that *P. aeruginosa* biofilms disappear after treatment with DNase [Okshevsky & Meyer, 2013]. Today, the significance of eDNA and its role in biofilm formation is becoming more obvious, with recent studies highlighting eDNA as one of the major components of the ECM and its involvement in many important biofilm functions, including adhesion, formation, and maintenance of structural integrity (Fig. 1.3) [Wu & Xi, 2009; Panlilio & Rice, 2021].

While most of the DNA found in the biofilm matrix is probably the result of cell lysis events, an increasing number of studies report that bacteria also apply active mechanisms of eDNA release for the purpose of creating cell aggregates [Hara & Ueda, 1981; Whitchurch et al., 2002; Hamilton *et al*., 2005; Qin *et al*., 2007]. As a result, eDNA is found in large quantities throughout the entirety of bacterial biofilms and microcolonies [Tang *et al*., 2013].

Production and purpose of eDNA have been extensively investigated for *P. aeruginosa* [Allesen-Holm *et al*., 2006]. The bulk of eDNA in *P. aeruginosa* biofilms is mostly generated by quorum sensing mechanisms, which control cell-lysis within the cell population. This leads to abundant eDNA concentrations in late-log phases. However, while bacterial (auto-)lysis is engaged in the production of eDNA in most, if not all bacterial species, there are usually additional pathways and mechanisms that are involved in the production process [Montanaro *et al*., 2011]. In gram-negative *Neisseria gonorrhoeae* for example, eDNA is actively secreted by the type IV secretion system in addition to cell lysis processes [Hamilton *et al*., 2005]. DNA can also be released in the form of lysis-independent membrane vesicles, as was shown for *Streptococcus mutans* [Liao *et al*., 2018]. Regardless, the abundance of eDNA in biofilms seems to be highly correlated to the overall cell density within the cell aggregate, supporting the hypothesis that release of eDNA is regulated by quorum sensing mechanisms [Ibánez de Aldecoa *et al*., 2017; Kim *et al*., 2018].

P. aeruginosa biofilms showcase a pronounced stabilizing ECM. eDNA deficiencies in this species hinders biofilm formation and eDNA-deprived biofilms tent to dissolve during early stages of development [Whitchurch *et al*., 2002]. This observation was affirmed by subsequent studies in many gram-positive and -negative bacteria, including *Staphylococcus aureus*, *Listeria monocytogenes*, *N. meningitidis*, and *V. cholerae*; further emphasizing the essential role of eDNA in biofilm organization, maturation, and initial attachment of cells to the substratum [Mann *et al*., 2009; Harmsen *et al*., 2010; Lappann *et al*., 2010; Seper *et al*., 2011]. In bacterial species expressing type IV pili, eDNA might be a strong supporting factor in the

formation of microcolonies. Studies highlighted the ability of type IV pili to interact with DNA; thus, eDNA might act as a connective linker that binds individual cells into clusters [van Schaik *et al*., 2005; Higashi *et al*., 2007]. Furthermore, eDNA was shown to be important for coordination of bacterial alignment and movements during biofilm growth [Gloag *et al*., 2013]. In contrast to these studies, however, eDNA was reported to inhibit *Caulobacter crescentus* from settling into biofilms and, also, to prevent biofilm formation of *Salmonella enterica ssp.'s* on abiotic surfaces [Berne *et al*., 2010; Wang *et al*., 2014].

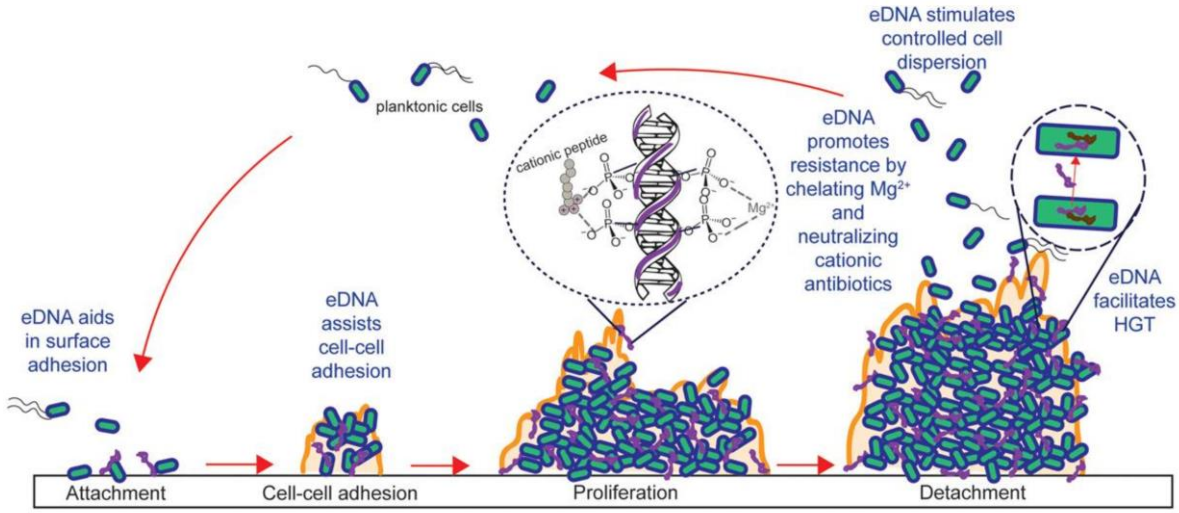

Figure 1.3: Known functions of extracellular DNA during different stages of biofilm growth.
Extracellular DNA (eDNA) is involved in numerous essential processes during biofilm development, including initial attachment, cell-cell-adhesion, biofilm proliferation, detachment and dispersion, antibiotic resistance, and horizontal gene transfer (HGT). Image adapted from Panlilio & Rice, 2021 and reproduced with permission.

The presence of extracellular DNA is often accompanied by production of extracellular nucleases, which, essentially, degrade DNA into an adjustable and flexible component, that can be modified according to the needs of the biofilm [Vorkapic *et al*., 2016]. Deletions of these nucleases often results in thick, compacted biofilms with increased biomass [Steichen *et al*., 2011; Kiedrowski *et al*., 2011; Cho *et al*., 2015]. These nucleases can degrade eDNA and enable its use as a nutrient-source during starvation [Mulcahy *et al*., 2010].

Extracellular DNA can aid pathogenic bacteria in overcoming the immune response and support the formation of biofilms within their respective hosts. For instance, the presence of eDNA in the matrix of *P. aeruginosa* biofilms triggers expression of lipopolysaccharide-modification pathway genes, which leads to resistance against antimicrobial peptides [Mulcahy

et al., 2008]. Similarly, the presence of eDNA leads to increased resistances against aminoglycosides, antimicrobial peptides, and ciprofloxacin in *S. enterica* Serovar Typhimurium, where eDNA was shown to be chelating Mg^{2+} cations; the presence of which hindered the expression of resistance operons in the organism [Johnson *et al*., 2013].

Moreover, eDNA is also contributing to the widespread exchange of genetic material in bacterial biofilms. This is due to heavily upregulated rates of horizontal gene transfer (HGT), which are typically much higher in biofilms compared to planktonic cell communities [Li *et al*., 2001; Hendrickx *et al*., 2003; Madsen *et al*., 2012].

1.1.4. Gene transfer in bacterial biofilms

Gene transfer is an important mean for bacteria to obtain beneficial genes and traits, e.g., antibiotic resistance, via exchange of genetic material. As such, gene transfer has contributed greatly to the evolution of bacterial and microbial species [Wiedenbeck & Cohan, 2011; Oliveira *et al*., 2017]. Bacterial genetic evolution is, usually, differentiated into two distinct pathways: vertical gene transfer, or vertical evolution, and horizontal gene transfer, or horizontal evolution (Fig. 1.4) [Sommer *et al*., 2017].

VGT is, essentially, cell division, whereby genetic traits and *de novo* mutations are simply passed on the progeny [Sommer *et al*., 2017]. HGT on the other hand, describes the non-genealogical transfer of genetic material between genetically distant organisms [Goldenfeld & Woese, 2007]. And while there is evidence that VGT is significantly involved in the exchange of genetic material, most focus is directed towards the HGT pathway [Li *et al*., 2019]. An increasing number of studies highlight that all three modes of HGT, namely conjugation, transduction, and transformation, do occur in bacterial biofilms [Broszat & Grohmann, 2014]. As a matter of fact, biofilms have often been described as hot spots for HGT, yet this assumption is not always critically questioned [Stalder & Top, 2016]. For example, introduction of plasmids into biofilm communities does not automatically trigger extensive horizontal transfer within the cell aggregate [Christensen *et al*., 1998]. Still, the concept of biofilms as HGT hot spots is generally accepted due to multiple factors: First, cells and organisms in biofilms are maintained in close physical proximity to one another, yet are not fully fix or immobilized and can, thus, exchange genetic material rather easily [Flemming *et al*., 2007]. Second, the biofilm forms a protective environment, which provides an ideal habitat for genetic exchange and, third, biofilms provide ample amounts of (extracellular) DNA that can be exchanged between organisms [Aminov, 2011; Tang *et al*., 2013].

Indeed, many studies highlight that HGT occurs with increased rates and efficiencies in bacterial biofilms. For example, a study by Hausner & Wuertz published in 1999 showed that conjugation rates are significantly higher in biofilms compared to planktonic populations. Furthermore, this study also highlighted that initial genetic exchange occurs much more frequently than previously expected, and that HGT rates are not reduced by nutrient limitations.

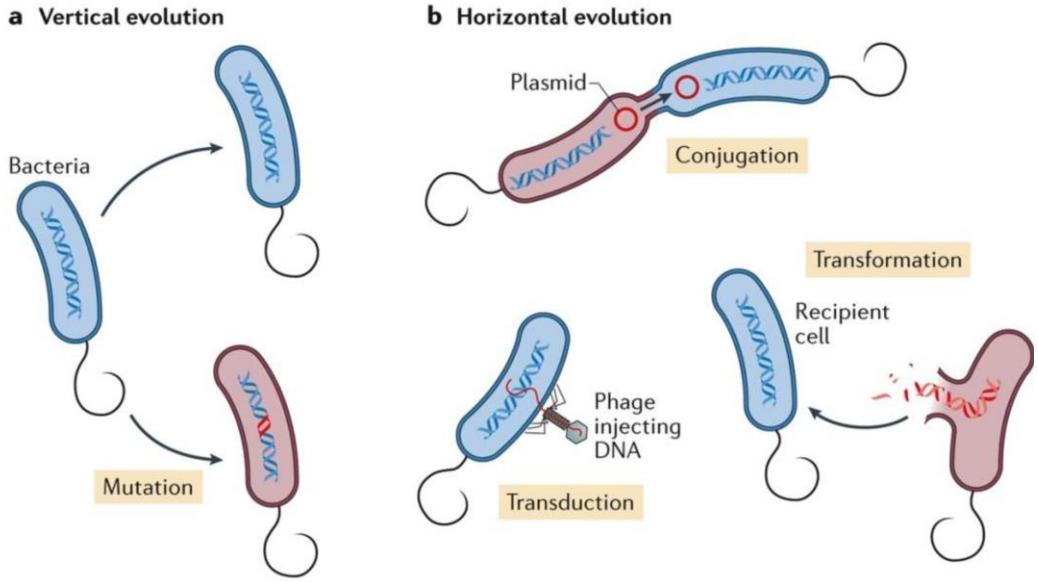

Figure 1.4: Evolution of bacteria – Vertical- and horizontal gene transfer.
Bacterial genomes can evolve by two distinct mechanisms of gene transfer. **(a)** Vertical evolution, or vertical gene transfer (VGT) represents the emergence of *de novo* mutations which are subsequently selected for and passed on to the progeny during cell division. **(b)** Horizontal evolution, or horizontal gene transfer (HGT), can occur through one of three mechanisms: Conjugation occurs through direct contact between donor and recipient, and mediates the exchange of movable genetic elements, e.g., plasmids. Transduction describes gene transfer via bacteriophages, which inject viral DNA into the host which is subsequently integrated into the genome. Transformation occurs if free DNA is taken up by naturally competent cells, which subsequently integrate the DNA into the genome by homologous recombination. Image adapted from Sommer *et al*., 2017 and reproduced with permission.

Comparable results were obtained for transformation events: transformation rates for biofilm-associated *S. mutans* are 10- to 600-fold higher compared to planktonic *S. mutans*, with transformation occurring optimally in 8 to 16 hours old biofilms [Li *et al*., 2001]. Additionally, biofilm-cultured *Acinobacter sp*. Strain BD413 transformed within 15 minutes of exposure to minor amounts of DNA, highlighting highly efficient gene transfer in biofilms [Hendrickx *et al*., 2003].

Transformation requires that cells can actively take up eDNA from their environment in order to change their genome by homologous recombination. This ability is known as competence [Mell & Redfield, 2014]. The development of natural competence in biofilms is believed to be coupled to the presence of eDNA and, given that biofilms contain large quantities of DNA, might indicate that efficient gene transfer and natural transformation are both a consequence *and* a cause of biofilm formation [Molin & Tolker-Nielsen, 2003; Madsen *et al*., 2012].

Rapid exchange of genetic material in biofilms leads to the emergence of single antibiotic- and multidrug resistance [Abe *et al*., 2020]. Resistance to antimicrobial agents is most likely already initiated during the early colonizer and attachment phase and further increases during biofilm growth [Patel, 2005]. Aside from increased HGT efficiencies, biofilms also tend to promote increased mutation rates, as was shown for biofilm-associated *S. aureus*; thereby, increasing the likelihood of obtaining heritable antibiotic resistance through spontaneous mutation [Ryder *et al*., 2012]. Thus, increased mutation frequencies of biofilm-associated cells compared to their planktonic counterparts, coupled with increased gene transfer rates in biofilms is the most likely explanation for the rapid spreading of resistances in bacterial biofilms [Driffield *et al*., 2008; Høiby *et al*., 2010; Savage *et al*., 2013].

A prime example for the emergence of antibiotic- and multidrug resistance is the human pathogen *N. gonorrhoeae*, also known as gonococcus; the causative agent of the sexually transmitted disease gonorrhea and the model organism used in this thesis. Gonococci are known to form microcolonies and biofilms which show efficient exchange of antibiotic resistance genes and acquisition of multidrug resistance in early stages of growth [Kouzel *et al*., 2015]. Furthermore, *N. gonorrhoeae* is naturally competent, highly recombinogenic and executes frequent natural transformation, making it a suitable organism to investigate biofilm formation and natural transformation [Hamilton & Dillard, 2005; Fiore *et al*. 2020].

1.2. *Neisseria gonorrhoeae* – a model organism to study biofilms and natural transformation

Neisseria gonorrhoeae, or the gonococcus, is a gram-negative bacterial pathogen that causes the sexually transmitted disease gonorrhea, which infects approx. 60 million people annually [Hill *et al*., 2016]. The organism infects a wide array of different mucosal surfaces in the human body, like the urethra, the endocervix, the pharynx or the rectum [Britigan *et al*., 1985]. Gonococci are microaerophilic organisms, but, given appropriate conditions, are also capable of anaerobic growth [Hill *et al*., 2016]. Growth of *N. gonorrhoeae* is also characterized by high autolytic activity. Gonococci lyse spontaneously, and the rate with which they do so is affected by various environmental factors, including pH, temperature or presence/absence of certain cations. The enzymes involved in autolysis of *N. gonorrhoeae* are, presumably, also responsible for a prolonged cell division phase, which is characterized by a diplococcal morphology [Elmros *et al*., 1976]. The role of autolysis during *N. gonorrhoeae*'s life cycle is not fully understood, but it is believed that excessive cell lysis releases cellular components which supply nutrients, modulate the immune response of the host during infection and provide DNA for access in natural transformation [Garcia & Dillard, 2006].

N. gonorrhoeae is naturally competent but, unlike many other bacteria, does not actively regulate its competence state. Instead, gonococci are competent throughout all phases of growth [Hamilton & Dillard, 2005]. However, *N. gonorrhoeae* is known to primarily take up genus-specific DNA, characterized by a sequence known as the DNA uptake sequence (DUS) that appears frequently within the genome of *Neisseria* species [Davidsen *et al*., 2004]. Transformation and uptake of DUS-bearing DNA in *N. gonorrhoeae* is reliant on type IV pili (T4P); thin cellular appendages formed at the cell surface that are part of a sophisticated DNA translocation complex (see section 1.2.2) [Chen & Dubnau, 2004]. As a result, gonococci undergo frequent and efficient transformation, which generates high genetic diversity and persistence of gonococcal infections in the human population [Hamilton & Dillard, 2005].

Proper treatment of gonococcal infections can be problematic. Appropriate antibiotic therapies are, for example, hampered by the ability of gonococci to develop antimicrobial resistance [Newman *et al*., 2007]. This is promoted by *N. gonorrhoeae*'s high recombinogenic activity, which is itself fostered by high rates of autolysis [Elmros *et al*., 1976; Fiore *et al*. 2020]. In addition, gonococci are also known to secrete DNA by the type IV secretion system (T4SS), further promoting frequent gene transfer by secreted eDNA [Hamilton *et al*., 2005].

Another important factor for complications in gonococcal infections is the fact that *N. gonorrhoeae* forms biofilms [Steichen *et al*., 2008].

1.2.1. Gonococcal biofilms and biofilm formation

N. gonorrhoeae forms biofilms and spherical microcolonies (Fig. 1.5). Aggregates of gonococci show reduced susceptibility to antibiotics, with dramatic effects for infections of its natural host [Wang *et al*., 2018]. Furthermore, gonococci feature highly efficient natural transformation within early colonies leading to rapid spreading of antibiotic resistance [Kouzel *et al*., 2015]. The matrix of *N. gonorrhoeae* biofilms is interlaced with pores and water channels and consist mostly out of large quantities of membrane structures, extracellular DNA, and type IV pili (T4P). However, gonococci lack genes for the production of exopolysaccharides [Greiner *et al*., 2005; Steichen *et al*., 2011; Todd *et al*., 1984].

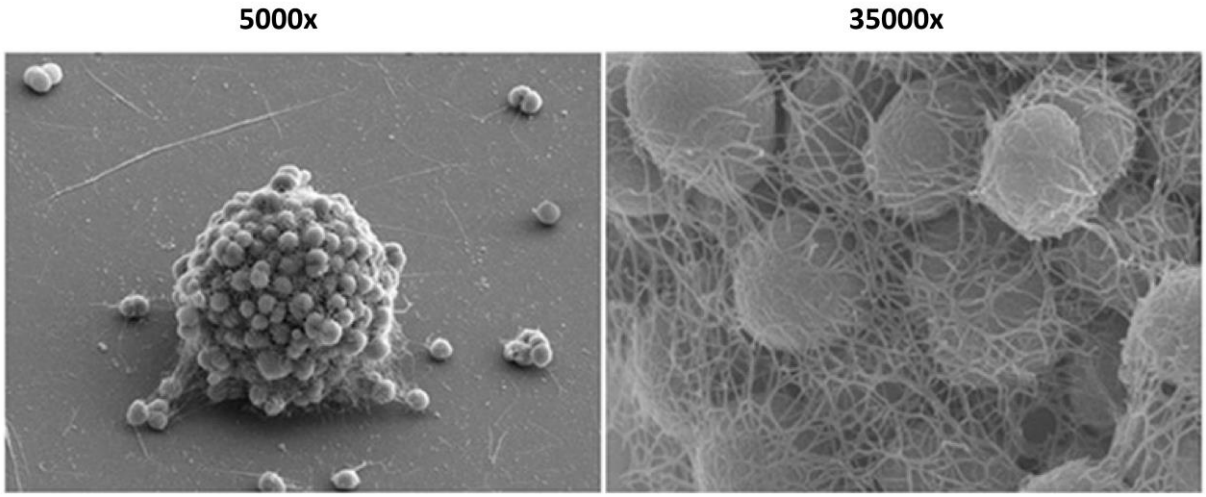

Figure 1.5: Scanning electron micrographs of microcolonies formed by *N. gonorrhoeae*.
Gonococci form spherical microcolonies (left) which develop into complex, layered biofilms. The matrix of gonococcal microcolonies is formed by type IV pili (T4P), which create a lattice-like structure with pores and water channels (right). The T4P lattice stabilizes the colony during growth. Values: x-fold magnification. Image adapted from Hockenberry *et al*., 2016 under the terms of the Creative Commons Attribution 4.0 International license.

The formation of biofilms and microcolonies is critically impacted by DNA and type IV pili (T4P). For instance, countless studies highlight the importance of T4P for biofilm formation and structuring [Hockenberry *et al*., 2016; Pönisch *et al*., 2017; Pönisch *et al*., 2018; Welker *et al*., 2018]. Variations in pilus-pilus interactions result in active cell sorting in colonies and

modify the structure of the cell aggregates, thus, T4P can mediate motility, social and infection behavior [Oldewurtel *et al*., 2015; Hockenberry *et al*., 2016].

In addition, biofilm formation was shown to be supported by secretion of ssDNA, whereas treatment of established gonococcal biofilms with isolated DNase results in rapid destruction of the cell aggregate [Steichen *et al*., 2011; Zweig *et al*., 2014]. There is evidence that eDNA in gonococcal biofilms is modelled by the thermonuclease Nuc, which is putatively secreted by *N. gonorrhoeae* into the extracellular space [Juneau *et al*. 2015]. Purified Nuc can degrade various sources of DNA and deletion of the nuclease results in thicker biofilms with increased biomass and amounts of eDNA. The mode of action of Nuc, however, is not fully understood and it is still not completely clear, for example, whether the location of Nuc is periplasmic or extracellular [Steichen *et al*., 2011].

1.2.2. Natural transformation in *N. gonorrhoeae*

Natural competence describes the ability of bacteria to efficiently take up extracellular DNA and incorporate it into the genome. Several steps are required to ensure successful transformation of DNA. First, extracellular DNA must be bound to the surface of the cell. Second, the bound DNA must overcome the cell envelope and reach the cytoplasm. In the case of gram-negative *N. gonorrhoeae*, DNA needs to overcome the inner- and outer membrane, as well as the periplasmic space that separates the two. Finally, the DNA must be integrated into the genome of the cell.

Most of the proteins of the DNA uptake machinery in *N. gonorrhoeae* are part of the type IV pilus system, a secretion system which maintains cellular surface structures which perform a variety of essential biological functions [Friedrich *et al*., 2014]. DNA uptake, natural transformation and type IV pili (T4P) are, thus, closely connected in gonococci. The complex molecular machinery that controls these vital cellular tasks, as well as all its important components, will be discussed in the following sections.

The Type IV pilus machinery (T4PM)

Type IV pili (T4P) are filamentous cell appendages that are exposed at the surface of a wide variety of bacterial species [Giltner *et al.*, 2012]. Each individual filament consists of thousands of copies of protein subunits and undergoes repeated cycles of extension and retraction [Craig *et al*., 2019]. This highly dynamic process creates strong mechanical forces of up to 150 pN, which renders T4P as one of the strongest bacterial molecular motors identified so far [Maier *et al*., 2002; Clausen *et al*., 2009]. As such, T4P are crucial drivers of a wide variety of cellular processes. For example, T4P facilitate cellular motility by performing cycles of surface-attachment and subsequent retraction, thereby translating the force exerted by the motor into locomotion [Holz *et al*., 2010]. Similarly, eDNA can be bound by pili and pulled into or towards the cell body during pilus retraction, which initiates DNA uptake [Long *et at*., 2003; Ellison *et al*., 2018]. However, there are countless other functions associated with T4P, like predation, cell adhesion to other microbes, host infection and, as previously mentioned, biofilm formation [Bieber *et al*., 1998; Merz *et al*., 2002; Klausen *et al*., 2003; Evans *et al*., 2007; Opitz *et al*., 2009; Oldewurtel *et al*., 2015; Craig *et al*., 2004].

The machinery that assembles and retracts these highly versatile cell appendices is highly conserved throughout different bacterial species. Its architecture in *Myxococcus xanthus* has recently been uncovered in great detail, which establishes a precise picture on how pili are controlled [Chang *et al*., 2016]. The type IV pilus machinery (T4PM) that assembles T4P fibers is a sophisticated protein complex that spans both the inner and outer membrane of the cell (Fig. 1.6). It is formed by four subcomplexes, all of which are necessary to form the functional machine and, ultimately, T4P [Leighton *et al*., 2015a].

The growing pilus is assembled and disassembled through the secretin-subcomplex, which forms at the outer membrane of the cell. It is arranged by PilQ, a multimeric protein that forms a pore through the outer membrane, and TsaP, which putatively fixates the complex to the peptidoglycan layer within the periplasm [Collins *et al*., 2004; Siewering *et al*., 2014].

The periplasm is gapped by the so-called alignment-complex, which consists of PilM and the PilNOP-complex which are primarily recruited to stabilize and arrange the structure of the T4PM within the cell envelope, although more recent studies suggest a contribution that goes beyond stabilization [Leighton *et al*., 2015b; Chang *et al*., 2016]. Pili originate from the motor-subcomplex, which is located at the inner membrane. It comprises the transmembrane protein PilG, which is located in the inner membrane, and the two antagonistic ATPases PilF and PilT

which are located in the cytoplasm. Together they orchestrate alternating cycles of pilus extension and retraction.

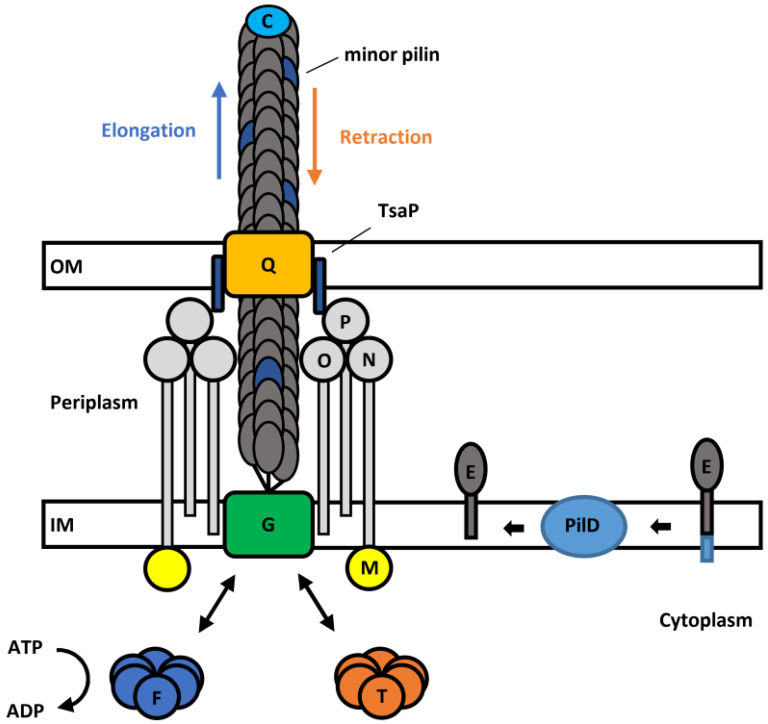

Figure 1.6: Schematic architecture of the type IV pilus machinery (T4PM).
The pilus fiber contains thousands of PilE copies and few minor pilins. The adhesin PilC is presumably located at the tip of the pilus. The fiber is anchored in the inner membrane of the cell by PilG and expends into the extracellular space through the outer membrane pore formed by PilQ and TsaP. PilM and the PilNOP complex stabilize the structure. The pilus is elongated and retracted by the ATPases PilF and PilT, which bind the cytoplasmic site of PilG in an antagonistic manner. Conformational changes of PilF/T during ATP-hydrolysis rotates the base in a clockwise/counterclockwise fashion, which shuffles PilE subunits in or out of the pilus fiber. A reservoir of pilin subunits is maintained in the inner membrane by the endopeptidase PilD, which processes prepilin into mature subunits through N-terminal cleavage and methylation. OM: outer membrane, IM: inner membrane.

The mechanism behind this is not fully understood. Based on the structure of the T4PM, however, a likely model has emerged that explains how pili are dis-/assembled [Chang *et al.*, 2016]. In this model, PilG acts as a platform for the base of the pilus and the hexameric ATPases PilF and PilT bind the cytoplasmic surface of PilG in a mutually exclusive manner. ATP-hydrolysis by PilF results in conformational changes within the hexamer which triggers a clockwise rotation of the inner membrane pilus-base PilG. The rotatory motion extracts a single pilin subunit from the membrane and merges it into the expanding pilus. PilT mediated ATP-

hydrolysis, on the other hand, results in a counterclockwise rotation of PilG and, thus, removal of pilus subunits from the fiber [Chiang *et al*., 2004; Takhar *et al*., 2013; Hospenthal *et al*., 2017; McCallum *et al*., 2017]. Approximately 700 subunits per second can be integrated and removed from the fiber, resulting in rapid dis-/assembly of T4P [Clausen *et al*., 2009].

The type IV pilus fiber (T4P) and the major pilin PilE

The final structural component of the T4PM is the pilus fiber itself. Pili represent helical polymers that are assembled from thousands of small protein subunits, called pilins. Most of the pilin subunits in a fiber are copies of the small protein PilE. [Parge *et al*., 1995; Hospenthal *et al*., 2017]. A single protein copy of PilE has a size of about 20 kDa and forms a ladle-shape molecule with a conserved, protruding N-terminal half and a hypervariable C-terminal half that forms a globular head (Fig. 1.7, right) [Craig *et al*., 2006]. Pilins are expressed as precursor proteins (prepilins) that expose a 7 amino acid long leader peptide at the N-terminus, which is eventually removed by the endopeptidase PilD [Strom & Lory, 1992; LaPointe & Taylor, 2000]. PilD then methylates the new N-terminal residue and creates mature pilin subunits, which represents an essential step in the biogenesis of T4P [Strom *et al*., 1993; Strom *et al*., 1994]. The mature N-terminus anchors the protein in the inner membrane and exposes the C-terminal globular domain to the periplasm [Thanassi *et al*., 2012].

During pilus assembly, single pilin subunits are gathered from the inner membrane and are incorporated at the base of the elongating pilus fiber by the T4PM (see Fig. 1.6). The core of the elongating filament is formed by the N-terminal domains, which adopt extensive hydrophobic interactions among individual subunits. At the same time, the C-terminal head domains are exposed at the surface of the filament, with little contact to one another (Fig. 1.7, left) [Craig & Li, 2008]. While the N-terminal region is highly conserved, there are high degrees of variability in the C-terminal domain, most notably in the surface-exposed D- and αβ-regions. The D-region contains a hypervariable loop that has been identified as a hot spot for pilin antigenic variation [Craig *et al*., 2004; Ramboarina *et al*., 2005], while the αβ-region contains two important serine residues, Ser63 and Ser68, which are targets for critical post-translational modifications of the pilus fiber [Parge *et al*., 1995; Hegge *et al*., 2004]. As such, the variable regions of the globular domains specify the outer surface area of the fiber and have important functional consequences for T4P [Thanassi *et al*., 2012; Craig *et al*., 2004].

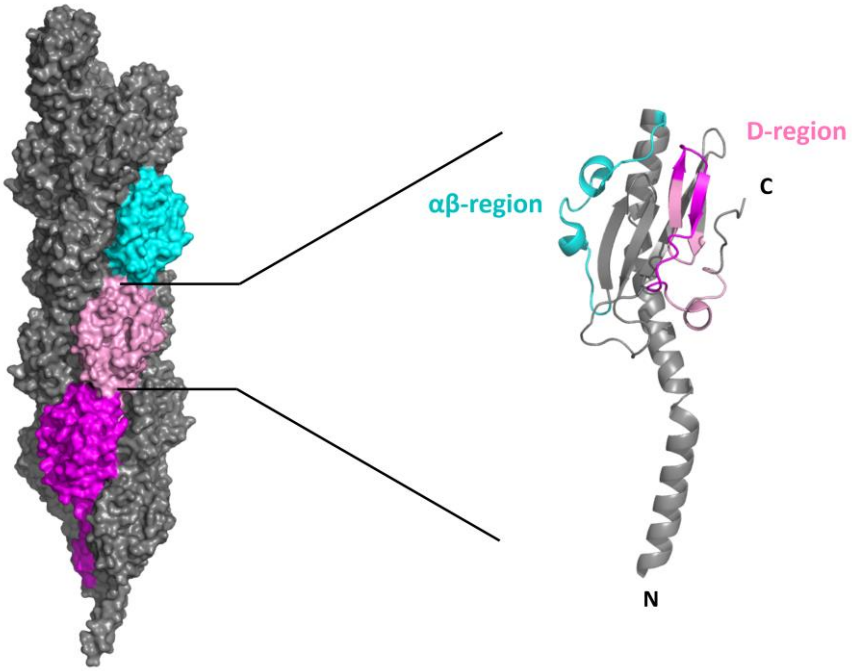

Figure 1.7: Structure of the pilus fiber and the major pilin PilE.

Type IV pili have a helical structure (as indicated by subunits colored in magenta, pink and cyan) and can reach a length of several microns, with a typical width of 6 nm (left). They are formed by polymerization of the major pilus subunit PilE, which has a globular C-terminal domain and a protruding N-terminal domain (right). The αβ-region, the structurally variable D-region and its hypervariable loop are highlighted again in cyan, pink and magenta, respectively. Image created with PyMOL Molecular Graphics System, Version 2.5.0a0 Open-Source, Schrödinger LLC., based on PDB IDs 2HI2 and 2HIL [Craig *et al*., 2006].

Minor pilins and the DNA-binding T4P component ComP

There are several identified pilin proteins besides the major pilin PilE. These so-called minor pilins share high structural similarity with PilE and become part of T4P by the same mechanisms, albeit at a much lower abundance [Jacobsen *et al*., 2020]. Yet, all minor pilins have important biological functions. For example, studies have suggested that PilC, which is presumably located at the tip of the pilus fiber, might be a major pilus adhesion molecule and, thus, important for adherence to host-cells [Rudel *et al*., 1995; Kirchner & Meyer, 2005]. Other adherence-associated minor pilins comprise PilV and PilX, which are essential to fine-tune pilus virulence and host cell infection [Winther-Larsen *et al*., 2001; Helaine *et al*., 2007].

Another important minor pilin is ComP, which is supposed to be a major contributor to natural transformation in *Neisseria* species [Wolfgang *et al*., 1999]. It is the only known pilus component that has DNA-binding capabilities and can interact with DNA via an electropositive stripe that is exposed at its surface. The stripe is flanked by a loop delimited by two disulfide

bridges, which essentially act as a docking platform for DNA und, thus, is crucial for DNA-binding [Cehovin *et al*., 2013]. Hence, ComP can be seen as the DNA-receptor within T4P and is, consequently, essential for DNA uptake.

While ComP can bind any DNA, it exhibits an increased binding-affinity for DNA originating from the *Neisseria* genus, which is denoted by a 10 - 12 bp gonococcal recognition sequence (5'-AT/GCCGTCTGAA-3') known as the "DNA Uptake Sequence", or DUS [Goodman & Scocca, 1988; Berry *et al*., 2013; Cehovin *et al*., 2013; Spencer-Smith *et al*., 2016]. These sequences represent up to 1 % of the entire genome and are 1000-fold more common than statistically expected. Given ComP's preference to bind the DUS, gonococci favor uptake of homospecific DNA, and efficient DNA uptake in *N. gonorrhoeae* is, consequently, sequence specific [Chen & Dubnau, 2004; Cehovin *et al*., 2013].

While the exact mechanism underlying (sequence-specific) DNA uptake in *N. gonorrhoeae* is not completely understood, there is a widely accepted model which is primarily focused on three molecules: ComP, the pilus component that interacts with extracellular DNA, the ATPase PilT, which retracts the pilus and, subsequently, brings the ComP-bound DNA into close proximity to the cell envelope, and the periplasmic DNA-binding protein ComE which translocates DNA from the extracellular- into the intracellular space [Aas *et al*., 2002; Chen & Dubnau, 2004].

The periplasmic DNA-binding chaperone ComE

ComE is a small, 8 kDa protein located in the periplasm. It binds DNA in a sequence unspecific manner through two conserved helix-hairpin-helix motifs [Chen & Gotschlich, 2001; Doherty *et al*., 1996]. The genome of *N. gonorrhoeae* has four identical copies of *comE*. While single gene deletions do not influence transformation frequencies in a measurable amount, serial deletions of these gene copies lead up to a 4×10^4 -fold reduction of transformation frequencies [Chen & Gotschlich, 2001].

Recent studies highlight ComE as the center piece of a dedicated DNA uptake machinery in *N. gonorrhoeae*. For instance, ComE was shown to be homogeneously distributed in the periplasm in the absence of transforming DNA, indicating free diffusion of the protein within the confines of the periplasm. However, upon contact with periplasmic DNA, ComE colocalizes to the DNA to form foci, which suggests that ComE molecules capture transforming DNA. Combined with the finding that ComE concentrations regulate the amount of DNA stored within the periplasm, this served as a strong indicator for an active role of ComE during DNA

uptake [Gangel *et al.*, 2014]. Furthermore, it was shown that the level of ComE expression defines the speed with which DNA is translocated into the periplasm [Hepp & Maier, 2016]. Most importantly, however, was the finding that the binding characteristics of ComE to DNA resemble those of a translocation ratchet.

Based on this finding, a model for DNA uptake in *N. gonorrhoeae* was derived which explains how eDNA enters the periplasmic space and is, subsequently, imported into the cytoplasm (Fig. 1.8) [Peskin *et al.*, 1993; Simon *et al.*, 1992; Chen & Dubnau, 2004; Yu & Luo, 2011; Hepp & Maier, 2016].

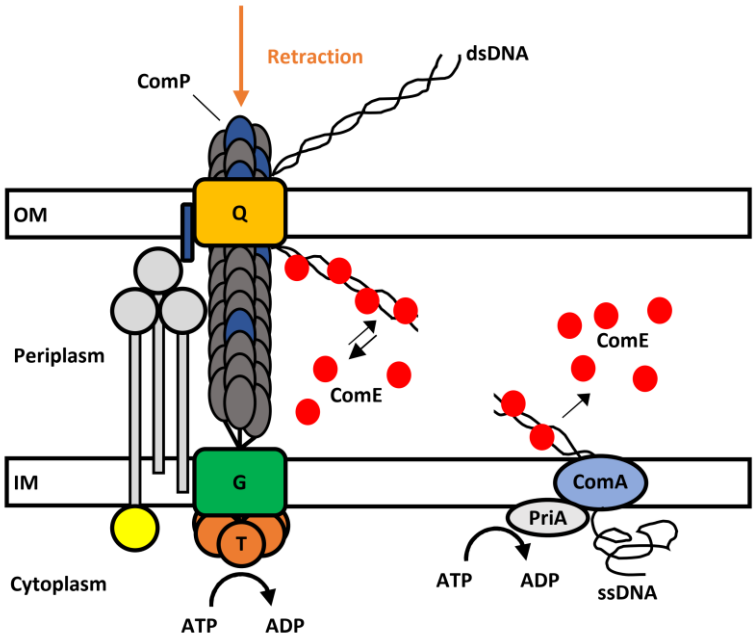

Figure 1.8: Putative model for DNA uptake in *N. gonorrhoeae*.

T4P fish for DNA in the extracellular space. ComP allows for sequence specific binding of DNA to the pilus fiber. Retraction, initiated by PilT at the pilus base PilG, drags ComP-bound DNA through the PilQ pore. ComE rapidly localizes to the area and binds the DNA, thereby biasing the direction of diffusion towards import. To overcome the inner membrane, ComE dissociates from the DNA, one strand is degraded, and the nucleotides enters the cytoplasm as ssDNA through a pore formed by ComA. The transport is likely driven by a PriA/ComFA-homologue. Once inside the cytoplasm, ssDNA is shuttled to RecA to induce homologues recombination into the gonococcal chromosome. OM: outer membrane, IM: inner membrane.

The most likely point of entry for DNA into the periplasm is the outer membrane pore formed by PilQ, since there is sufficient data which indicates that DNA uptake is directly linked to T4P retraction through the opening in the outer membrane [Aas *et al.*, 2002; Assalkhou *et al.*, 2007]. Therefore, pili need to interact with eDNA at an early stage of the transformation process. This

interaction is formalized by the minor pilin ComP and its inherent property to bind DNA bearing the DUS motif [Cehovin *et al*., 2013]. ComP mediated DNA-binding to the pilus is, thus, the first step in gonococcal transformation and used to differentiate between self- and foreign DNA. Once the pilus retracts due to PilT mediated depolymerization, the pilus-bound DNA will be exposed at the outer membrane of the cell, where it is immediately gathered by ComE, which biases the direction of transport towards import into the periplasm.

However, ComE binding to DNA is reversible and dissociation of ComE from DNA molecules is a requirement for its subsequent transport into the cytoplasm [Hepp & Maier, 2016]. This process, as well as the subsequent integration into the genome of *N. gonorrhoeae* by homologous recombination, requires a few more critical components and mechanisms, which will be described in the following sections.

Crossing the cytoplasmic membrane

How DNA is transported across the cytoplasmic membrane is still not completely understood. Studies in *B. subtilis*, show that the permease/channel protein ComEC and the ATP-binding protein ComFA are required for DNA transport [Inamine & Dubnau, 1995; Chen & Dubnau, 2004]. Orthologs of ComFA have not been found in gonococci or other gram-negative bacteria; however, the orthologue to ComEC has been identified: ComA [Facius & Meyer, 1993]. ComA is a polytropic membrane protein that is believed to form an aqueous channel across the cytoplasmic membrane that is dispensable for DNA-binding but essential for DNA transport [Dubnau, 1999; Chen & Dubnau, 2004]. In *N. gonorrhoeae*, ComA is not required for DNA uptake, but mutants lacking ComA retain dsDNA in the periplasm [Facius *et al*., 1996]. ComA has a binding-protein domain (BPD), which is a signature motif characteristic of ABC transporter permeases and mutations of a specific residue in the BPD reduce the level of transformation [Chen & Dubnau, 2004]. Transport across the inner membrane into the cytoplasm is uncoupled from transport through the outer membrane and is likely to occur at a membrane pore formed by ComA [Facius *et al*., 1996, Chen & Dubnau, 2004].

The ATP-binding protein ComFA is required for competence in *B. subtilis* [Chen & Dubnau, 2004]. Mutations in this membrane-associated protein lead up to a 1000-fold reduction in transformation frequencies but show no effect on DNA-binding [Chen & Dubnau, 2004]. Its homologue in *E. coli*, PriA, is an ATP-driven DNA translocase with similarities to DNA and RNA helicases [Chen & Dubnau, 2004]. The protein has Walker-A and -B motifs and mutations of Walker-A result in reduced transformation efficiencies [Dubnau, 1999]. While not yet

identified, it is conceivable that, due to its similarities to helicases, a PriA/ComFA homologue in *Neisseria* unwinds dsDNA and drives the passage of ssDNA through the ComA channel by ATP-hydrolysis [Londoño-Vallejo & Dubnau, 1993; Chen & Dubnau, 2004]. This hypothesis is supported by the finding that most DNA is double stranded when taken up into the periplasm, but most of the DNA translocated into the cytoplasm is single stranded instead [Chausse & Hill, 1998].

Homologous recombination into the genome

Homologous recombination has been extensively researched in *E. coli* [Kowalczykowski *et al*., 1994]. Here, recombination is mediated mostly by the RecBCD and RecF pathways [Horii & Clark, 1973; Kushner *et al*, 1971]. Several homologues of enzymes involved in these pathways have been identified in the genome of *N. gonorrhoeae* and it was shown that the RecBCD pathway is required for efficient gonococcal transformation, while the RecF pathway is not necessary [Hamilton & Dillard, 2005].

The essential protein in both the RecBCD and RecF pathways is the recombinase RecA, a highly conserved enzyme found in almost all bacteria [Brendel *et al*., 1996]. RecA is essential for homologous recombination, DNA repair and initiation of SOS responses to DNA damage [Clark, 1973; Koomey & Falkow, 1987; Cox, 2007]. The recombinational function of RecA has been extensively studied: RecA binds ssDNA and produces a right-handed helical filament that contains one RecA monomer for every three nucleotides. Subsequently, homologous duplex DNA is aligned to the ssDNA encaged within the helical RecA-filament, after which the DNA strand exchange is promoted through ATP-hydrolysis [Kowalczykowski *et al*., 1994; Cox, 2003; Kidane & Graumann, 2005; Cox, 2007].

1.3. Aims of this study

Bacteria and microbes usually organize into highly structured, multicellular aggregates called biofilms. This alternative lifestyle of bacterial growth provides many advantages and benefits, as biofilms pose protective environments that facilitate survival under otherwise adverse conditions. The underlying mechanisms behind the protective capabilities of bacterial biofilms are complex and numerous; however, many of them are attributed to the extracellular matrix which is secreted during biofilm development. While highly diverse in its composition, it is now well established that extracellular DNA is one of the most important components of the matrix and, thus, biofilms. Nevertheless, many of the functions and mechanisms provided by DNA in the broader context of bacterial biofilms are still not completely understood.

For example, it is currently unknown how mobile DNA is within cellular aggregates. In this study, we addressed this gap of knowledge by investigating the spatio-temporal dynamics of eDNA penetration into early biofilms of *Neisseria gonorrhoeae*. We hypothesized that the dynamics strongly depend on length of the DNA molecule and might be affected by the presence of DNA uptake sequences. Furthermore, we also investigated the effects of the thermonuclease Nuc, which was reported to act as an eDNA-structuring enzyme in biofilms.

Next, we related our understanding of the diffusion and penetration dynamics to DNA uptake and transformation events in bacterial colonies. Biofilms are often labeled as hot spots for horizontal gene transfer, however, data on the spatio-temporal dynamics of both pathways in biofilms is limited. Here, we characterized the efficiency of both processes in gonococcal colonies with spatial and temporal resolution. Moreover, we also delineate direct gene transfer events in between reporter strains in mixed colonies.

While it is straightforward to think of eDNA solely as a target for horizontal gene transfer, an increasing number of studies suggest additional functions for DNA in biofilms. In particular, eDNA is often conceptualized as a stabilizing component of the ECM within bacterial biofilms. Utilizing a high-affinity DNA stain we visualized the release of free eDNA within gonococcal colonies. We show that released DNA forms impressive networks of eDNA. These experiments are a first step towards understanding how the extracellular matrix is formed and remodeled to stabilize bacterial biofilms.

2. Materials and methods

2.1. Media and solutions

Table 2.1: Protocol for the preparation of Isovitalex.

Isovitalex was sterile filtered through a 0.2 µm membrane, split into 10 ml aliquots and stored at -20 °C.

Substance	Amount	Company
D(+)-Glucose	100 g	Carl Roth
L-Glutamine	10 g	Carl Roth
L-Cysteine · HCl · H_2O	28,9 g	Carl Roth
Cocarboxylase (Thiamine Pyrophosphate)	0,1 g	Sigma Aldrich
Ferric Nitrate ($Fe(NO_3)_3 \cdot 9\ H_2O$)	0,02 g	Sigma Aldrich
Thiamine · HCl	0,003 g	Carl Roth
4-Aminobenzoic Acid (PABA)	0,013 g	Sigma Aldrich
B-Nicotinamide Adenine Nucleotide (NAD)	0,25 g	Carl Roth
Cyanocobalamin (Vitamin B_{12})	0,01 g	Sigma Aldrich
ddH_20	1 l	

Table 2.2: Protocol for the preparation of GC-agar plates.

All components, except for Isovitalex, were mixed and autoclaved. The agar solution was cooled to 55 °C in a water bath and Isovitalex (see Table. 2.1) was added before plates were poured in a laminar flow hood.

Substance	Amount	Company
NaCl	5 g	Carl Roth
K_2HPO_4	4 g	Carl Roth
KH_2PO_4	1 g	Carl Roth
Proteose Peptone No. 3	15 g	BD
Bacto Agar	10 g	BD
Soluble Starch	0,5 g	Sigma Aldrich
Isovitalex	10 ml	-
ddH_20	1 l	

Table 2.3: Protocol for GC-medium.

All components, except for Isovitalex, were mixed and autoclaved. The medium was stored at 4 °C. Isovitalex (see Table 2.1) was added shortly before use.

Substance	Amount	Company
NaCl	5 g	Carl Roth
K_2HPO_4	4 g	Carl Roth
KH_2PO_4	1 g	Carl Roth
Proteose Peptone No. 3	15 g	BD
Isovitalex	10 ml	-
ddH_20	1 l	

2.2. Bacterial strains and growth conditions

2.2.1. Cultivation of *Escherichia coli*

Chemically competent *Escherichia coli* strains *10-beta* (New England Biolabs) and *DH5α* (genotype: *fhuA2 lac(del)U169 phoA glnV44 Φ80' lacZ(del)M15 gyrA96 recA1 relA1 endA1 thi-1 hsdR17*) were grown in LB-broth (Carl Roth) or on LB plates (LB-broth with 1.5 % Agar) at 37 °C. All LB media were prepared according to manufacturer instructions and supplemented with antibiotics if necessary.

2.2.2. Cultivation of *Neisseria gonorrhoeae*

All *Neisseria gonorrhoeae* strains used in this study are shown in Table 2.4. Prior to any experiments, cells were grown overnight at 37 °C and 5 % CO_2 on GC-agar plates. GC-agar was prepared according to Table 2.2. The solution was autoclaved and subsequently cooled to 55 °C in a water bath. Isovitalex (see Table 2.1) was added to a final concentration of 1 % and plates were poured in a laminar flow hood where they were stored at room temperature for 1-2 days before usage to ensure proper drying of the agar. For long-term storage, GC plates were transferred to plastic bags and stored at 4 °C.

After overnight incubation on the plates, cells were picked and transferred into GC-medium (see Table 2.3). The medium was sterile filtered with a 0.2 µm syringe filter (VWR) before usage. To create bacterial stocks, cells were scraped from plates, resuspended in a 10 % milk-powder solution and frozen in liquid nitrogen. The stocks were stored at -80 °C.

Table 2.4: Bacterial strains used in this study.

List of *Neisseria gonorrhoeae* strains used in this study.

Strain	Genotype	Number	Reference
*wt**	MS11, opa-selected, G4::*aac*, *lctp::PpilE-sfgfp-speR::aspC*	NG194	Welker *et al*., 2021
Δnuc	MS11, opa-selected, G4::*aac*, *lctp::PpilE-sfgfp-speR::aspC, nucA::kanR*	NG235	This study
comE-PAmcherry	N400 GV1, *recA:tet*, *PAmcherry-comE4:KanR*	NG069	This study
*comE-mcherry**	MS11, opa-selected, G4::*aac*, *igA::gfp:ermR, comE4-mcherry:kanR, comE1-5'-UTR-apraR-pilE1*	NG195	This study
wt sfgfp$_{nf}$*	MS11, opa-selected, G4::*aac*, *lctp::PpilE-sfgfp$_{nf}$-speR::aspC, igA::PpilE mcherry ermR*	NG233	This study
mcherry	MS11, opa-selected, G4::*aac*, *igA::PpilE mcherry ermR*	NG232	This study
ΔcomP	MS11, opa-selected, G4::*aac*, *comP::m-Tn3erm*	NG236	This study
comE-mcherry	MS11, opa-selected, G4::*aac*, *comE4-mcherry:kanR, comE1-5'-UTR-apraR-pilE1*	NG192	This study
ΔG4	MS11, opa-selected, G4::*aac*	NG150	Welker *et al.*, 2018
gfp	MS11, opa-selected, G4::*aac* , *igA::gfp:ermR, ComE1-5'-UTR-apraR-pilE1*	NG151	Welker et al., 2018
GV1	N400, *ΔpilV*, *recA:tet(recAind)*	NG005	Winther-Larsen *et al*., 2001
GV1 Δnuc	N400 GV1, ΔpilV(pilVfs), *recA6ind(tetM), nucA::kanR*	NG058	Hepp, PhD Thesis, 2017
comE-mcherry ΔpilV	N400, *ΔpilV*, *recA:tet(recAind), comE4-mcherry:kanR*	NG068	Gangel *et al*., 2014
N400 mcherry	N400 *igA::PpilE mcherry ermR, recA6ind(tetM)*	NG065	Zöllner *et al*., 2017
MW104	N400, *recA:tet; comP::m-Tn3erm*	NG031	Wolfgang *et al*., 1999

2.3. Microbiological methods

The methods outlined in the following sections were mainly used for cloning and DNA sample preparation.

2.3.1. Isolation of genomic DNA

To isolate genomic DNA of *Neisseria gonorrhoeae*, bacteria were plated on GC-agar plates and incubated overnight at 37 °C with 5 % CO_2 (see section 2.2.2). Cells were resuspended in PBS (Gibco/Life Technologies) and pelleted by centrifugation. For isolation of *E. coli* genomic DNA, cells were grown overnight in a 5 ml liquid culture of LB-broth at 37 °C. Again, cells were pelleted by centrifugation.

DNA was purified using the DNeasy Blood & Tissue Kit (Qiagen) according to manufacturer instructions. Elution of the DNA was done in ddH_2O instead of the provided buffer. Isolated genomic DNA was stored -20 °C and concentrations were determined by absorption measurements at 260 nm and 280 nm wavelengths using a BioPhotometer D30 (Eppendorf).

2.3.2. Plasmid isolation from *E. coli*

Bacteria were grown overnight in 5 ml LB-broth (Carl Roth) at 37 °C in a shaking incubator (250 rpm). Plasmid DNA was subsequently purified with the GenUP Plasmid Kit (biotechrabbit GmbH) according to manufacturer instructions. DNA was eluted in ddH_2O instead of the provided buffer and subsequently stored at -20 °C. The concentration of the eluted plasmid DNA was determined via absorption measurements at wavelengths 260 nm and 280 nm using a BioPhotometer D30 (Eppendorf).

2.3.3. Polymerase Chain Reaction

All Polymerase Chain Reaction (PCR) were done using the Q5 High-Fidelity DNA Polymerase (M0491, New England Biolabs). Reaction setups and thermocycling conditions were adopted from instructions and recommendations by New England Biolabs. Primer design was done with the SnapGene molecular cloning tool (GSL BioTech LLC.). PCRs were prepared in 25 µl-volume reactions at room temperature and were transferred to a thermocycler preheated to 98 °C. Annealing temperatures were calculated with the help of the open-access tool NEB Tm Calculator (New England Biolabs) [SantaLucia J., 1998]. NEB Tm Calculator was also used

during primer design to ensure that differences in melting temperatures between forward- and reverse-primers do not exceed 5 °C.

2.3.4. Agarose gel electrophoresis

To check DNA fragments in terms of length or size, agarose was dissolved in 1x TAE buffer through heating in a microwave. After cooling, Midori Green Advance DNA Stain (NIPPON Genetics) was added, and a gel was formed in a suitable mold.

DNA samples were mixed with Gel Loading Dye, Purple (6X, New England Biolabs) and loaded into the agarose gel. Electrophoresis was performed at 100 V for 1 hour in 1x TAE buffer. Generuler 1 kb DNA Ladder (Thermo Scientific) was used as a size standard, and DNA was visualized with a GENi gel documentation system (Syngene).

2.3.5. PCR purification

DNA amplified by PCR was purified with either one of two different methods based on the purity of the sample after amplification (determined by gel electrophoreses). In most cases, DNA samples were purified via the gel extraction approach and isolated using the QIAquick Gel Extraction Kit (Qiagen): After gel electrophoreses (see section 2.3.4), amplified DNA was excised from the agarose gel and subsequently purified according to the manual instructions of the kit.

In case that the DNA sample was already sufficiently pure after PCR, purification was instead performed with a silica-membrane-based procedure. To this end, the QIAquick PCR Purification Kit (Qiagen) was used, and all steps were performed according to the instructions of the Kit's manual. Isolated, purified DNA was eluted in ddH_2O for both gel extraction- and membrane-based purification procedures.

2.3.6. Restriction enzyme digestion

All digestion reactions were done with restriction enzymes and buffers supplied by NEB (New England Biolabs). The open-access tool NEBcloner was used to set up each restriction reaction.

In short, 1 µg of DNA was mixed with the chosen restriction enzyme(s) in a final dilution of 1x of a suitable buffer. ddH_2O was used to bring the total volume to 50 µl and the reaction was incubated at 37 °C for 2 hours. The reaction was stopped by heat-inactivation at 80 °C for 2 minutes.

2.3.7. Dephosphorylation of DNA

To prevent re-ligation of linearized DNA after restriction digests the sample was treated with Antarctic Phosphatase (New England Biolabs). The enzyme and associated buffer were directly added into the ongoing restriction reaction (see section 2.3.6) and incubation at 37 °C was continued for a further 30 minutes. The reaction was terminated by heat-inactivation at 80 °C for 2 minutes. Dephosphorylated DNA samples were purified with a silica-membrane (see section 2.3.5) before subsequent cloning steps were performed.

2.3.8. Ligation

T4 DNA Ligase (New England Biolabs) was used to ligate DNA into a restriction digested and dephosphorylated target-vector. 1 µl of vector DNA was mixed with 15 µl of the desired DNA insert, 1 µl ligase and 2 µl of T4 buffer. 1 µl of ddH_2O was added to adjust the final reaction volume to 20 µl. The mix was incubated at 16 °C overnight and the process was stopped by heat-inactivation at 65 °C for 10 minutes.

2.3.9. Transformation of *N. gonorrhoeae*

Naturally competent *N. gonorrhoeae* were transformed with the spot transformation method. 5 µl of DNA were pipetted onto an GC-agar plate so that it forms a drop in the center of the plate. Once the drop of DNA had dried, the cells were streaked onto the spot of the DNA-drop and incubated overnight (see section 2.2.2). Cells were harvested the next day and re-streaked onto fresh GC-agar plates containing selective antibiotics. After overnight incubation, single colonies were picked from the plate and transferred to 50 µl of GC-medium in separate tubes. The cell suspensions were plated on separate GC-agar plates, and, after overnight incubation, a stock was created and stored at -80 °C. The stocks were checked by PCR and sequencing (see section 2.3.11) to identify which stock contains the desired integration of target DNA.

2.3.10. Transformation of chemically competent *E. coli*

Preparation and transformation of chemically competent *E. coli* were performed according to a previously published protocol [Sambrook & Russel, 2001]. In short, a 200 µl aliquot of chemically competent *E. coli* was thawed on ice and the desired DNA insert was added. After 30 minutes the tube was transferred to a pre-heated 42 °C thermo-block, to expose the cells to a 90 second heat-shock. Subsequently, the tube was transferred back to ice for another 1-2 minutes before 800 µl of SOC Outgrowth medium (New England Biolabs) were added and the

suspension was incubated at 37 °C for 45 minutes, shaking. Transformation was finalized by briefly pelleting the cells in a benchtop centrifuge to enable removal of 900 µl of medium. The remaining 100 µl of the suspension were resuspended and plated on LB-agar plates containing an appropriate antibiotic. After overnight incubation, single colonies were picked and screened for the desired DNA insert.

2.3.11. Sanger Sequencing

Sanger sequencing was used to obtain the exact nucleotide sequence of sample DNAs, PCR products and plasmids. Sequencing was carried out by GATC services (Eurofins Genomics) in Cologne, Germany. To this end, DNA was diluted and mixed with the sequencing primers according to the instructions of the sequencing service. The sample was shipped, and sequencing was usually finished within 48 hours.

2.4. Construction of mutant strains

2.4.1. Construction of a green fluorescent wildtype strain (*wt**)

To be able to observe dynamics within colonies by confocal microscopy, we opted to create a new strain of green fluorescent *N. gonorrhoeae*. Superfolder green fluorescent protein (sfGFP) [Pédelacq *et al*., 2006] was a suitable candidate protein, since it features an enhanced fluorescent signal and is less prone to bleaching effects compared to conventional GFP, thus we stably integrated *sfgfp* into the genome of our lab strain *ΔG4* (NG150) and put it under the control of the strong, constitutive *pilE* promoter. The procedures to achieve this were published previously [Welker *et al*., 2021].

In short, we amplified the PilE promoter region (*PpilE*) from genomic DNA of strain *ΔG4* (NG150) with primers TC22 and NB065 (see section 2.3.3) whereas the *sfgfp* gene sequence was amplified from plasmid *pET28a-sfGFP* (obtained from Addgene; Plasmid #85492) with primers TC21 and NB066. Both fragments were subsequently merged in a fusion-PCR: fragments were mixed in 1:1 ratio, and PCR was performed for 20 cycles without any primers. Afterwards, primers NB065 and NB066 were added to the reaction and the PCR was continued for another 20 cycles. The obtained *PpilE-sfgfp* fusion-product was subcloned into the vector *pLAS* via FseI and PacI digest (see section 2.3.6). The generated plasmid *pLAS-sfgfp* was transformed into *E. coli* (see section 2.3.10) and positive transformants were selected on LB-agar plates containing kanamycin. The correct sequence of the vector insert was verified by sequencing (see section 2.3.11) with primers TC19 and TC20.

Finally, the *pLAS-sfgfp* plasmid was transformed into strain *ΔG4* (NG150) according to the procedure described in section 2.3.9 and transformants were selected on GC-agar plates containing spectinomycin. Expression of sfGFP was confirmed with a fluorescent microscope.

2.4.2. Construction of a *nuc* deletion strain (*Δnuc*)

To determine the potential impact of the thermonuclease Nuc on the spatio-temporal dynamics of extracellular DNA in gonococcal colonies, we created a *nuc* deficient mutant of the previously generated green fluorescent wildtype strain *wt** (NG194). This mutant strain was generated by transforming genomic DNA of strain *GV1 Δnuc* (NG058) into strain *wt** (NG194). Transformants were selected on GC-plates containing kanamycin. The correct insertion of the kanamycin cassette into the *nuc* gene was checked by PCR with primers NB084 and NB085.

2.4.3. Construction of a red fluorescent strain (*mcherry*)

The strain was created by inserting *mcherry* into the *igA*-locus of the *ΔG4* lab strain (NG150). This allowed for the monitoring of the colony structure during confocal imaging. A *PpilE-mcherry* fusion was amplified from genomic DNA of strain *N400 mcherry* (NG065) using primers NB069 and NB070. The product was ligated into vector *pIGA* by XhoI and KpnI digestion, which eventually yielded the plasmid *pIGA-mcherry*. The plasmid was transformed into the *ΔG4* strain (NG150) and transformants were selected on GC-agar plates containing erythromycin, yielding clones of the final strain *mcherry* (NG232).

2.4.4. Construction of a transformation reporter strain (*wt* sfgfp$_{nf}$*)

In order to observe single transformation and gene transfer events within gonococcal colonies with spatial and temporal resolution, we opted to create a new reporter strain based on our green fluorescent lab strain *wt** (NG194), which is expressing sfGFP. The reporter strain was generated by introducing a single point mutation into the chromophore region of *sfgfp*. The mutation creates a premature stop-codon within the *sfgfp* open reading frame (ORF) and thus leads to the expression of a truncated, non-fluorescent form of sfGFP. Fluorescence of sfGFP is recovered once the ORF of the gene is reverted to its native sequence, which can be achieved by means of transformation of suitable DNA and, hence, enables the direct visualization of genetic exchange by means of transformation.

We inserted the mutated *sfgfp* sequence into the *lctp-aspC* locus of strain *mcherry* (NG232). As a first measure, an adenine to cytosine substitution at position 201 of the *sfgfp* coding sequence (c.201A>C) was inserted into the previously constructed *pLAS-sfgfp* plasmid (see section 2.4.1) via site-directed mutagenesis, using back-to-back primers NB073 and NB074. The resulting *pLAS-sfgfp$_{nf}$* vector, which contained the coding sequence for the truncated, non-fluorescent protein, was then transformed into strain *mcherry* (NG232) by spot transformation. Clones were selected on plates containing erythromycin, and subsequently sequenced to confirm the integration of the c.201A>C point mutation; thus, yielding the final strain *wt* sfgfp$_{nf}$* (NG233).

2.4.5. Construction of a *comP* deletion strain (*ΔcomP*)

To investigate the putative role of DNA-binding and type IV pili (T4P) on the formation of DNA filaments and bundles within gonococcal colonies, we created a strain lacking the DNA-binding minor pilin ComP. To this end, genomic DNA of strain *MW104* (NG031) was transformed into strain *ΔG4* (NG150) via the spot transformation method (see section 2.3.9).

Clones were subsequently selected on GC-agar plates containing erythromycin and insertion of the m-Tn3erm transposon into *comP* was confirmed with PCR using primers NB067 and NB068.

2.4.6. Construction of a ComE-PAmCherry fusion strain (*comE-PAmcherry*)

Super resolution imaging of individual ComE molecules required a strain expressing the DNA-binding protein as a fusion with a photoactivatable fluorescent protein. Here, we choose photoactivatable-mCherry (*PAmcherry*) and fused it to the 3'-end of one of the four gene copies of *comE* (*comE4*). The cloning procedures outlined below were performed by Dr. Christof Hepp.

In short, the genetic construct was generated in a series of multi-step PCR's. First, *comE4* and parts of the 5'-UTR were amplified from genomic DNA of strain *GV1* (NG005) with primers P1 and P2 (fragment 1). Second, *PAmcherry* was amplified from vector *pGCC4-PAmcherry* with primers P3 and P4 (fragment 2). The kanamycin-resistance cassette was amplified from vector *pUP6* with primers P5 and P6 (fragment 3), while the 3'-UTR of *comE4* (fragment 4) was produced from genomic DNA of strain *GV1* (NG005) with primers P7 and P8. The four fragments were subsequently merged with fusion-PCR's and transformed back into strain *GV1* (NG005). Clones were selected on GC-agar plates containing kanamycin and integration of *comE-PAmcherry* was confirmed by sequencing.

2.4.7. Construction of a ComE-mCherry fusion strain (*comE-mcherry**)

In order to investigate ComE foci dynamics within gonococcal colonies we created a strain expressing the protein as a fusion to *mcherry*. Furthermore, we choose to also add *gfp* into a neural locus of the genome to monitor cell and colony positions during confocal imaging.

We created this strain by, first, transforming genomic DNA of strain *comE-mcherry ΔpilV* (NG068) into strain *ΔG4* (Ng150), thereby transferring the *comE-mcherry* fusion into the *ΔG4* background. Transformants were selected on GC-agar plates containing kanamycin. The resulting strain *comE-mcherry* (NG192) was subsequently transformed with genomic DNA of strain *gfp* (NG151) and transformants were selected on GC-agar plates containing erythromycin; thus, creating the final strain *comE-mcherry** (NG195). Both transformation steps were performed according to the spot transformation method (see section 2.3.9).

Table 2.5: Primers and Nucleotides.

Listed are all primers and oligonucleotides that were used in this study.

Name	Sequence
P1	GGATCCATGCCGTCTGAACGTCGCAAGATGCGG
P2	TGAAGGCGATGGTGACGGAGATGGTTTTTTAACCGCAGGCAGCACCGGTTTGGCGGG
P3	CCATCTCCGTCACCATCGCCTTCAATGGTGAGCAAGGGCGAGG
P4	TTATTCCTCCTAGTTAGTCACTTGTACAGCTCGTCCATGCCG
P5	CTGTACAAGTGACTAACTAGGAGGAATAAATGATTGAACAAGATGGATTGCACGCAG
P6	CCCCTTCCTTTACAGGTTCCCCTATCAGAAGAACTCGTCAAGAAGGCGATAG
P7	TAGGGGAACCTGTAAAGGAAGGGGCATCGGCTGCCGCCGGC
P8	GAATTCTTGCCTTCCACCCTTCG
TC19	CCTTAATTAAGGTTATTTATACAGTTCATCCATACCGTG
TC20	TCTGGCCGGCCTTCCGACCCAATCAACACACC
TC21	CATTTCCCCTTTCAATTAGGAGTAATTTTATGGTTAGCAAAGGTGAAGAACT
TC22	AGTTCTTCACCTTTGCTAACCATAAAATTACTCCTAATTGAAAGGGGAAATG
NB065	TTTTAATTAATTCCGACCCAATCAACACACCC
NB066	TTGGCCGGCCTTATTTATACAGTTCATCCATACCGTG
NB067	TACACGATTCTCATTCCATCAAGG
NB068	CATACTGCTGAATGGGATAGTAAG
NB069	CCGCTCGAGCGGTTCCGACCCAATCAACAC
NB070	CGGGGTACCCCGCTACTTGTACAGCTCGTCC
NB073	AAGCACTGAACGCCCTAGGTCAGGGTG
NB074	TAGCCGCTATCCGGATCATATGAAACGC
NB077	TTCAGACGGCATCAGATTCC
NB078	CAATACGCCGTTTTCCGATACTGC
NB079	ACACTAAAAATGAAAGTTTACTCGTAAAAG
NB080	CAGATTCCCTTCCTCAATCTTCTCC
NB081	GGAAAGGTTCAGCAATACGCCGTT
NB082	AAATTCGTTTCAACACTAAAAATGAAAGTTT
NB084	GTTGCGCGTCTCCGCAAAAATG
NB085	CAAGGGTAATCCTGACGTTAAGATG
NB088	TTCAGACGGCATTCTGAAATCCGCAAAAACTTGGGC
NB089	GTACGGCCAGCAACGTCGGTTCGAG
NB090(2)	TTCAGAGCGCCCTTCAAATTTAACTTCCGCACG
NB091	GAACTGGATGGTGATGTGAATGGCC

2.5. Determining the dynamics of DNA in early gonococcal biofilms

In this study we investigated the spatio-temporal dynamics of external DNA penetrating gonococcal colonies. To this end, we labelled DNA with the red fluorescent dye Cy3, supplemented the labelled DNA to the growth medium of early cell aggregates formed by *N. gonorrhoeae* and subsequently imaged the colonies with confocal microscopy. Finally, the position of Cy3-DNA within gonococcal colonies at different time points was determined with a Matlab (MathWorks) image processing pipeline.

2.5.1. Preparation of Cy3-DNA samples

Genomic DNA (gDNA) was isolated from *N. gonorrhoeae* strain *ΔG4* (NG150) and *E. coli* strain *DH5α* (see section 2.3.1) while 300 bp and 3 kb DNA fragments were generated with PCR (see section 2.3.3). Primer NB077 was used as the forward primer for DNA fragments containing a DNA uptake sequence (DUS) and the segment length was defined by the reverse primer used during PCR: NB078 for 300 bp and NB079 for 3 kb fragments. Conversely, primer NB080 was used as the forward primer for DNA fragments lacking a DUS, with NB081 and NB082 serving as reverse primers for 300 bp and 3 kb fragments, respectively. Genomic DNA of the *ΔG4* lab strain (NG150) was used as template DNA for all PCR reactions.

To enable the observation of DNA molecules during confocal imaging, we used the "Label IT Nucleic Acid Labelling Kit, Cy3" (MIR3600, Mirus Bio LLC) to covalently attach Cy3-fluorescent molecules to DNA. All labelling steps were performed according to the instructions lined out in the manual of the kit. However, incubation times were extended to 2 hours to ensure that proper labelling densities were reached. To ensure sufficient yield of sample DNA, multiple labelling reactions were pooled before any experiments were started. Finally, absorption of all Cy3-labelled DNA samples was measured with a spectrometer at a wavelength of 562 nm (Table 2.6) to be able to adjust for fluorescence intensity fluctuations and indifferences between different samples during image analysis.

Table 2.6: Absorption of Cy3-DNA samples at 562 nm.

Absorption was measured to adjust for indifferences between individual labelling reactions. Each sample was measured 3x, and the average value (final row) was used to adjust intensities during image analysis (see section 2.5.3).

gDNA (*ΔG4*)	gDNA (*DH5α*)	300 bp	300 bp DUS	3 kb	3kb DUS
0.707	0.821	0.859	1.053	0.731	1.082
0.695	1.066	0.660	1.162	0.595	0.931
0.835	0.927	0.429	1.052	0.539	0.803
0.745	0.938	0.649	1.089	0.621	0.938

2.5.2. Confocal imaging of colonies and Cy3-DNA

Cells of green fluorescent strain *wt** (NG194) were grown overnight on GC-agar plates (see section 2.2.2), scraped and resuspended in GC liquid medium (see Table 2.3) supplemented with IsoVitalex (1 %) and 7 mM $MgCl_2$. The medium was sterile filtered with a 0.2 µm syringe filter (VWR) and heated to 37 °C before usage. Optical density (OD_{600}) of the suspension was adjusted to 0.1 and a 500 µl aliquot was incubated in a shaking-incubator (250 rpm) at 37 °C, 5 % CO_2 for 30 minutes. Afterwards, 200 µl of the cell suspension was transferred into a well of a poly-L-lysine coated "µ-Slide 8 Well" plate (Cat.No. 80824, Ibidi). The plate was incubated for another 30 minutes without shaking.

In the meantime, a 100 µl sample of GC-medium containing 1.5 µg of fluorescently labelled Cy3-DNA (see section 2.5.1) was prepared and warmed to 37 °C. The DNA-medium mix was carefully added to the cell suspension in the well plate once the 30-minute incubation period was over and imaging was started immediately. Subsequently, image acquisition was started, and colonies were imaged for 2 hours.

Cy3-DNA within colonies was imaged with a Ti-E inverted microscope (Nikon) equipped with a CSU-X1 (Yokogawa) spinning disk unit and a 100x CFI Apo Tirf objective (Nikon). Image acquisition was done with an EMCCD camera (iXon 897, Andor). Fluorophores were excited using lasers with a wavelength of 561 nm (Cy3-DNA) and 488 nm (sfGFP, denoting cell and colony positions), respectively. Exposure times were set to 50 ms, with laser powers of 50 % and 5 %, respectively.

For each colony, 27 images with a z-spacing of 0.2 µm per image were obtained close to the equatorial, lateral plane of the colony; resulting in a 3D data set that resembles a total height of 5 µm within colonies.

2.5.3. Image and data analysis

In order to uncover the spatio-temporal dynamics of DNA in gonococcal colonies we needed to detect fluorescence intensities of Cy3-DNA with respect to their position within the colony, i.e., the distance to the colony contour. Thus, we aimed at detecting both Cy3-DNA, as well as the position of the colony in each recording. This was done with proprietary Matlab (MathWorks) scripts developed together with the help of Dr. Marc Hennes. The principles of the data analysis procedures are exemplified in Figures 2.1, 2.2 and 2.3.

Colony detection

Colony detection was based on identification of sfGFP fluorescence in each recording (Fig. 2.1a). The center of mass (COM) of the colony and its radius (*r*) were extracted from confocal microscopy data sets by, first, creating a single averaged image of the 3D stack (Fig. 2.1b). On this average, we subsequently apply a gaussian blur with a radius of 10 µm. Finally, colonies are detected by applying the Matlab function *imfindcircles* with a range of 100 - 300 pixels, which corresponds to the typical colony radius of 15 µm we expect at a resolution of 80 nm per pixel (Fig. 2.1c).

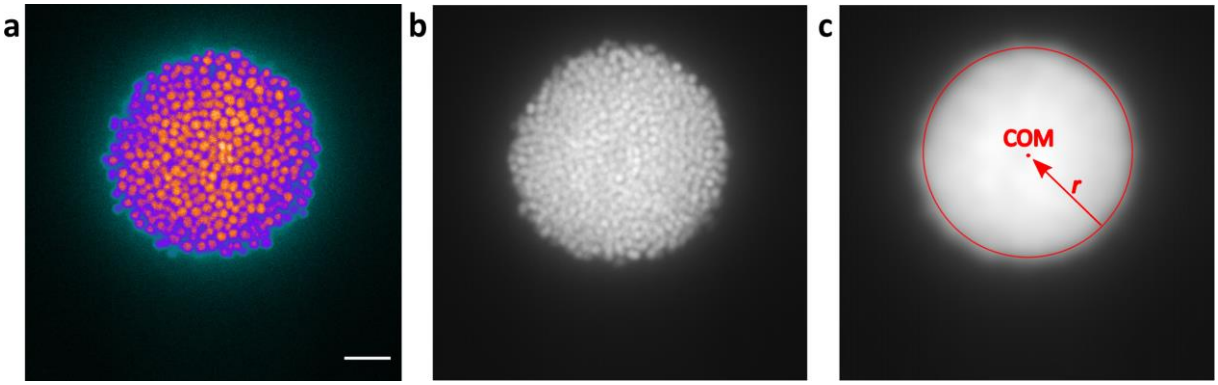

Figure 2.1: Principle of the colony detection process.

Images from 3D confocal data sets **(a)** are imported into Matlab. Afterwards, all images are averaged into a single image **(b)**, which is subsequently blurred with a 10 µm kernel gaussian filter. The blurred image **(c)** is then used to detect the contour of the colony (red highlight) with the *imfindcircles* function and a range of 100-300 pixels. Detection of the contour allows the extraction of the center of mass (COM) and the colony radius *r*. Scale bar: 5 µm.

Detection of radial fluorescence intensities of Cy3-DNA

Detection of Cy3-DNA fluorescence intensities was performed by, first, normalizing the intensities of the raw data. For this purpose, we scaled the pixel values of each image according to the absorbances we measured for different Cy3-DNA samples (see Table 2.6), resulting in intensity equalized image stacks. The scaled stack is subsequently averaged to create a single averaged image (Fig. 2.2a). This average is saved, as it is also the basis for Cy3-DNA foci detection (see below).

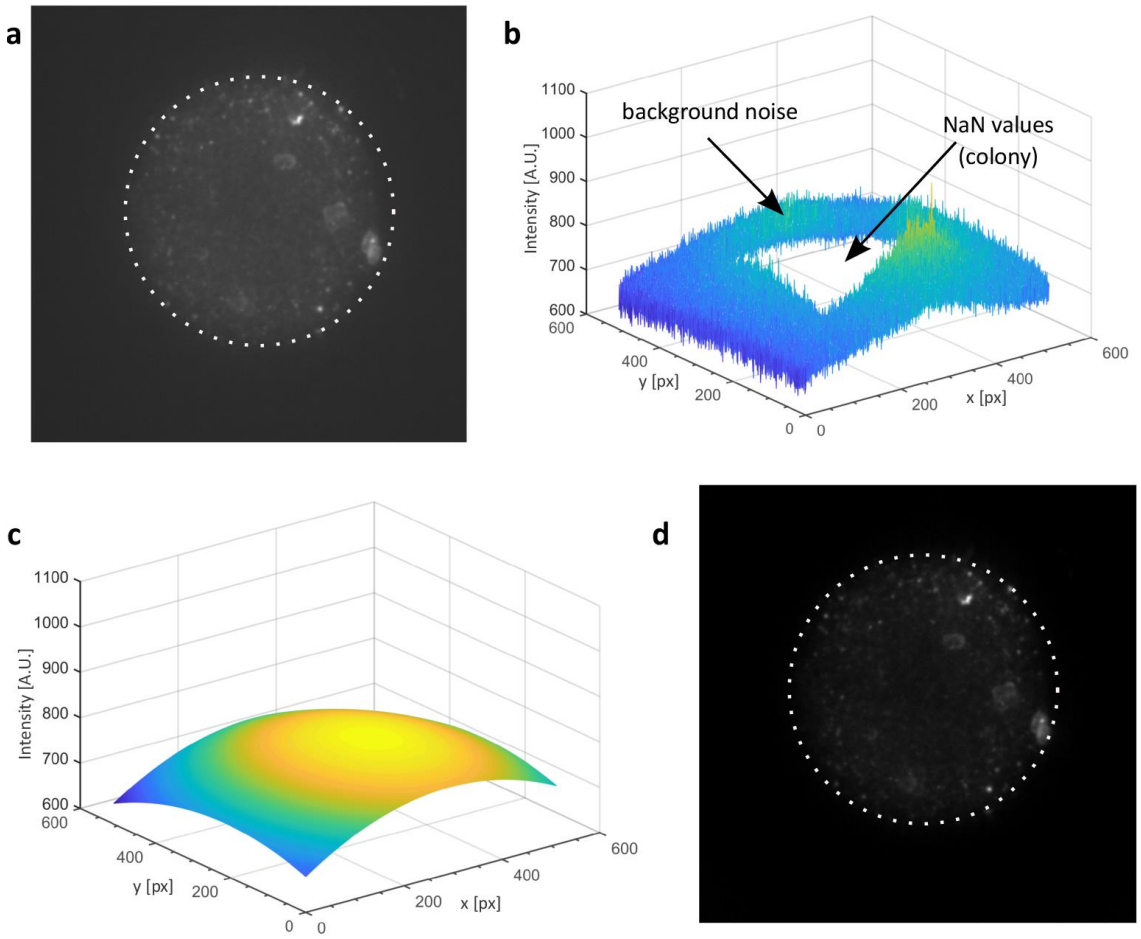

Figure 2.2: Basic principle of fluorescence intensity detection and background removal in colonies.
In order to detect fluorescence intensities of Cy3-labelled DNA we, first, equalized the intensities of all images in the data set according to the absorbance we measured for each DNA sample. Next, we averaged all images in the data set into a single image **(a)**. From this average we remove all pixels denoting positions of the colony, retaining only background fluorescence intensities **(b)**. By fitting a second degree 2D polynomial to these intensities, we obtain a background intensity map **(c)**, which is subsequently removed from the data average (a) to obtain the final image. The image is now devoid of any shot noise while retaining Cy3 fluorescence intensities within the colony **(d)**. Detailed descriptions of the proceeding are found in the main text. White dotted lines in (a) and (d) indicate the colony contour.

Next, we performed a background subtraction by, first, removing the intensity of the regions beyond the colony from the image. We then obtain the background intensities by fitting a second degree 2D polynomial $p_0 + p_{10}x + p_{01}y + p_{11}xy + p_{20}x^2 + p_{02}y^2$ with coefficients p_{ij} to an image where the colony has been removed by setting the corresponding values to NaN (Fig. 2.3b) and subsequently subtract the obtained intensity map (Fig. 2.3c) from the average image. The final fluorescence intensity values (Fig. 2.3d) are subsequently distributed in radial bins to obtain radial fluorescence intensities and intensity profiles within gonococcal colonies with respect to their distance to the colony contour.

Detection of Cy3-DNA foci and foci densities

As mentioned earlier, detection of fluorescence foci, or spots, was performed on the saved averaged image of the 3D data set (Fig. 2.3a). From this average, we create a median-smoothed duplicate using the *immedfilt2* Matlab function with a 20 x 20 pixel smoothing window (Fig. 2.3b). The median-smoothed copy is subsequently subtracted from the initial average image. Doing so, eliminates any background noise and leaves only the intensity peaks of DNA foci (Fig. 2.3c). The detection of these peaks is performed with the *pkfnd* and *cntrd* functions of the IDL-tracking suite (from The Matlab Particle Tracking Code Repository by Daniel Blair & Eric Dufresne), for which we chose a blob diameter of 11 pixel and an intensity threshold of 200 (in A.U.). The threshold was chosen as the Gauss radius of the noise intensity distribution extracted from the histogram of the intensity in the image. The obtained peak i.e., foci positions (Fig. 2.3d) are subsequently distributed in radial bins to obtain the DNA foci density with respect to the distance to the colony contour.

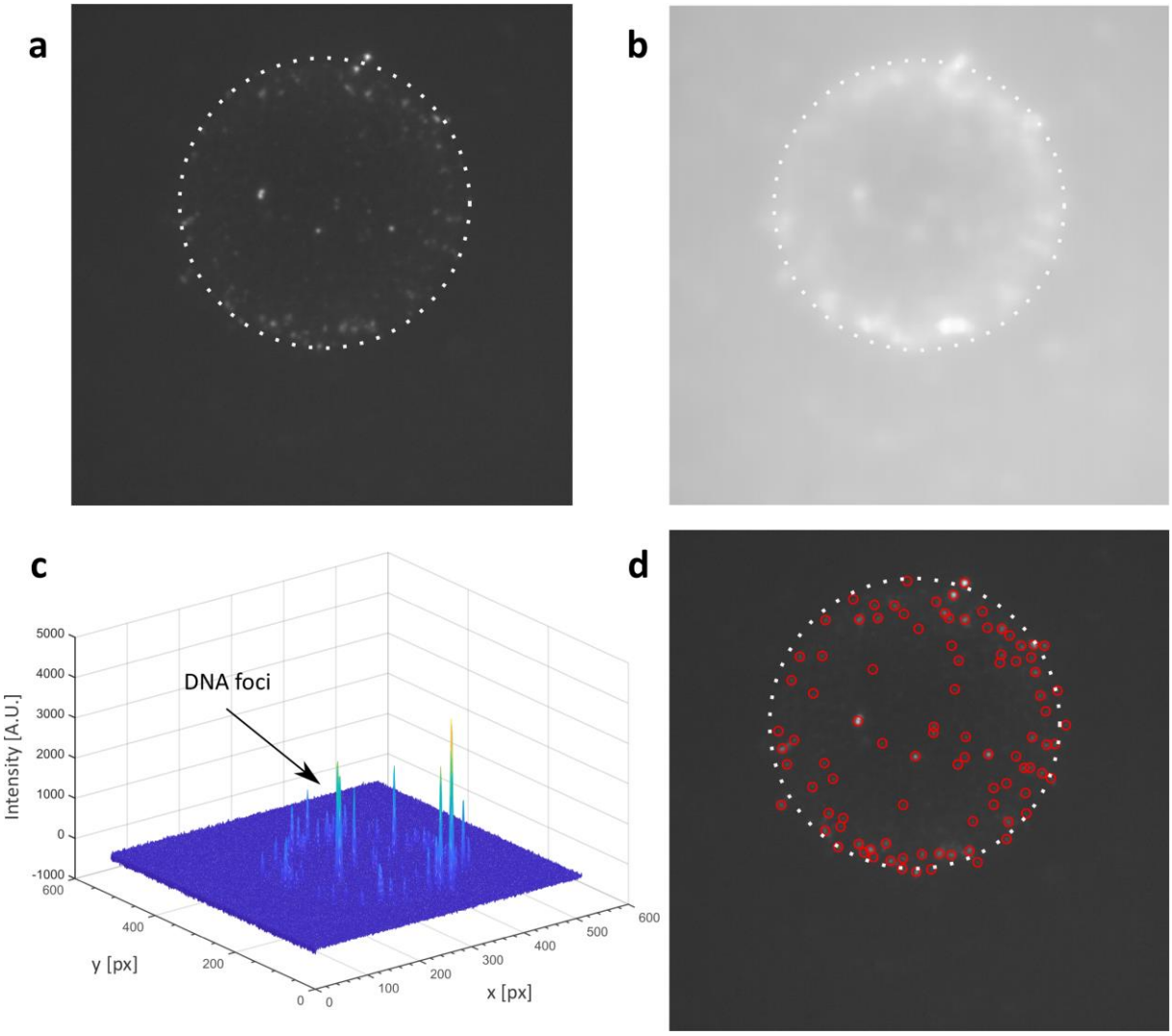

Figure 2.3: Basic principle of fluorescence foci detection for Cy3-DNA in colonies.

From the normalized, averaged image of the 3D data set **(a)** we create a median-smoothed duplicate **(b)**, which is subsequently subtracted from the average image, thereby removing any background flouresence while retaining flourescence intesity peaks, or foci, formed by Cy3-DNA **(c)**. These are subsequently detected using the IDL-tracking suite in Matlab **(d)**, and their positions are subsequently distributed in radial bins in a distance from the colony edge to obtain the DNA foci density in the colony. Detailed descriptions of the proceeding are found in the main text.

2.6. SytoX - dead stain

We observed that a small fraction of cells showed a strong accumulation of Cy3-labelled DNA at the cell periphery (see Fig. 3.5). We wondered whether this accumulation was caused by cell death, resulting in Cy3-DNA penetrating the outer cell envelope. To test this hypothesis, we performed Live/dead stainings with the green dead stain SytoX, which were performed to the following protocol:

Cells of strain *ΔG4* (NG150), grown overnight on agar plates, were harvested, and resuspended in GC medium supplemented with 1 % IsoVitalex and 7 mM $MgCl_2$. The optical density (OD_{600}) of the cell suspension was adjusted to 0.1 and 300 µl were given into a well of a poly-L-lysine coated "µ-Slide 8 Well" plate (Cat.No. 80824, Ibidi) together with 0.2 µM of SytoX (Invitrogen). The SytoX working solution was prepared by mixing the dye with an appropriate amount of GC-medium. Subsequently, the well plate was incubated for one hour at 37 °C before 1 µg of Cy3-labelled 300 bp fragments (see sections 2.5.1 & 2.5.2), mixed in a total volume of 30 µl GC-medium, were added into the well plate. The 300 bp fragments had a single DNA uptake sequence (DUS^+).

After an additional hour of incubation at 37 °C, imaging was performed with a Ti-E inverted microscope (Nikon) equipped with a CSU-X1 (Yokogawa) spinning disk unit and a 100x CFI Apo Tirf objective (Nikon). Image acquisition was done with an EMCCD camera (iXon 897, Andor). Fluorophores were excited with lasers with a wavelength of 561 nm (Cy3-DNA) and 488 nm lasers (SytoX), set to 50 % and 1.5 % respectively. In addition, we acquired a brightfield image of the colony. Exposure times were set to 50 ms.

2.7. Determining the dynamics of ComE foci formation in gonococcal colonies

We investigated the spatio-temporal dynamics of DNA uptake in microcolonies of *N. gonorrhoeae*. To this end, we visualized the formation of ComE foci in gonococcal colonies by means of confocal microscopy. Subsequently, we extracted the radial ComE foci densities within colonies with proprietary Matlab (MathWorks) image processing pipelines; thereby identifying single DNA uptake events within early bacterial biofilms.

2.7.1. Confocal imaging of ComE foci within gonococcal colonies

Cells of strain *comE-mcherry** (NG195) were grown on GC-agar plates overnight. Cells were harvested and resuspended in GC medium supplemented with 1 % IsoVitalex and 7 mM $MgCl_2$. The optical density (OD_{600}) of the cell suspension was adjusted to 0.1 in a volume of 500 µl. Depending on the sample we, subsequently, added either 10 Units of DNaseI (New England Biolabs) or 1.5 µg of genomic DNA derived from *N. gonorrhoeae* strain *ΔG4* (NG150) to the suspension, while an equal amount of medium was added for untreated (control) samples. The mix was shaken for 30 minutes in a 37 °C incubator before 200 µl were added into a poly-L-lysine coated "µ-Slide 8 Well" plate (Cat.No. 80824, Ibidi). Imaging of colonies was started as soon as possible.

Colonies were imaged with a Ti-E inverted microscope (Nikon) equipped with a CSU-X1 (Yokogawa) spinning disk unit and a 100x CFI Apo Tirf objective (Nikon). Image acquisition was done with an EMCCD camera (iXon 897, Andor). Colonies were imaged after 0, 1 and 2 hours. For every colony imaged, a stack of 27 images, with a z-spacing of 0.2 µm was acquired at the equatorial, lateral plane of the colony, resulting in a 3D data set resembling a total height of 5 µm within colonies. Fluorophores were excited with 488 nm (GFP, denoting cell and colony positions) and 561 nm lasers (ComE-mCherry), set to 5 % and 15 % power, respectively. The exposure time was adjusted to 50 ms.

2.7.2. Detection of ComE foci and data analysis

Data analysis was performed with the same Matlab routines we used for the detection of Cy3-DNA foci (see section 2.5.3). However, we adjusted the intensity threshold for spot detection to account for different fluorescence intensities of ComE-mCherry compared to Cy3-DNA. Moreover, we had to set a separate threshold value for each time point individually, as we found that the intensity of ComE-mCherry decreased over the course of the experiment due to some form of bleaching (see Fig. S13). We deemed this the simplest way of ensuring proper detection of ComE foci across all time points.

2.8. Photo activatable localization microscopy (PALM) of ComE molecules

We investigated DNA uptake with a resolution beyond the diffraction limit. To this end, we prepared a strain that expresses the DNA-binding protein ComE as a fusion with photoactivable-mCherry (PAmCherry), which allowed us to visualize the formation of individual ComE foci, or DNA uptake events, with photoactivable localization microscopy, or PALM. All procedures to acquire PALM images of ComE foci are described in the following sections.

2.8.1. Sample preparation

Cells of strain *comE-PAmcherry* (NG069) were grown on GC-agar plates overnight, harvested and resuspended in GC-medium supplemented with 1 % IsoVitalex and 7 mM $MgCl_2$. The optical density (OD_{600}) was adjusted to 0.1 and 500 µl of the suspension were incubated for 3 hours at 37 °C, shaking at 250 rpm. For samples lacking DNA, we supplemented 10 U of DNaseI (New England Biolabs) prior to incubation. For DNA-samples we added 850 ng of vector DNA (*pIGA*-vector) after two hours and continued incubating for the remaining hour. Afterwards, samples were centrifuged for 5 minutes at 5000 x g to pellet the cells. The medium was carefully discarded, and cells were resolved in 1x PBS before cells were transferred onto a coverslip (High Precision No. 1.5H, Marienfeld). Finally, a microscopy slide was placed on top of the coverslip and the sample was sealed using Valepp (Vaseline, wool fat and paraplast in a ratio of 1:1:1).

2.8.2. Image acquisition and data analysis

Super resolution imaging was done on a Ti-E inverted microscope (Nikon) equipped with a N-STORM unit, a LUA4 laser unit, a 100x CFI Apo Tirf objective (all obtained from Nikon) and an EMCCD camera (iXon 897, Andor). Imaging was done in "EM Gain 10 MHz 14-bit" readout mode with EM Gain multiplier set to 300 and conversion gain at 5.1, with the TIRF angle adjusted to 2815. For imaging, the 561 nm laser was operated at maximum intensity (100 %), while the 405 nm activation laser was set to 0.5 % power; both at 50 ms exposure time and operated in continuous mode. To reduce unspecific blinking and autofluorescence in the final recording, we prebleached the sample area by solely activating the 561 nm laser for a couple of seconds before, eventually, activating the molecules (i.e., 405 nm laser). We recorded movies of 5000 images each. While recording, we gradually increased the power of the activation laser to ensure proper activation of all molecules. Finally, the obtained raw data was analyzed, and super resolution images were created, using the Nikon NIS Ar Imaging Software (Ver. 4.13.05, Build 933).

2.9. Analysis of the dynamics of transformation within gonococcal colonies

In this thesis we investigated the dynamics of transformation in colonies formed by *N. gonorrhoeae* with spatial and temporal resolution. Utilizing a suitable reporter strain, we designed an experimental approach that allowed us to visualize and detect individual transformation events within gonococcal colonies. All required steps to replicate the experimental approach are described in the following sections. In addition, we visualized gene transfer events between two bacterial strains in well mixed colonies. The proceedings for these experiments are included as well.

2.9.1. Preparation of transformable DNA samples

Genomic DNA of strain *wt** (NG194) was isolated according to section 2.3.1. 300 bp and 3 kb fragments were generated by PCR, with primer pairs NB090(2) and NB091 for 300 bp, and primers NB088 and NB089 for 3 kb fragments, respectively. In both cases the primers added a single DNA uptake sequence (DUS) to the fragment. After PCR, the fragments were purified with the "QIAquick PCR Purification Kit" (see section 2.3.5). To yield sufficient amounts of sample DNA, multiple reactions were pooled.

2.9.2. Confocal imaging of transformation events within gonococcal colonies

Strain *wt** *sfgfp*$_{nf}$ (NG233) was grown overnight on GC-agar plates and cells were scraped and resuspended in GC medium supplemented with 1 % IsoVitalex and 7 mM $MgCl_2$. The optical density (OD_{600}) of the cell suspension was adjusted to 0.1 and 500 µl were transferred to a fresh tube, which was subsequently incubated at 37 °C and 5 % CO_2 for 30 min under shaking conditions (250 rpm). Afterwards, 200 µl were given into one well of a poly-L-lysine coated "µ-Slide 8 Well" plate (Cat.No. 80824, Ibidi). Subsequently, the well plate was incubated for another 30 minutes. 1.5 µg of the chosen DNA sample (see section 2.9.1) was mixed with GC-medium so that a final volume of 100 µl was reached. The DNA-medium mix was subsequently warmed to 37 °C and added to the colonies in the well plate, once the 30-minute incubation period was over. Afterwards, imaging of colonies was started as soon as possible.

Transformation events within gonococcal colonies were visualized with a Ti-E inverted microscope (Nikon) equipped with a CSU-X1 (Yokogawa) spinning disk unit and a 100x CFI Apo Tirf objective (Nikon) in multipoint recordings. Four areas in the well plate were chosen and imaged every 15 minutes for a total time interval of 4 hours. Tiling of 5x5 images was used

to expand the recorded area within the well plate. This was done to increase the sampling size of each recording, i.e., to image more colonies simultaneously. During each imaging step, a brightfield image and a 5 µm z-stack, comprising of 27 images with a z-spacing of 0.2 µm, were acquired. The stack was acquired with a 488 nm laser set to 5 % and 50 ms exposure time and was recorded approx. 10µm above the bottom of the well, so that we obtain a 3D data set spanning the equatorial, lateral plane of colonies.

2.9.3. Image and data analysis

In order to uncover the spatio-temporal dynamics of transformation in gonococcal colonies we needed to detect single transformant cells with respect to their position within the colony, i.e., the distance to the colony contour. Thus, we had to detect both single, fluorescent cells, as well as the position of the colony in each recording. This was done with proprietary Matlab (MathWorks) scripts developed together with Dr. Marc Hennes. The principles of the data analysis are outlined below.

Colony detection

Detection of transformation events within gonococcal colonies was performed according to the following steps. First, we extracted colony radii (*r*) and center of mass (COM) from the brightfield images. We removed salt and pepper noise by smoothing the images with a gaussian blur filter with a sigma radius of 2. Next, we utilized high local intensity variance in a window of 15 x 15 pixels as the basis for colony detection, with high variation of dark and bright pixels for colonies and small variance for pixels outside of colonies, resulting in a binary representation of the brightfield image [Oldewurtel *et al.*, 2015]. From the histogram of this binary image, we define a threshold so that the noise distribution in the image is ignored. The image is then processed by binary dilations and erosions to ensure connected segments for each colony. Using the Matlab function *regionprops* we extract centroids (x- and y-positions) and the area for all colonies. This information is subsequently used to determine the extent of each colony (*r*). The height (z-position) of the colony COM was calculated by multiplying *r* with a factor of 0.85, which we obtained from previous measurements [Welker *et al.*, 2021].

Detection of transformant cells

Single transformants were detected by thresholding, for which we defined 7x the standard deviation of the image intensity as the threshold value. Similar to the detection of colonies in the brightfield image (see above), we again used the Matlab function *regionprops* to obtain x-, y- and z-positions for each transformed cell, or fluorescent spot. As a consequence, we detect single transformants across multiple z-plains, thus vastly overestimating the transformants in colonies. To account for this problem, we combined all spots within a range of 2.4 µm in z-direction into a single spot. We found this procedure to be an appropriate solution to obtain the true number of transformants in z. Similarly, we combined spots if they are within a range of 4 µm in x- and y-orientation to account for multiple transformants in close proximity to one another. This was done as to avoid detecting cell division events as opposed to transformation events.

To link detected transformants to their respective colony we calculate the distance to all colony COMs in the brightfield image in x and y and pick the colony for which this distance is smallest. From here, we calculate the transformant density by dividing the number of spots in a certain spherical shell of the colony by the area of this shell. In addition, we save the total number of transformant cells, as well as the number of colonies in which we detected at least a single transformation event, such that we can calculate the average fraction of transformants per colony for different times.

2.9.4. Visualization of gene transfer in mixed gonococcal colonies

The assay for the detection of gene-transfer events in mixed colonies relied on a flow chamber setup (Fig. 2.4) which allowed us to grow and image bacterial colonies for many hours. The setup consisted out of a commercially available growth chamber (Ibidi, µ-Slide I Luer, ibiTreat #1.5 polymer, channel height of 0.8 mm), a custom-made bubble trap to reduce the likelihood of air bubbles interfering with colony growth, and some silicon tubing. Prior to the experiment, the flow chamber was poly-L-lysine coated by adding a sterile mix of ddH_2O and poly-L-lysine (Sigma Aldrich, conc.: 0.01%) in a 1:1 ratio into the channel of the chamber. To ensure proper coating, the chamber was incubated overnight at room temperature. To reduce the likelihood of contaminations, the coating step was done in a laminar flow hood.

The bubble trap was assembled by cutting both a 1.5 ml reaction tube and a plastic syringe (B. Braun Injekt® Luer Solo, 5 ml) in half. The upper part of the reaction tube was incised into the lower part of the syringe. Also, an opening was made to fit in the silicon tubing. Finally, all

components were fixed with epoxy glue (Yachtcare Epoxy Fix Mix). The outlet of the system was created with a silicon tube and an Elbow luer connector (Ibidi). Bubble traps and outlet tubing were autoclaved before usage. For inoculation of the system, cell suspensions were transferred into syringes and subsequently injected through the outlet tube. The puncture site was sealed with silicon glue (Scrintec RTV-1 Silicone Rubber) to prevent leakage of the system. Finally, the outlet tube was connected to a peristaltic pump to apply a continuous flow of fresh medium through the channel.

The experimental procedure itself was adapted from Nadzeya Kouzel [Kouzel *et al*., 2015]. The optical density (OD_{600}) of both the *wt** (NG194) and the *wt** *sfgfp*$_{nf}$ (NG233) were adjusted to 0.1 and subsequently mixed in a ratio of 1:1. For proper mixture of the two strains, 5 % of ddH_2O (sterile filtered) was added and the cell suspension was incubated shaking (250 rpm) at 37 °C for 15 minutes. 300 µl of the mix were subsequently used to inoculate the flow chamber as described earlier. The inoculated chamber was incubated at 37 °C for 1 hour to allow proper settling of the colonies to the coated surface. Finally, the flow of medium was started at a rate of 1 rpm.

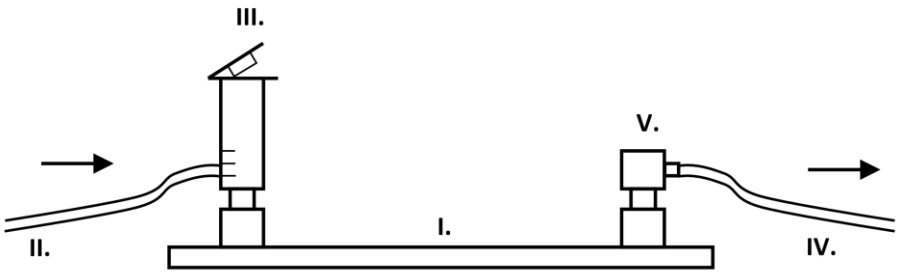

Figure 2.4: Schematic of the flow chamber setup used to detect single gene-transfer events.
The setup allows for the culturing of gonococcal colonies and biofilms over many hours under continuous flow of fresh medium. The center piece of the setup is a commercially available flow chamber **(I.)** in which colonies were grown. Prior to the experiment the chamber was coated with poly-L-lysine. Fresh medium was supplied over a silicon tube **(II.)** which was connected to a custom-made bubble trap **(III.)**. Another silicon tube **(IV.)** was connected to the outlet with a luer connector **(V.)**. The outlet tube was connected to a peristaltic pump (not shown) to generate continues flow through the channel of the chamber. Arrows indicate the direction of medium flow during the experiment.

After 24 hours of growth, colonies were fixated with paraformaldehyde (PFA). This was done to minimize cellular motility and, thus, to simplify cell detection during image processing. To this end, the channel was flushed with 4 % PFA, which was injected through the opened bubble trap. The inlet tube was pinched off and the flow was continued until the trap was emptied. Subsequently, colonies were incubated for 30 minutes before the flow chamber was transferred to a microscope for imaging.

Imaging of single, 24 hour-old colonies was performed with a Ti-E inverted microscope (Nikon) equipped with a CSU-X1 (Yokogawa) spinning disk unit and a 100x CFI Apo Tirf objective (Nikon). Image acquisition was done with an EMCCD camera (iXon 897, Andor). For each colony, we acquired a 10 µm z-stack with a 0.4 µm spacing between each slice of the stack. Since most colonies were quite large after 24 hours of growth, we used tiling of 3x3 images to increase the area we can cover during imaging. Fluorophores were excited with 488 nm (sfGFP-expressing cells) and 561 nm lasers (mCherry-expressing cells), set to 5 % and 100 % at 50 ms exposure time, respectively. In addition to the z-stack, we acquired a brightfield image for every recording.

2.10. Visualization of free eDNA in gonococcal colonies

In this study we visualized the release of free, extracellular DNA in colonies of *N. gonorrhoeae*. The purpose of these experiments was to characterize the accumulation and processing of DNA within early biofilms of *N. gonorrhoeae*; a process which eventually leads to the formation of a DNA network within gonococcal colonies. All steps performed during these experiments are outlined in the following sections.

2.10.1. Imaging of free, extracellular DNA within gonococcal colonies

The basis for the staining of free DNA within colonies is the nucleic acid dye YOYO-1-iodide (Invitrogen), which we found to be a useful dye to stain extracellular DNA due to its high affinity to nucleic acids and its cell-impermeability. We diluted the 1 mM Stock solution (in DMSO) to a 1 µM working solution in TE50 buffer (50 mM Tris-HCl, 50 mM NaCl, 1 mM EDTA, pH 7.5) [Schoen *et al.*, 2011]. For imaging, we prepared 100 µl of 1 nM YOYO-1 in TE50 buffer and added the mix into a poly-L-lysine coated "µ-Slide 8 Well" plate (Cat.No. 80824, Ibidi).

Depending on the experiment, cells of strain *ΔG4* (NG150), or *ΔcomP* (NG236), were grown on GC-agar plates overnight, scarped from the plates and suspended in GC-medium supplemented with 1% IsoVitalex and 7 mM $MgCl_2$, with the optical density (OD_{600}) adjusted to 0.1. 200 µl of the cell suspension were added to the 1 nM YOYO-1/buffer mix in the poly-L-lysine well plate, which was subsequently incubated for 15 minutes to allow colonies to form and to properly settle on the coated surface. Afterwards, imaging was started immediately. For all samples treated with DNase, we added 10 U of recombinant DNase I (New England Biolabs) to the growth medium before imaging.

Timeseries imaging of single colonies was performed with a Ti-E inverted microscope (Nikon) equipped with a CSU-X1 (Yokogawa) spinning disk unit, a 100x CFI Apo Tirf objective (Nikon) and an EMCCD camera (iXon 897, Andor). Recording and imaging of selected colonies was done in automated multi-point recordings, in which we specified 10 random colonies to be imaged every 30 minutes for a total time interval of 4 hours. For each round of imaging, we recorded a 10 µm z-stack, starting at the bottom of the colony or well plate, with a z-spacing of 0.2 µm per slice. YOYO-1 was excited with a 488 nm laser set to 5 % power at 50 ms exposure time. Furthermore, we used 2x2 tiling to increase the total imaging-area. In addition to the 3D data set, we also acquired a brightfield image for every colony.

3. Results

In this thesis, we investigated the biological role and significance of extracellular DNA (eDNA) in the context of multicellular aggregates of the gram-negative bacterium *Neisseria gonorrhoeae*. DNA is key to the formation and development of bacterial biofilms and is now widely accepted as a critical component of cellular aggregates [Whitchurch *et al*., 2002; Seviour *et al*., 2021]. Biofilm-associated populations produce more DNA compared to their planktonic counterparts, and it has been suggested that the presence of DNA triggers natural competence and enhanced exchange of genetic material during biofilm growth [Molin & Tolker-Nielsen, 2003; Liao *et al*., 2014; Kim *et al*., 2018]. DNA's role in biofilm development is multifaceted and affects structure, architecture, and stability [Panlilio & Rice, 2021]. However, many processes regarding DNA's role in biofilm development still remain unknown. For instance, it is not known how mobile DNA is within bacterial biofilms. Given DNA's multitude of important functions in biofilms, it is critical to assess the mobility of DNA molecules to fully understand DNA's role during the development of multicellular aggregates.

This chapter is divided into four sections, each focusing on a different subset of experiments and findings. In the first section we will focus on the mobility of external DNA within gonococcal colonies. We show that, the spatio-temporal dynamics of fluorescently labelled, external DNA penetrating gonococcal microcolonies depends on the length of the diffusing DNA. Moreover, we found that the dynamics are strongly affected by the presence of DNA uptake sequences (DUS), which are specific for genomic DNA of *Neisseria* species. In addition, there is also evidence that the thermonuclease Nuc controls the amount of eDNA within the colony and that cells embedded in colonies interact non-uniformly with DNA.

In the second section we will address the dynamics of DNA uptake events in gonococcal colonies with spatial and temporal resolution. We found that, in the presence of transformable DNA, uptake is more abundant in the outer periphery of gonococcal colonies. Interestingly, we also observed that removal of external DNA from the growth medium did not drastically reduce, let alone abrogate, DNA uptake in colonies, which could indicate that colony formation simultaneously triggers DNA uptake.

The third section will focus on the spatio-temporal dynamics of transformation. Here, we found that transformation is, again, affected by the size of the transforming DNA. Interestingly, we also found that DNA is almost exclusively transformed in the periphery of colonies, indicated by poor transformability of cells in the colony center. Furthermore, we found that

transformation is only efficient within a rather short interval during colony growth. In addition, we also investigated horizontal gene transfer in mixed colonies of two different gonococcal strains. Here, we found that direct exchange of genetic material between both strains was inefficient.

In the fourth and final section, we investigate free, external DNA which is released within gonococcal colonies. We found that eDNA forms filaments, which, in turn, assemble an intricate mesh, or lattice, of DNA that, eventually, cocoons the cell aggregate. We also found evidence that the DNA lattice affects the structural integrity of colonies, suggesting a stabilizing function of DNA in colonies and biofilms of *N. gonorrhoeae*.

3.1. Spatio-temporal dynamics of DNA in early gonococcal biofilms

Here, we characterize the spatio-temporal diffusion dynamics of extracellular DNA penetrating early gonococcal biofilms of *Neisseria gonorrhoeae*. Using DNA samples that are either specific for *Neisseria*, i.e., DNA bearing DNA uptake sequences (DUS^+), or DNA samples which are *Neisseria*-unspecific (DUS^-), we highlight that the dynamics of DNA within bacterial microcolonies are affected by size or length of the diffusing molecules. For DUS^+ DNA, we find altered diffusion dynamics compared to DUS^- DNA. More specifically, we find that gonococcal genomic DNA diffuses poorly in gonococcal colonies. Furthermore, we also address whether the DNA-degrading thermonuclease Nuc, which is putatively secreted into the extracellular space, does affect the dynamics of DNA diffusion in any shape or form. Finally, we will briefly highlight that cellular interaction with DNA is non-uniform in gonococcal colonies

3.1.1. Spatio-temporal diffusion dynamics of unspecific (DUS^-) DNA in gonococcal colonies

First, we characterized the spatio-temporal dynamics of DNA lacking the DNA uptake sequence (DUS^-) in gonococcal colonies. Colonies were grown for one hour in a poly-L-lysine coated well plate before fluorescently labeled Cy3-DNA fragments were added to the growth medium. Colony forming cells expressed *sfgfp* under the strong *pilE* promoter, which allowed to detect the colony contour in confocal imaging. Random colonies were imaged for a period of 2 hours and the radial fluorescence intensity profiles (Fig. 3.1 & Fig. S1) were determined computationally (see section 2.5.3).

We find that short, 300 bp DNA fragments caused only a small increase in fluorescence intensities compared to the background (Fig. 3.1a, d). For larger 3 kb fragments the increase is much more obvious (Fig. 3.1b, e). Here, intensities of Cy3-DNA increased as a function of time but saturate after 1.5 hours. Initially, we observe a decline towards the center of the colony, which suggests that penetration of the colonies is impaired (violet and dark blue; 0.5 and 1 hour, respectively). However, after 1 hour the profile becomes flat, which indicates heterogeneous distribution of DNA across the entire colony.

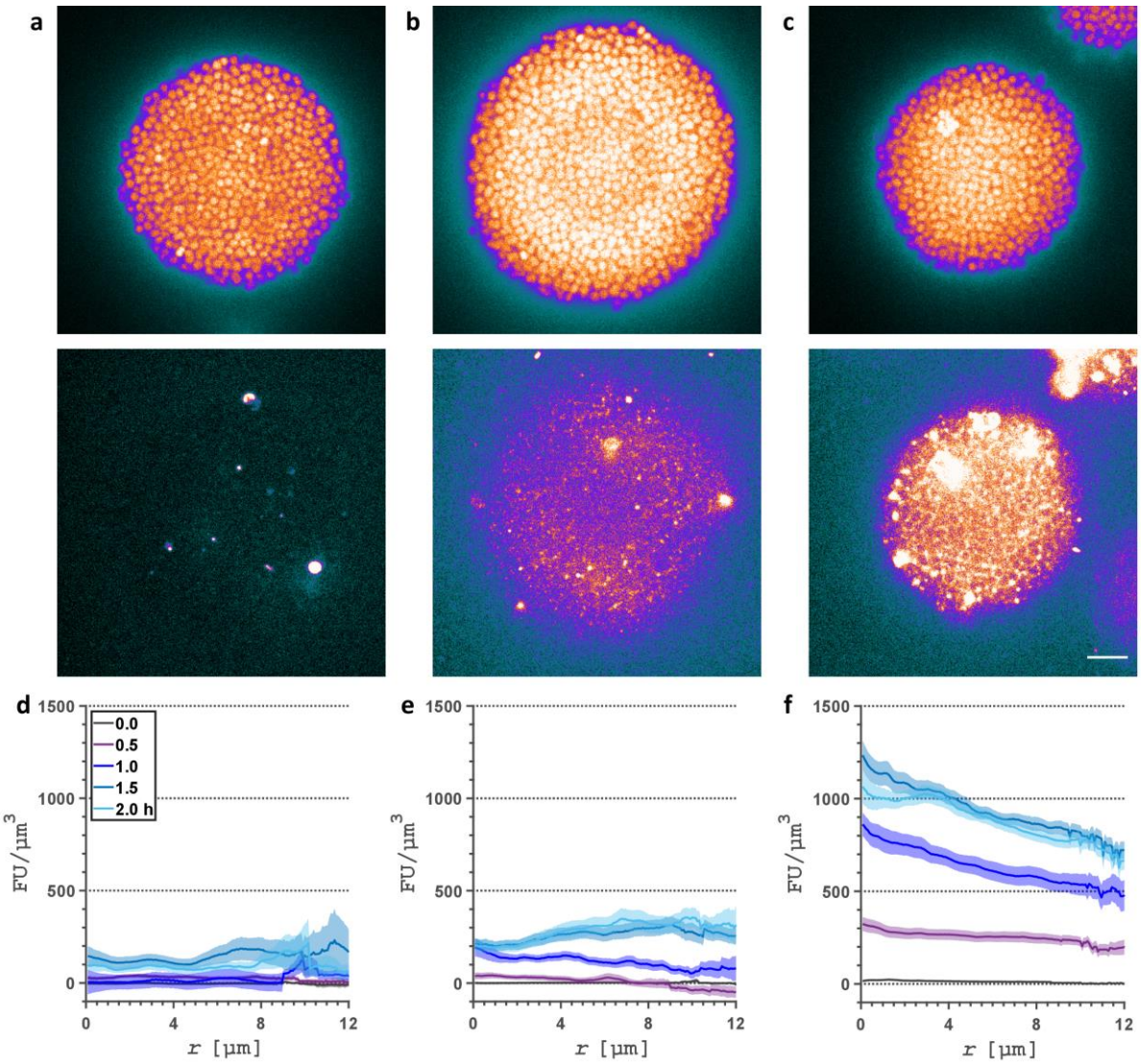

Figure 3.1: Spatio-temporal dynamics of Cy3-labelled DUS⁻ DNA in gonococcal colonies.
Exemplary confocal slices of colonies formed by strain *wt** (NG194) imaged 2 hours after addition of Cy3-DNA lacking DUS **(a-c)**. Upper row: Colony and cell positions as denoted by sfGFP expression. Lower row: Cy3-DNA. **(a)** 300 bp fragments, **(b)** 3 kb fragments, **(c)** gDNA of *E. coli*. **(d-f)** Mean radial fluorescence intensities (FU, in arbitrary units) of Cy3-DNA as a function of the distance (*r*) to the colony contour. **(d)** 300 bp fragments, **(e)** 3 kb fragments, **(f)** gDNA of *E. coli*. Shaded areas represent standard errors of 26 - 38 colonies. Scale bar: 5 µm.

Furthermore, we investigated the dynamics of genomic DNA (gDNA) from a genetically distinct species. Interestingly, we find that DNA of *E. coli* accumulates strongly in gonococcal colonies, as indicated by overall much higher intensities compared to 300 bp and 3 kb fragments (Fig. 3.1c). Fluorescence intensities increase gradually over the first 1.5 hours but saturate during the final stages of the experiment (Fig. 3.1f). The profiles show a strong decline from the colony contour towards inner layers of the colony, suggesting that DNA does not distribute homogenously in the colony. Still, a fraction of DNA molecules can penetrate the colony rather

freely and reach the colony core. It should be noted though, that the *E. coli* genome contains few DUS sequences which could, potentially, affect the dynamics we present here due to DNA-binding. Performing a basic sequence screening, we identified twelve truncated 10 bp DUS, but no 12 bp DUS in the genome of *E. coli*.

In conclusion, we find that DNA with no or few DUS can penetrate gonococcal colonies efficiently. However, the penetration dynamics depends on the length of DNA; with increasing length, colonies incorporate an increasing amount of DNA.

3.1.2. Diffusion dynamics of DNA are affected by DNA uptake sequences (DUS)

The DUS is known to strongly enhance DNA-binding and uptake dynamics of gonococci (Elkins *et al*., 1991). We, therefore, hypothesized that the presence of DUS affects the diffusion and penetration dynamics of DNA fragments within gonococcal colonies. Hence, we repeated the experiment explained in the previous section with DNA molecules bearing one or more DUS (Fig. 3.2 & Fig. S2).

When adding 300 bp fragments, bearing a single DUS (DUS^+), we find that they accumulate more strongly within gonococcal colonies compared to fragments lacking the DUS (Fig. 3.2a, d). The intensity profiles are flat throughout the 2-hour experiment, indicating homogenous spatial distribution of DNA across colonies. In addition, we find that fluorescence intensities increase as a function of time, and fluorescence is, overall, much higher compared to DUS^- 300 bp fragments (see Fig. 3.1d). Combined, this indicates that short fragments efficiently penetrate gonococcal colonies.

Similarly, the DUS enhances the fluorescence intensity caused by penetration of 3 kb fragments (Fig. 3.2b, e). Fluorescence intensities are increased compared to DUS^- fragments as well (see Fig. 3.1e). Initially, profiles show a decline towards the colony center, indicating hindered penetration. After 1 hour (dark blue) the profile becomes flat, suggesting homogenous distribution of DNA within the colony.

Addition of genomic DNA of *N. gonorrhoeae* to the growth medium revealed a markedly different intensity profile compared to shorter DNA fragments. Gonococcal gDNA is almost completely retained at the outer periphery of the colony (Fig. 3.2c). Fluorescence intensities (Fig. 3.2f) increase as a function of time and saturate after 1.5 to 2 hours; however, even after 2 hours there is little Cy3-fluorescence, i.e., DNA, detectable within the inner layers of the colony. Thus, penetration of homospecific genomic DNA is highly retarded and strictly limited to the outer layers of the cell aggregate.

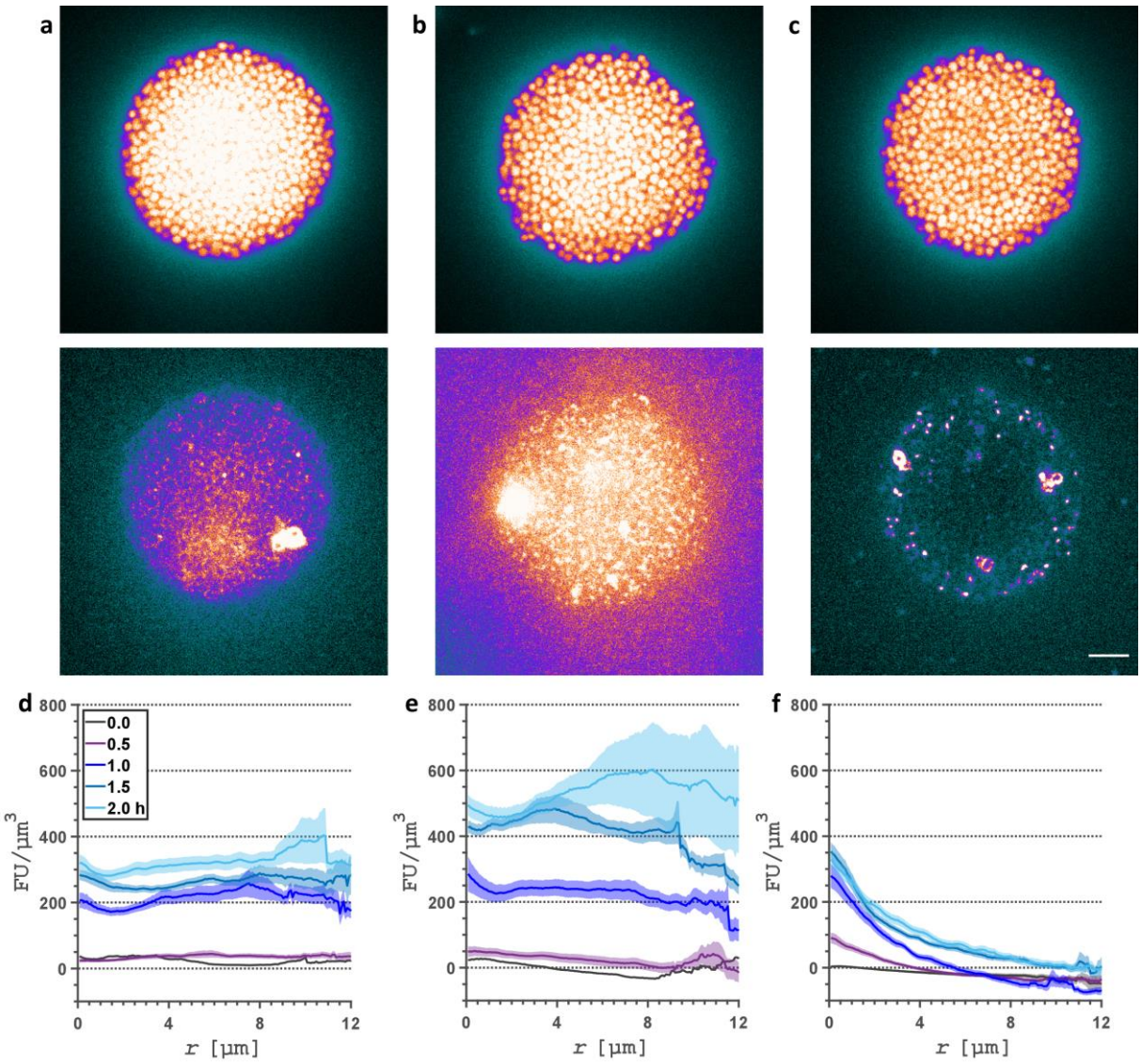

Figure 3.2: Spatio-temporal dynamics of Cy3-labelled DUS$^+$ DNA in gonococcal colonies.
Exemplary confocal slices of colonies formed by strain *wt** (NG194) imaged 2 hours after addition of Cy3-DNA bearing DUS **(a-c)**. Upper row: Colony and cell positions as denoted by sfGFP expression. Lower row: Cy3-DNA. **(a)** 300 bp fragments, **(b)** 3 kb fragments, **(c)** gDNA of *N. gonorrhoeae*. **(d-f)** Mean radial fluorescence intensities (FU, in arbitrary units) of Cy3-DNA as a function of the distance (*r*) to the colony contour. **(d)** 300 bp fragments, **(e)** 3 kb fragments, **(f)** gDNA of *N. gonorrhoeae.* Shaded areas represent standard errors of 30 - 39 colonies. Scale bar: 5 µm.

We conclude that the presence of DUS strongly affects the spatio-temporal dynamics of DNA diffusing within gonococcal colonies. Penetration of short DNA is efficient and eventually leads to uniform retention of DNA across the colony, while genomic DNA derived from *N. gonorrhoeae* penetrates colonies poorly.

3.1.3. The thermonuclease Nuc degrades genomic DNA within gonococcal colonies

N. gonorrhoeae expresses the thermonuclease Nuc, which resides within the periplasm and is supposed to also be secreted into the extracellular space. The enzyme has been described as a DNA modulating component within gonococcal biofilms [Steichen *et al*., 2011; Juneau *et al*. 2015]. We hypothesized that Nuc, as a DNA-degrading enzyme, might affect the abundance and diffusion dynamics of DNA within gonococcal colonies. Hence, we repeated the experiment described in section 3.1.2 with a *nuc* deletion strain (*Δnuc*).

When comparing the fluorescence intensity profiles of the *wt** strain with the ones of *Δnuc* we find that gDNA is persistently more abundant in colonies formed by *Δnuc* compared to *wt** colonies (Fig. 3.3 & S3), indicating that Nuc actively degrades genus-specific gDNA within gonococcal colonies. This could, potentially, explain the restricted penetration of DNA we observed for genomic DNA in our previous experiments (see Fig. 3.2c, f).

By contrast, lack of *nuc* has only minor effects on the intensity profiles for 300 bp and 3 kb fragments (Fig. S4 & S5). However, determining the average fluorescence intensity of Cy3-DNA (per pixel) reveals that deletion of *nuc* decreases the global amount of 300 bp and 3 kb fragments in *Δnuc* colonies compared to *wt** colonies (Fig. 3.4). Interestingly, this finding implies that Nuc does not actively degrade shorter 300 bp and 3 kb fragments compared to gDNA. This observation was unexpected, as we assumed that deletion of a DNA degrading enzyme (Nuc) would lead to an increase in DNA levels independent of the nucleotide sample being used. However, the outcome suggests that Nuc, by some unknown mechanism, regulates the amount of DNA of various different sizes which penetrates or diffuses within colonies.

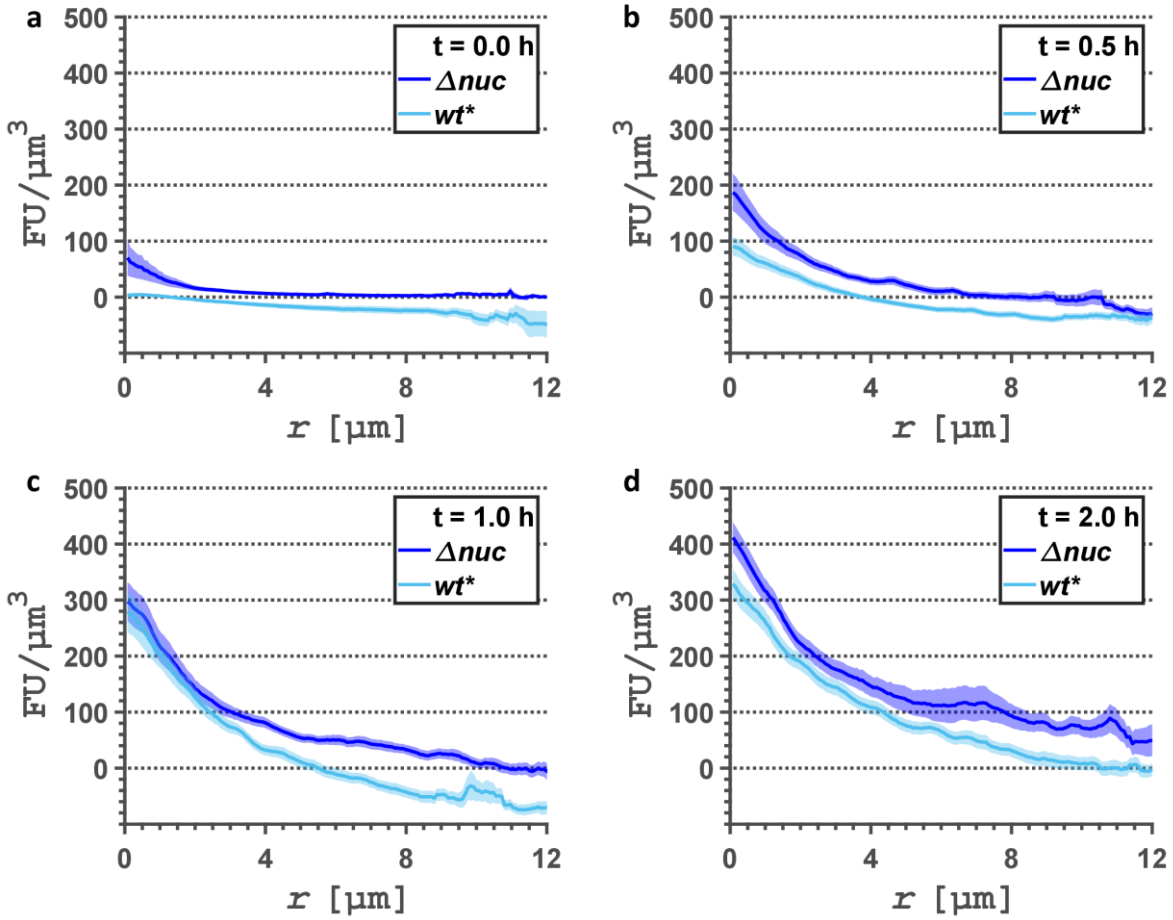

Figure 3.3: Colonies formed by strain *Δnuc* (NG235) retain a higher amount of genomic DNA.

Mean radial fluorescence intensities (FU, in arbitrary units) of DUS$^+$ Cy3-gDNA derived from *N. gonorrhoeae* as a function of the distance (*r*) to the colony contour immediately after addition to the medium **(a)**, and after 0.5 h **(b)**, 1 h **(c)** and 2 hours **(d)**, for colonies formed by wildtype (*wt**, NG194) and *nuc*-deletion strains (*Δnuc*, NG235). Shaded areas represent standard errors of 33 - 40 colonies.

While the reason behind this outcome is unclear, it could, nevertheless, provide a hint to Nuc's mode of action in modifying eDNA within gonococcal colonies and biofilms.

In summary, we find that Nuc degrades genomic DNA within gonococcal colonies, thus, contributing to the rather poor penetration dynamics we observed earlier. By contrast, our findings suggest that 3 kb and 300 bp fragments are not actively degraded by Nuc in *wt** colonies.

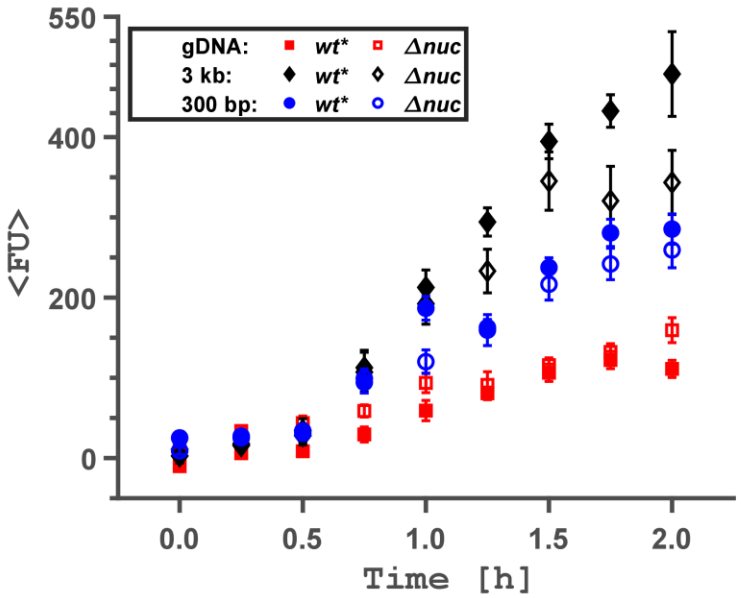

Figure 3.4: Nuc regulates the amount of various DNA fragments that penetrate gonococcal colonies.
Mean fluorescence intensities, averaged over an area of 80 x 80 nm (one pixel), of DUS^+ Cy3-DNA within gonococcal colonies formed by *Δnuc* (NG235) and *wt** (NG194) strains. Genomic DNA: red. 3 kb: black. 300 bp: blue. Error bars represent standard errors of 30 – 40 colonies.

3.1.4. Cellular interaction with DNA is non-uniform

While investigating the dynamics of fluorescently labelled DNA within gonococcal colonies (see Fig. 3.1 - 3.4), we found that the fluorescent signal of Cy3-DNA in colonies of *N. gonorrhoeae* is not homogenous. For example, we noted that Cy3-DNA forms spots, or fluorescence foci, within gonococcal colonies. They appeared with different lengths of DNA fragments and in the presence and absence of DNA uptake sequences; however, they appear most prominently with genomic DNA (see Fig. 3.2c). Formation of Cy3-fluorescence foci was already reported in a previous study, where they indicated DNA-uptake in single-cells of *N. gonorrhoeae* [Gangel *et al*., 2014]. In that study, focus formation was related to DNA uptake. In the current study, foci may represent either extracellular or intracellular DNA. If focus formation signaled DNA uptake, we expected that the spatial distribution of foci and total fluorescence intensity were different, in particular for unspecific DNA (DUS^-) which is not taken up by gonococci. Thus, we asked whether the distribution of foci reflected the distribution of fluorescence intensity within colonies. Using image analysis pipelines in Matlab described in section 2.5.3, we achieved to detect Cy3-foci reliably within gonococcal colonies. We found that the patterns of foci agreed qualitatively with the fluorescence intensity profiles shown in previous chapters (see Fig. S6 - S9).

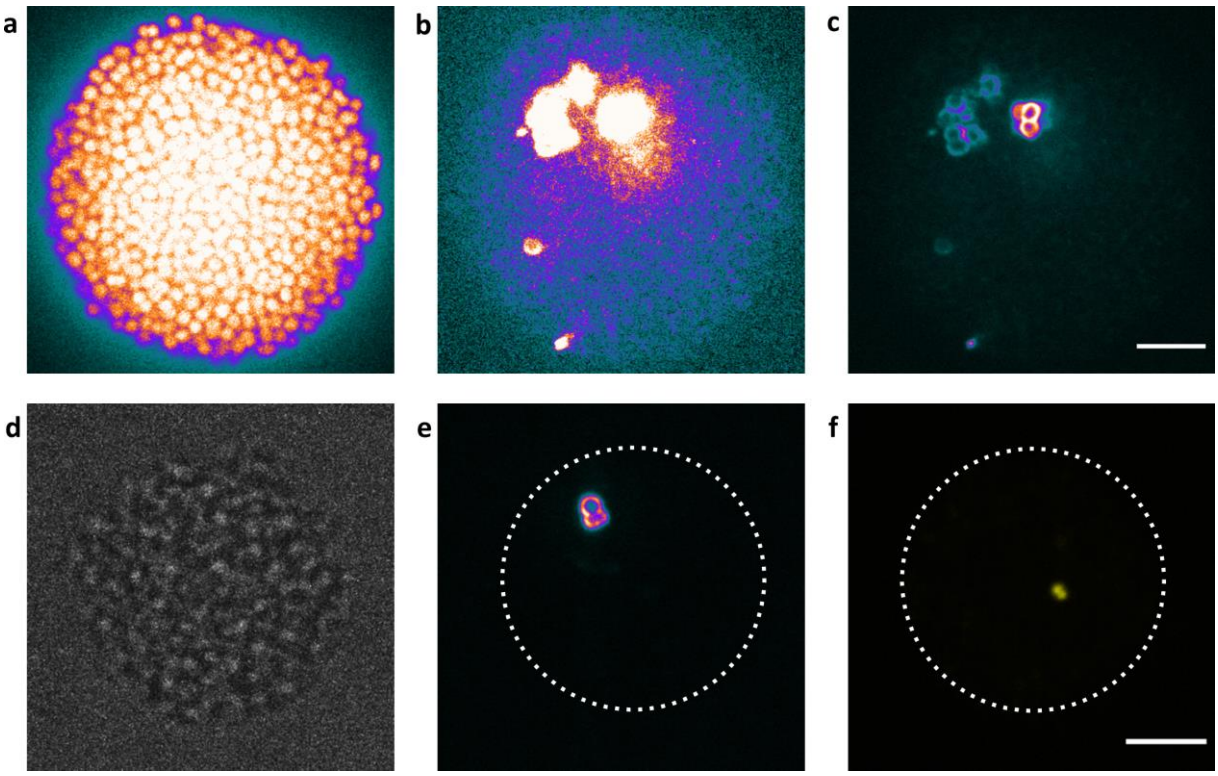

Figure 3.5: Interaction with Cy3-DNA is heterogenous in gonococcal colonies.

A small fraction of cells shows very strong accumulation of Cy3-DNA at the cell periphery. Upper row: Colony formed by strain *wt** (NG194), treated with DUS$^+$ 300 bp DNA fragments. **(a)** Colony and cell positions as denoted by sfGFP expression. **(b)** 300 bp Cy3-DNA with intensities adjusted as in Fig. 3.1 & Fig. 3.2. **(c)** Adjusting the intensity reveals staining of the cell envelope by Cy3-DNA. Lower row: Life/dead-staining with SytoX of a colony formed by strain *ΔG4* (NG150), treated with DUS$^+$ 300 bp fragments. The staining reveals that the effect is not caused by cell death; implying heterogenous interaction with DNA within colonies. **(d)** Brightfield image denoting colony and cell positions. **(e)** 300 bp Cy3-DNA. **(f)** SytoX signal. Scale bars: 5 µm.

More importantly, however, was the observation that, in some cases, a small fraction of cells within gonococcal colonies exhibits a much stronger fluorescence signal compared to the "average" signal within the colony (Fig. 3.5a, b). Adjustments to image contrast and brightness reveals that the signal is localized at the outer cell periphery, which is stained by Cy3-DNA (Fig. 3.5c). The occurrence of these bright cells was completely independent of DNA sample, presence of DNA uptake sequences, time or even bacterial strain used during experiments (*wt** and *Δnuc*).

We hypothesized that the random nature of the appearance could be caused by cell death. In this case, cell lysis would allow DNA to permeate the ruptured, outer cell envelope. To address this hypothesis, we performed a life/dead staining in the presence of 300 bp Cy3-DNA, utilizing SytoX to stain dead or lysed cells (Fig. 3.5d-f). However, we find no correlation, or overlap,

between the signals of Cy3-DNA and SytoX (Fig. 3.5f). Thus, the effect is not caused by cell death, suggesting a more specific reason for the strong accumulation of Cy3-DNA. This most likely implies, that interaction with DNA is heterogenous in gonococcal colonies, with some cells showing a strikingly stronger and DUS-independent interaction compared to others.

To conclude, we find that cellular interaction with Cy3-DNA is not uniform in gonococcal colonies. DNA forms fluorescence foci and a small fraction of cells in the colony interacts strongly with external Cy3-DNA. Both phenomena are independent of DNA sample length, the presence of DNA uptake sequences or time of exposure to DNA. The strong interacting cells capture Cy3-DNA at their outer periphery or cell envelope; however, this effect is not caused by cell death.

3.2. Dynamics of ComE foci formation and DNA uptake in *N. gonorrhoeae*

Recently, several studies have focused on DNA uptake and the molecular machinery that drives this process in *N. gonorrhoeae* [Gangel *et al*., 2014; Chang *et al*., 2016; Hepp & Maier, 2016]. Hence, we now have a rather complete and detailed picture on how DNA uptake is controlled and maintained on a molecular level. However, we lack detailed information on DNA uptake processes in cellular communities. Many studies have focused on horizontal gene transfer in bacterial biofilms, but to our knowledge few have actually addressed the preceding step of DNA uptake in cellular aggregates.

Here, we investigate the dynamics of DNA uptake and ComE foci formation in *N. gonorrhoeae*. The periplasmic, DNA-binding chaperone ComE has previously been identified as a reporter for DNA uptake events on a single cell level [Gangel *et al*., 2014]. The study highlighted that ComE colocalizes with transforming DNA within the periplasm of *N. gonorrhoeae* to form foci.

First, we investigate ComE focus formation using super resolution microscopy and confirm recent results obtained by fluorescence microscopy. We moved on to investigate ComE foci formation within gonococcal colonies. We find that foci are more abundant in the outer periphery of gonococcal aggregates in the presence of transformable eDNA. Furthermore, we highlight that removal of DNA from the growth medium of colonies results in less foci overall but does not abrogate their formation completely.

3.2.1. ComE forms periplasmic aggregates in the presence of transformable DNA

First, we visualized DNA uptake on a single-molecule level. To this end, we created a strain generating ComE as a fusion with photoactivatable mCherry (PAmCherry). This allowed the investigation of the DNA ratcheting chaperone by means of photoactivable localization microscopy, or PALM [Betzig *et al*., 2006]. The method is based on the stochastic activation of only a very sparse subset of fluorescent proteins at any given time, which can be achieved with brief laser pulses of a specific wavelength. Activated PAmCherry molecules fluoresce until they are irreversibly bleached, thus, repeated cycles of activation eventually inactivate the entire population of PAmCherry within the specimen [Subach *et al*., 2009]. This process is recorded and results in a series of images, in which individual molecules are represented as isolated fluorescent spots. Summing all images across time, results in a diffraction-limited image of all activated molecules; however, fitting an assumed Gaussian point spread function to each fluorescent spot in each individual image allows for precise localization of single

molecules within cells. Finally, a super resolution image is reconstructed from these localizations, in which single molecules are rendered as spots [Rust *et al*., 2006; Hess *et al*., 2006; Betzig *et al*., 2006]. In doing so, we were able to visualize DNA uptake events with a resolution beyond the diffraction limit (Fig. 3.6).

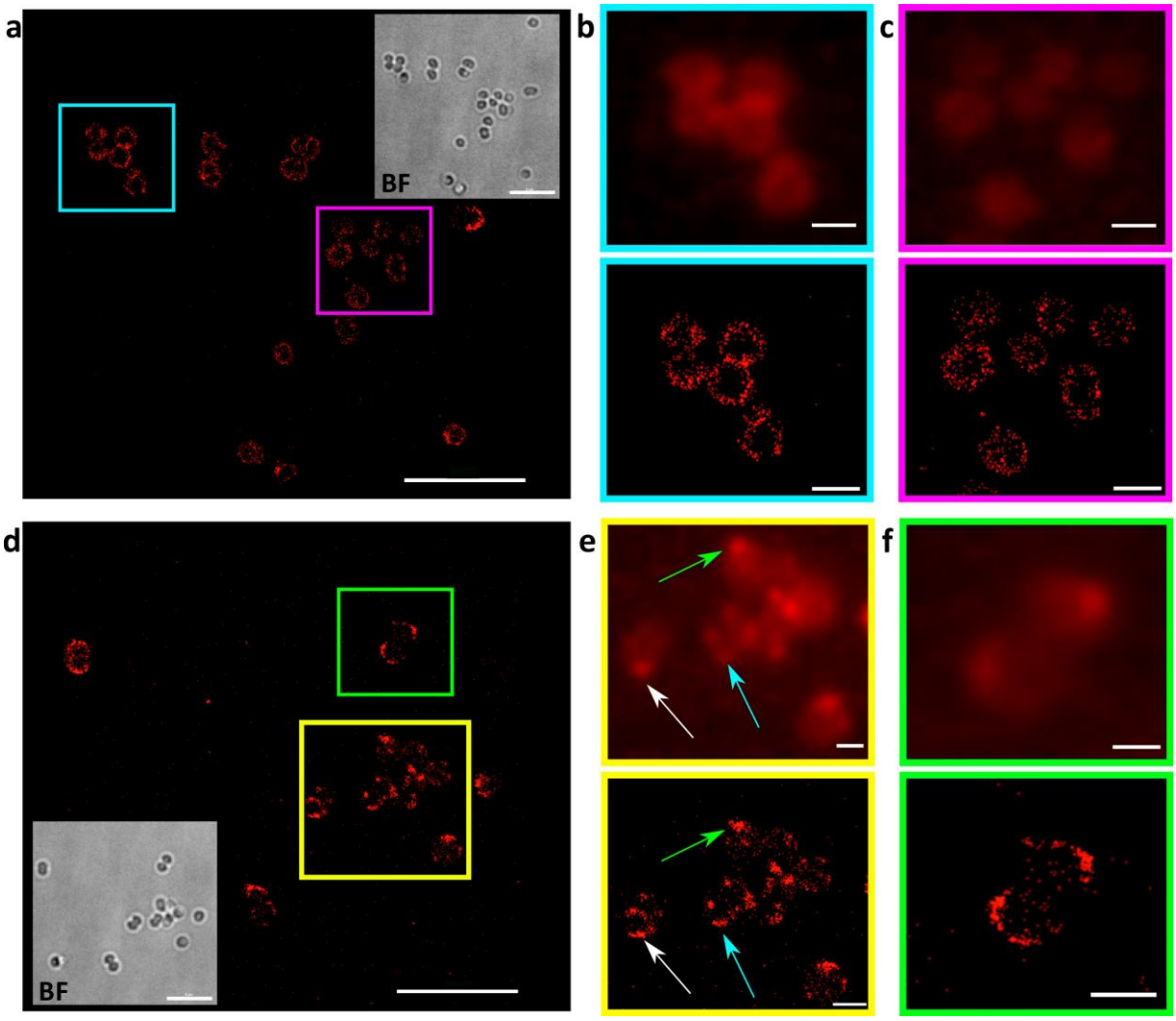

Figure 3.6: ComE aggregates in the presence of transformable DNA to form foci.
Photoactivatable localization microscopy (PALM) images of *N. gonorrhoeae* strain *comE-PAmcherry* (NG069). **(a)** Exemplary image of cells treated with DNase. In the absence of DNA ComE is homogeneously distributed within the periplasm **(b, c)**. Upper row: Diffraction limited images. Lower row: Localized single molecules. **(d)** Exemplary image of cells treated with DNA. In the presence of transformable DNA ComE forms aggregates and diffraction limited foci (colored arrows) within the periplasm **(e, f)**. Upper row: Diffraction limited images. Lower row: Localized single molecules. Scale bars in (a) and (d): 5 µm, else 1 µm.

When treating cells with DNase; thereby degrading transformable DNA in the growth medium, we find that ComE-PAmCherry molecules are homogenously distributed within the confines of the periplasm (Fig. 3.6b, c). Conversely, we find that ComE forms foci in the presence of transformable eDNA (upper row, Fig. 3.6e, f). Both observations are in good agreement with previous reports [Gangel *et al*., 2014]. Utilizing PALM, we find that ComE foci are, in fact, aggregates of many accumulated ComE molecules as denoted by the obtained super resolution images (lower row, Fig. 3.6e, f).

Based on our findings we conclude that ComE is an excellent reporter to detect DNA uptake in isolated *N. gonorrhoeae.* Single ComE molecules aggregate in the presence of eDNA to form foci. Given ComE's mode of action, each of these foci, essentially, represents a single DNA ratchet machinery [Hepp & Maier, 2016]. Hence, detection of ComE foci can be used to detect individual DNA uptake events in isolated gonococci.

3.2.2. Spatio-temporal dynamics of ComE foci formation in gonococcal colonies

Next, we set out to uncover the dynamics of DNA uptake in biofilms, by investigating ComE foci formation in colonies formed by *N. gonorrhoeae*. As mentioned in the previous section, ComE foci are indicators of single DNA uptake events in isolated bacteria (see section 3.2.1). In order to observe these uptake events in gonococcal microcolonies, we created a strain expressing one of the four gene copies of *comE* as a fusion to *mcherry*. In addition, we inserted *gfp* into the *igA*-locus, which enabled the localization of cell and colony positions within the cell aggregate. The resulting strain (*comE-mcherry**, see Table 2.4) could, thus, be utilized to observe ComE-mCherry foci formation in early gonococcal biofilms by means of confocal imaging (Fig. 3.7).

Unexpectedly we find that numerous, homogenously distributed ComE foci are formed within gonococcal colonies even in the absence of externally added DNA (Fig. 3.7a-c, lower row). We determined the positions of ComE foci as a function to the distance to the colony contour (see section 2.7.2); thus, obtaining density profiles of ComE foci within gonococcal colonies for different time points (Fig. 3.7d-f). We find that the profiles of untreated colonies (blue curves) show a slope towards the colony center, indicating that focus formation is more abundant within the inner layers of the colony compared to the periphery.

We asked whether the presence of transformable DNA changes dynamics of ComE foci formation within cell aggregates and repeated the experiment by adding DNA to the growth medium. Previous experiments showed that gonococcal gDNA penetrates colonies poorly and

is retained in the outer periphery (see Fig. 3.2). Thus, we hypothesized that addition of gDNA elevates DNA uptake, and ComE foci formation, in the outer periphery of colonies as well. Immediately after addition of external DNA, we find higher foci densities in colonies grown in the presence of eDNA compared to untreated colonies (Fig. 3.7d-f, red curves), indicating a general increase of DNA uptake within colonies when transformable nucleotides are present. Moreover, the profile lacks the slope found in the profile of untreated colonies, indicating increased DNA uptake in the periphery of colonies (Fig. 3.7d). After 1 hour of incubation with external DNA, the density profiles of ComE-mCherry foci are independent of extracellular DNA (Fig. 3.7e).

We previously showed that formation of ComE foci and, thus, DNA uptake can be abrogated by DNase treatment of single cells (see Fig. 3.6). Therefore, we were interested to investigate the effects of DNase treatment on DNA uptake in gonococcal colonies as well. Thus, we repeated the experiment yet again by adding recombinant DNase I to the growth medium of colonies. The resulting foci density profiles show that, initially, ComE foci are reduced in colonies (Fig. 3.7d, black curve); however, their formation is not abrogated completely, indicating that ComE foci can form in colonies by a mechanism different from DNA uptake from the extracellular space. Furthermore, the profile has a strong slope towards the inner regions of colonies, indicating that focus formation in the periphery of the colony is limited by the presence of DNase. For later times we find that the effect of DNase treatment gradually disperses (Fig. 3.7e, f).

Altogether, we find that ComE focus formation within colonies is induced by the addition of extracellular DNA, indicating that it signals DNA uptake. However, ComE foci form even in the presence of DNase, suggesting that there is an additional mechanism of ComE focus formation within colonies that has been overlooked so far. Combined, our data suggests that eDNA penetrating colonies of *N. gonorrhoeae* is mainly taken up by the cells in the outer layers of the cell aggregate, with limited uptake in the core region of the colony. Moreover, our data shows that ComE foci formation cannot be abrogated in gonococcal colonies, indicating that colony formation might, simultaneously, trigger ComE foci formation and, thus, DNA uptake.

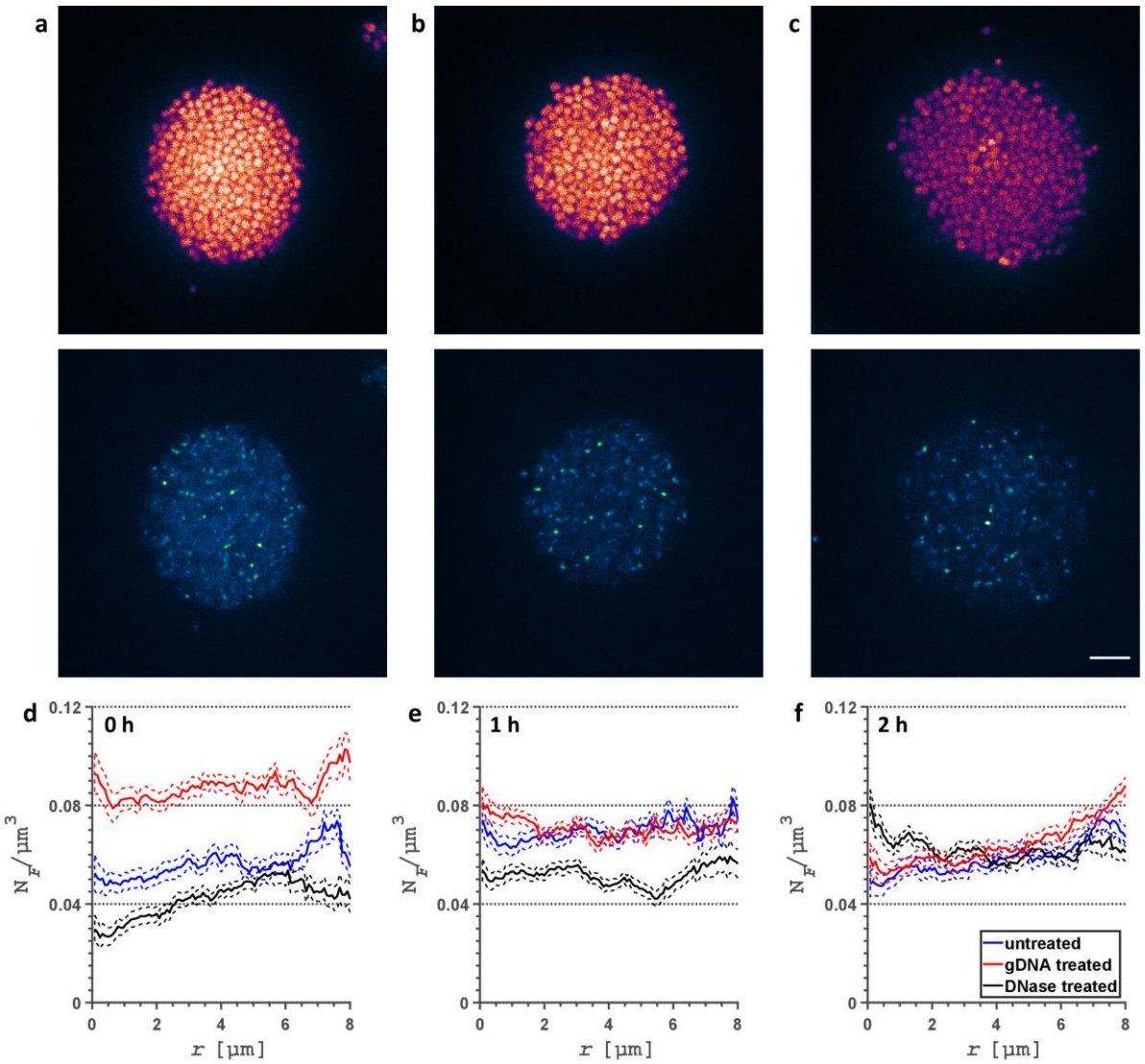

Figure 3.7: Spatio-temporal dynamics of ComE foci formation in gonococcal colonies.

Exemplary confocal slices of colonies formed by strain *comE-mcherry** (NG195) under untreated conditions **(a-c)**. Upper row: Colony and cell positions as denoted by GFP expression. Lower row: ComE-mCherry. **(a)** 0 h. **(b)** 1 h. **(c)** 2 hours of incubation. **(d-f)** Density (N_F) of ComE-mCherry foci within colonies as a function of the distance (r) to the colony contour after **(d)** 0 h, **(e)** 1 h, and 2 hours **(f)**. Colonies were treated with DNase (black), with gDNA of *N. gonorrhoeae* (red) or not at all (blue). Shaded areas represent standard errors of 30 colonies. Scale bar: 5 µm.

3.3. Spatio-temporal dynamics of transformation

Biofilms have been reported as hot spots for horizontal gene transfer (HGT) and, thus, transformation [Stalder & Top, 2016]. While reports concerning HGT in biofilms gained in significance in recent years, especially in the context of potential effects on human health, many of the mechanisms involved in this process remain poorly understood [Lerner *et al*., 2017; Lerminiaux & Cameron, 2019]. We already investigated transformation efficiencies in early gonococcal biofilms in a previous study and found that transformation was more efficient in biofilms compared to planktonic cells, but the low fraction of transformants prevented direct visualization of transformation under non-selective conditions [Kouzel *et al*., 2015].

In this section, we present the dynamics of transformation within gonococcal colonies with spatial and temporal resolution. To stay in line with our previous experiments, we determined transformation efficiencies in colonies transformed with genomic DNA, 3 kb and 300 bp fragments. We find that 3 kb fragments, which achieve highest abundance in gonococcal colonies, are also the most efficiently transformed. Moreover, we also find that transformation is only efficient within a short, early period of colony growth, and that transformation is limited to the outer periphery of the colony.

3.3.1. Detection of transformation events with spatial and temporal resolution

Detection of single transformation events with spatial and temporal resolution within gonococcal colonies (Fig. 3.8) required the creation of a new reporter strain. We used strain *wt** (NG194) and introduced a point mutation into the *sfgfp* gene sequence (c.201A>C) which creates a premature stop codon within the residue-triplet of the chromophore. This, in turn, results in expression of truncated sfGFP (Fig. 3.8a). Consequently, colonies grown from this new strain (*wt* sfgfp*$_{nf}$) are non-fluorescent. Transformation of the reporter strain with DNA containing the native chromophore sequence, replaces the point mutation and restores fluorescence of sfGFP (Fig. 3.8b). Because *sfgfp*$_{nf}$ and the native sequence only differ by a single nucleotide, we expected transformation probabilities to be high. However, fluorescent cells may also arise due to cell division of an already transformed cell, which would result in fluorescent diplococci or small clusters of fluorescent cells. Yet, the mobility was low enough so that one can identify such a fluorescent sector (e.g., cluster or diplococcus) as the result of a single transformation event.

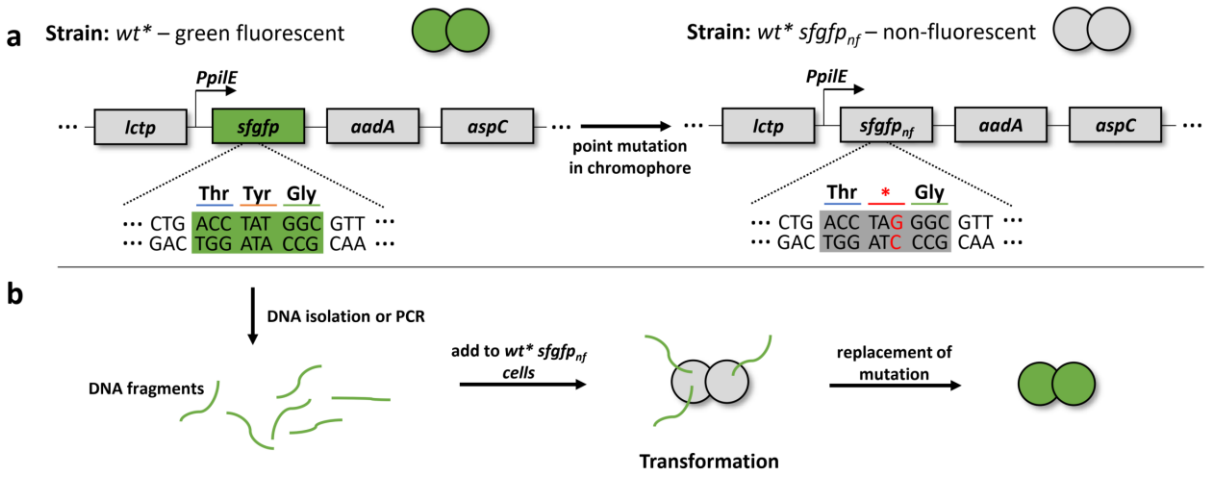

Figure 3.8: Scheme – principle for detection of transformation events within gonococcal colonies.
The figure outlines the principles of the experiment described throughout this section of the manuscript. **(a)** Creation of the reporter strain. Strain *wt** contains *sfgfp* and is green fluorescent (left). Insertion of a point mutation disrupts the chromophore (Thr-Tyr-Gly triplet) and introduces a premature stop-codon (red asterisk, right), resulting in expression of truncated, non-fluorescent sfGFP. **(b)** Transformation procedure. DNA samples, containing the native chromophore sequence are derived from strain *wt** and subsequently added to the growth medium of colonies formed by *wt* sfgfp$_{nf}$*. Transformation of DNA replaces the mutation and recovers fluorescence of sfGFP.

3.3.2. Transformation is most efficient in the periphery of early colonies

To remain coherent to our previous experiments, we prepared gDNA from strain *wt**, as well as 3 kb and 300 bp fragments of native *sfgfp* and added these to 1-hour old colonies formed by *wt* sfgfp$_{nf}$*. Subsequently, colonies were imaged for 4 hours in intervals of 15 minutes (Fig. 3.9).

We find that 3 kb fragments were transformed in gonococcal colonies within 4 hours (Fig. 3.9a). By contrast, we did not observe any transformants for gDNA or 300 bp fragments after 4 hours of incubation (not shown), highlighting the impact of fragment length on transformation efficiency. For 3 kb fragments, we find that transformants start to appear 1 hour after addition of transformable DNA to the growth medium. However, the overall number of transformants after 4 hours of growth was small (Fig. 3.9b). The average fraction of transformants increases over the course of the second hour in rather even increments in between timepoints; but shortly thereafter the fraction of transformants saturates, indicating that colonies become arrested for transformation. This suggests that transformation is most efficient within a short period during the early stages of gonococcal colony development.

Furthermore, transformation is limited to the outer periphery of gonococcal colonies (Fig. 3.9c). We do not detect transformants beyond a penetration depth of 6 µm (at an average colony radius of ~10 - 15 µm), indicating that cells within the core region of colonies transform poorly. Previous experiments have shown that 3 kb DNA reaches the center of gonococcal colonies within 1 hour (see Fig. 3.2); therefore, limited transformation in the colony core is likely not the result of a lack of transformable eDNA but instead suggests some form of transformation arrest of gonococcal cells within the colony center.

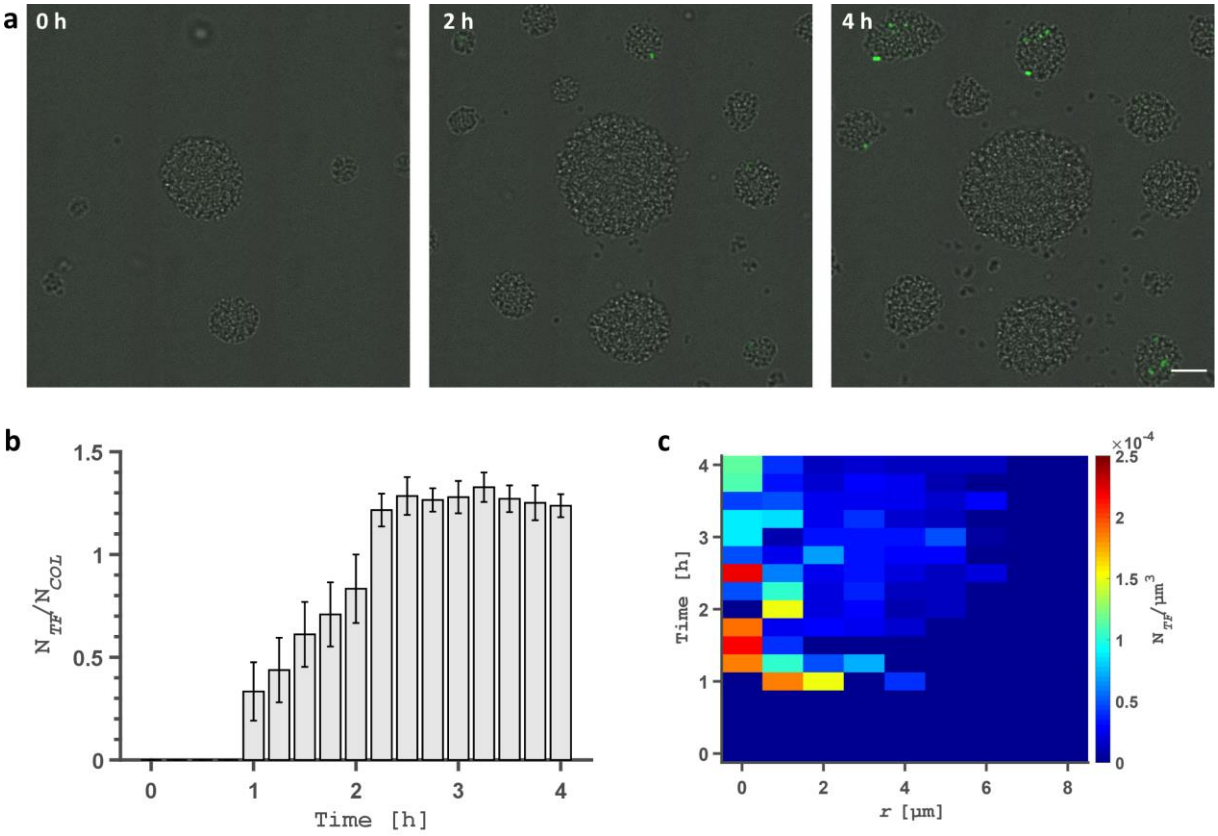

Figure 3.9: Spatio-temporal dynamics of transformation in colonies of *N. gonorrhoeae*.

Exemplary confocal slice merged with brightfield images of one-hour old colonies of the non-fluorescent mutant strain *wt* sfgfp$_{nf}$* (NG233) after addition of 3 kb DNA fragments after 0 h, 2 h and 4 hours **(a)**. **(b)** Fraction of average transformants (N_{TF}) per colony with at least one transformation event (N_{COL}). **(c)** Average number of transformants per volume ($N_{TF}/\mu m^3$), as a function of the distance (r) to the colony contour. Scale bar: 10 µm.

In conclusion, we find that transformation of naked, 3 kb DNA fragments is efficient in early gonococcal colonies. Furthermore, we find that gene transfer is limited to the outer periphery of colonies. Poor transformation of cells residing in the center of colonies is most likely not the result of a lack of transformable DNA, but of reduced transformability of the cells. Genomic DNA and 300 bp fragments did not transform within 4 hours, implying that the length of DNA

fragments critically affects the efficiency with which they are transformed. However, we adjusted the different DNA samples according to the total weight of DNA added to the growth chamber, not according to the number of native *sfgfp* sequences. Thus, gDNA might have a lower probability to replace the *sfgfp$_{nf}$* mutation, yet actual transformation rates might be higher compared to 3 kb fragments.

3.3.3. Gene transfer between two strains is inefficient in mixed gonococcal colonies

Next, we wanted to also address direct horizontal gene transfer between two bacterial strains that were well mixed within gonococcal colonies, utilizing a similar approach we used to detect naked, transforming DNA (see Fig. 3.8). To this end, we inserted the gene encoding for *mcherry* into a different locus of strain *wt* sfgfp$_{nf}$* (strain 1), which allowed the detection of cells during confocal microscopy. The now red fluorescent strain was mixed in a ratio of 1:1 with strain *wt** (strain 2), which is green fluorescent. Strain 2 carries the native *sfgfp* sequence. Both were grown in poly-L-lysine coated flow chambers for 24 hours under continuous flow of fresh medium. Transformation of red fluorescent strain 1 with genomic DNA of green fluorescent strain 2 leads to replacement of the *sfgfp$_{nf}$* mutation and, thereby, restores native *sfgfp*. Thus, successful transformation generates cells which are, simultaneously, red and green fluorescent (Fig. 3.10).

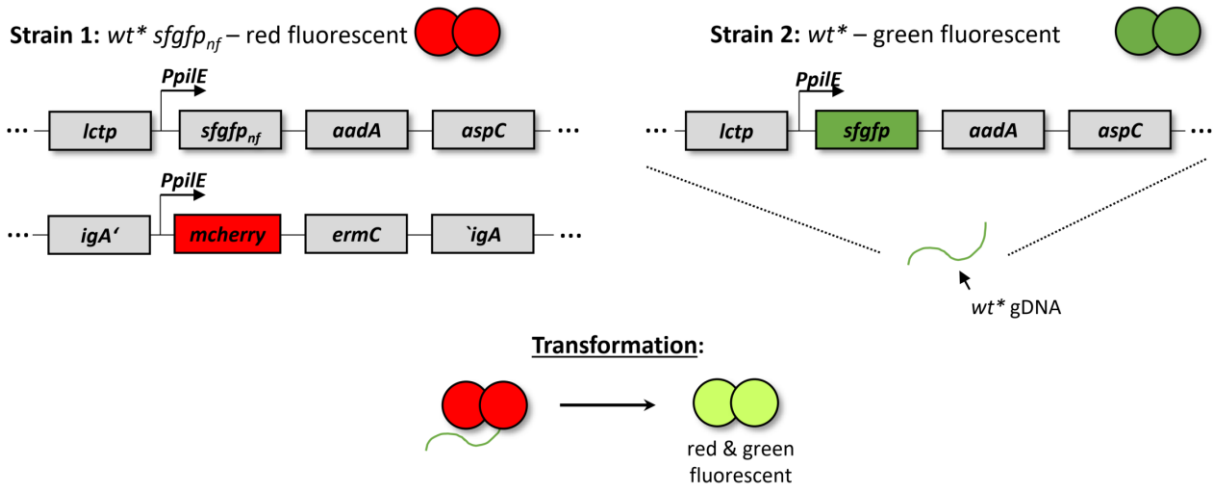

Figure 3.10: Detection scheme for gene transfer events in mixed colonies.

Red fluorescent strain 1 was genetically modified to carry both non-fluorescent *sfgfp$_{nf}$* and *mcherry* in the *igA* and *lctp-aspC* loci of the genome. The strain is cocultured with green fluorescent strain 2, which carries unmodified *sfgfp*. Genomic DNA (gDNA) originating from strain 2 can, thus, be transformed by strain 1 resulting in the replacement of *sfgfp$_{nf}$* with the native sequence by homologous recombination, generating cells that are both red- and green fluorescent.

We observe that after 24 hours of growth, only a small fraction of cells was transformed (Fig. 3.11), emphasizing that gene exchange within colonies was inefficient, which was unexpected. Given that *sfgfp* and *sfgfp$_{nf}$* only differ by a single nucleotide we expected transformation to be efficient between the two strains. However, we noted that fluorescence of mCherry deteriorated throughout the experiment, which, presumably, impedes our ability to properly visualize, let alone detect, transformed cells (Fig. S10). Thus, it is likely that we underestimate the true extent of gene exchange between the two strains.

Even so, we conclude that substitution of the *sfgfp$_{nf}$* point mutation by means of horizontal gene transfer between two strains is inefficient within gonococcal colonies.

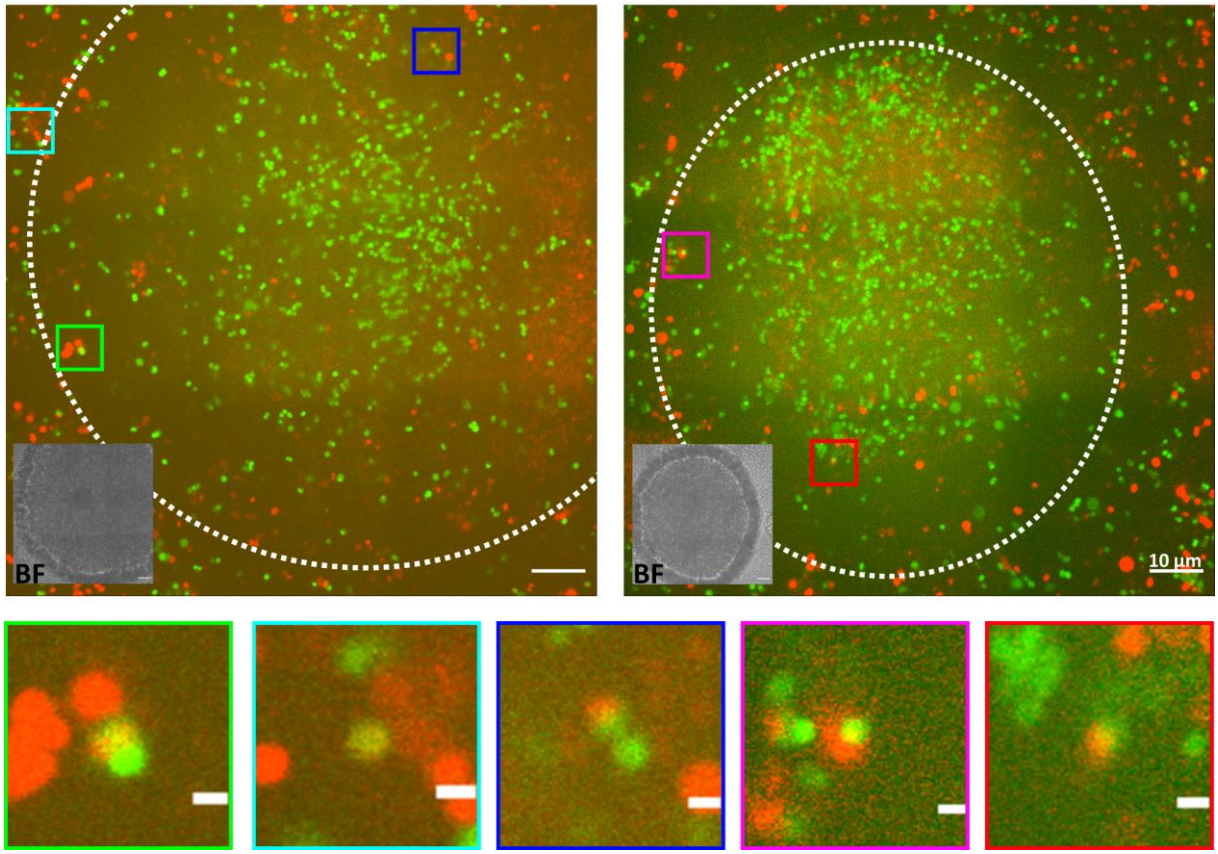

Figure 3.11: Repair of *sfgfp$_{nf}$* by means of gene transfer is inefficient in mixed gonococcal colonies.
Typical merge-images of mixed colonies of strains *wt** (NG194) and *wt* sfgfp$_{nf}$* (NG233) after 24 hours of growth. Upper row: z-slice of two random colonies, imaged close the bottom of the growth chamber. White dotted lines indicate colony contours. Inlets: brightfield images. Only a small fraction of cells shows green and red fluorescence simultaneously (colored boxes). Lower row: close up images of random transformed cells, as indicated by colored boxes. Scale bar: 1 µm.

3.4. Release of free DNA stabilizes gonococcal colonies

N. gonorrhoeae is known to release DNA in an independent manner. Gonococci possess a type 4 secretion system (T4SS), which, in conjunction with autolysis, is used to release chromosomal (ss-)DNA into the extracellular surrounding [Elmros *et al*., 1976; Callaghan *et al*., 2017]. The released DNA is not only used to transform *Neisseria* cells and species but was also shown to play an important role during initial biofilm formation [Hamilton & Dillard, 2005; Zweig *et al*., 2014]. For instance, free, extracellular DNA has been reported to be a strong stabilizing component in biofilms of other bacterial species [Montanaro *et al*., 2011]. While we know that DNA is present in the biofilm matrix of *N. gonorrhoeae* [Steichen *et al*., 2011], the architecture and the dynamics of the eDNA network are unknown.

In the experiments outlined here, we visualized extracellular, free DNA in colonies of *N. gonorrhoeae* with the DNA-binding dye YOYO-1-iodide. Our data indicates that DNA is processed into elongated filaments of various sizes, which in turn form an extensive network, or lattice. The formation of the filament-lattice can be completely abolished by supplementing DNase into the growth medium of the colonies, which also affects colony surface morphology. Thus, our data suggest a strong stabilizing function for extracellular DNA. Furthermore, we show that the bulk of DNA is released by cell death and (auto-)lysis, and that released DNA is not locally confined, but with time redistributes across the colony. Finally, our data also suggest that aggregation of DNA molecules into filaments is independent of type IV pili (T4P) and ComP-mediated DNA-binding.

3.4.1. Free eDNA forms a filamentous lattice within gonococcal colonies

Visualization of extracellular DNA in biofilms and microcolonies requires a dedicated dye that specifically binds to free DNA only, ignoring chromosomal nucleic acids in viable cells. We choose the DNA-binding dye YOYO-1-iodide (YOYO-1) for the experiments described here, since it has an excellent signal-to-noise ratio and stains both ds- and ssDNA [Åkermann & Tuite, 1996]. To visualize free eDNA within gonococcal biofilms, we supplemented the growth medium of *N. gonorrhoeae* with 0.33 nM YOYO-1 and cultured the growing biofilm in poly-L-lysine coated well plates.

After 4 hours of incubation, we imaged selected colonies with confocal microscopy and found that eDNA formed a network of elongated filaments within gonococcal colonies (Fig. 3.12). Interestingly, the lattice is most pronounced within the outer periphery of colonies, suggesting that DNA cocoons the cell aggregate. In addition, we found DNA fibers which are

extended into the extracellular space, were they associate with the underlying colony surface (Fig. S11). Combined, these findings suggest that DNA filaments act as a stabilizing or structural component within gonococcal colonies. Moreover, the results highlight the fact that formation of extensive DNA networks in gonococcal colonies is rapid and occurs within few hours.

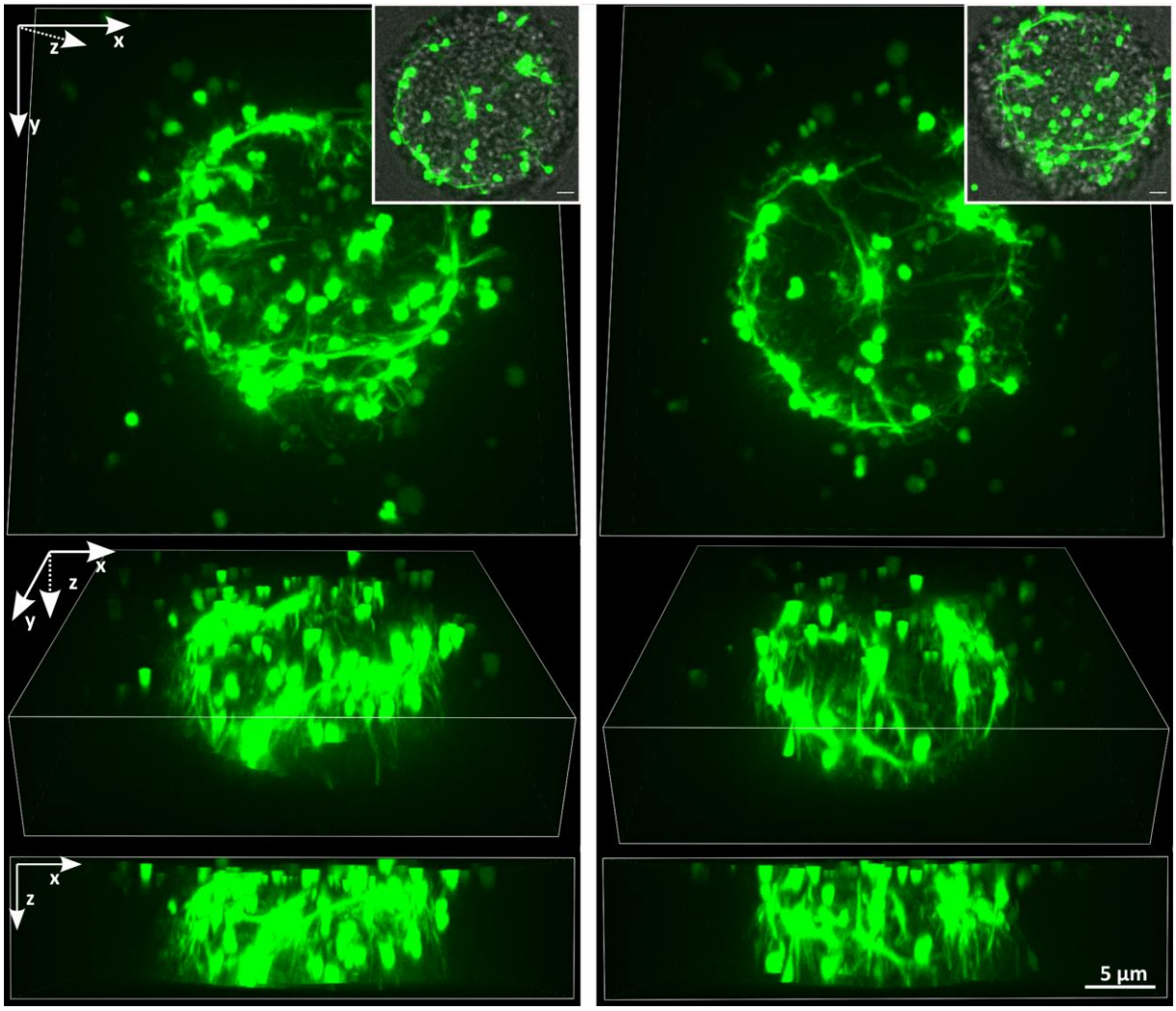

Figure 3.12: Free DNA forms a lattice of filaments which cocoons the colony.

3D volume projection of two 4-hour old colonies of strain *ΔG4* (NG150), grown in medium supplemented with 0.33 nM of the cell-impermeable DNA stain YOYO-1-iodide; represented in various 3D viewing angles. Inlets: Merge with brightfield image. Scale bars: 2.5 µm.

Next, we performed timelapse imaging to characterize the formation of DNA filaments and the resulting DNA network. Thus, we repeated the experiments, but imaged selected colonies in intervals of 30 minutes after initial colony formation.

The resulting images show that, initially, eDNA is sparse within gonococcal colonies (Fig. 3.13a). However, more DNA is progressively released into the cell aggregate which, eventually, forms the lattice in the periphery (Fig. 3.13b, c).

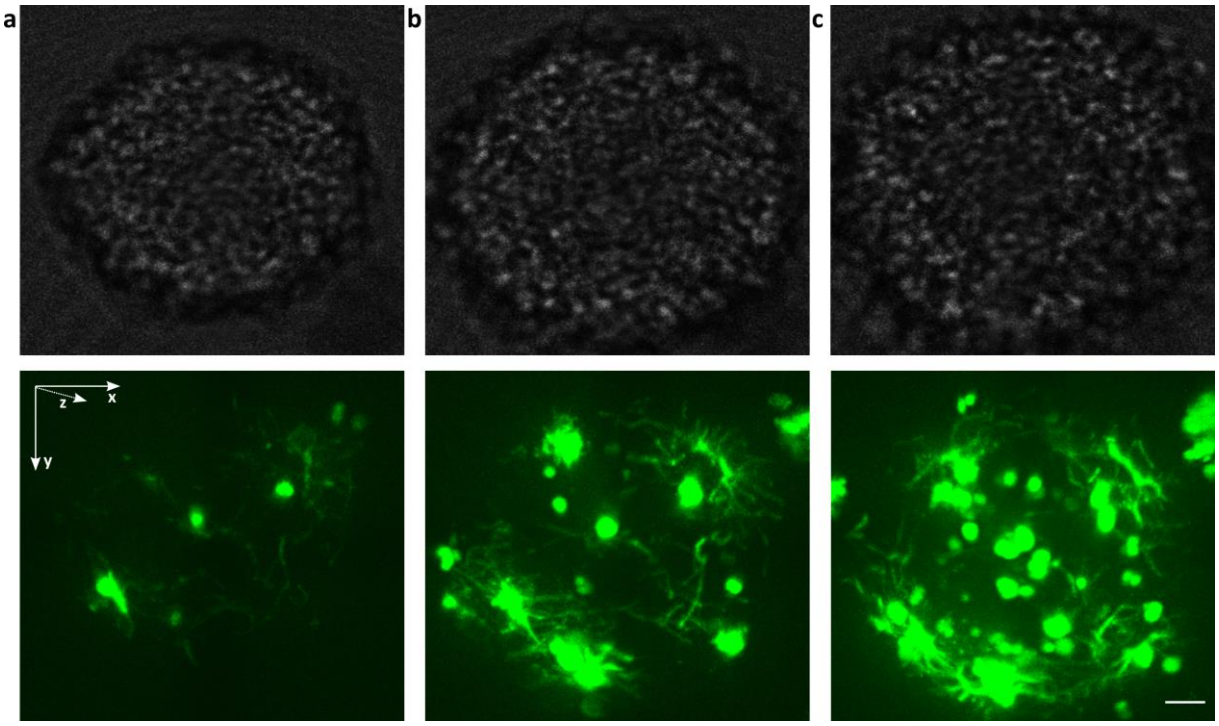

Figure 3.13: DNA is progressively released into colonies by cell death.

Typical YOYO-1 fluorescence within a single colony of *N. gonorrhoeae* formed by strain *ΔG4* (NG150), immediately after colony formation **(a)**, after 2 h **(b)** and 4 hours of incubation **(c)**. Upper row: brightfield images. Lower row: volume projections of YOYO-1 fluorescence intensities represented in aerial 3D view. Scale bar: 2.5 µm.

Furthermore, the images strongly suggest that DNA filaments sheer off from lysed cells and are more abundant in areas with increased cell lysis; indicating that the bulk of eDNA is released by cell death. At the same time, the images also imply that DNA released by cell death is not locally confined but rather distributed throughout the colony in the form of DNA filaments.

Thus, we conclude the following: Free DNA in gonococcal colonies is processed into elongated filaments and bundles which eventually spread through the entire cell aggregate and form an intricate mesh, or lattice-like, structure that cocoons the colony. Formation of the lattice is rapid, since it occurs within few hours, and is primarily driven by cell death and/or auto-lysis.

3.4.2. Removal of DNA affects structural integrity of gonococcal colonies

We asked whether the presence of the DNA lattice affects the stability or structure of gonococcal colonies. In order to address this question, we repeated our experiments by supplementing DNase I to the growth medium of colonies, thereby degrading external DNA.

Indeed, we find that the presence of DNase in the growth medium of colonies prevents the formation of any DNA filaments (Fig. 3.14). Furthermore, we note that cell aggregates which are grown in the presence of DNase showcase a rough and bloated surface morphology compared to untreated colonies (Fig. S12).

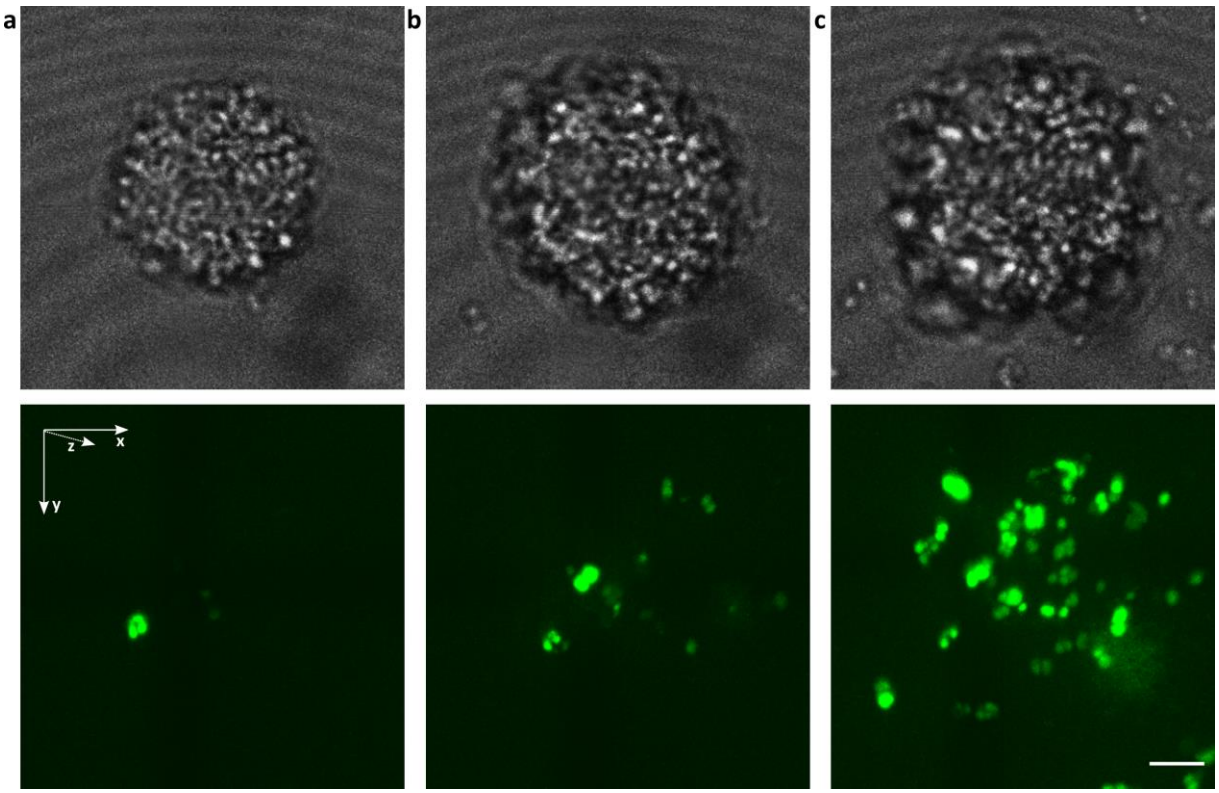

Figure 3.14: The presence of DNase prevents formation of DNA fibers and bundles.
Typical YOYO-1 fluorescence within a single colony of *N. gonorrhoeae* formed by strain *ΔG4* (NG150), immediately after colony formation **(a)**, after 2 h **(b)** and 4 hours of incubation **(c)**, grown in medium supplemented with 10 U of DNase I. Upper row: brightfield images. Lower row: volume projections of YOYO-1 fluorescence intensities represented in aerial 3D view. Scale bars: 2.5 µm.

We asked whether the removal of the eDNA lattice was also possible if the network was already well established. To address this, we added DNase to the medium of 4-hour old colonies which had already formed the DNA mesh (Fig. 3.15a). Interestingly, we find that DNase removes preexisting DNA networks instantly (Fig. 3.15b, lower row). At the same time, colonies

immediately adopt the bloated morphology mentioned earlier, further emphasizing that removal of DNA affects the structural integrity of gonococcal colonies negatively (Fig. 3.15b, upper row). However, colonies relax back into the initial state, or morphology, within few minutes (Fig. 3.15c).

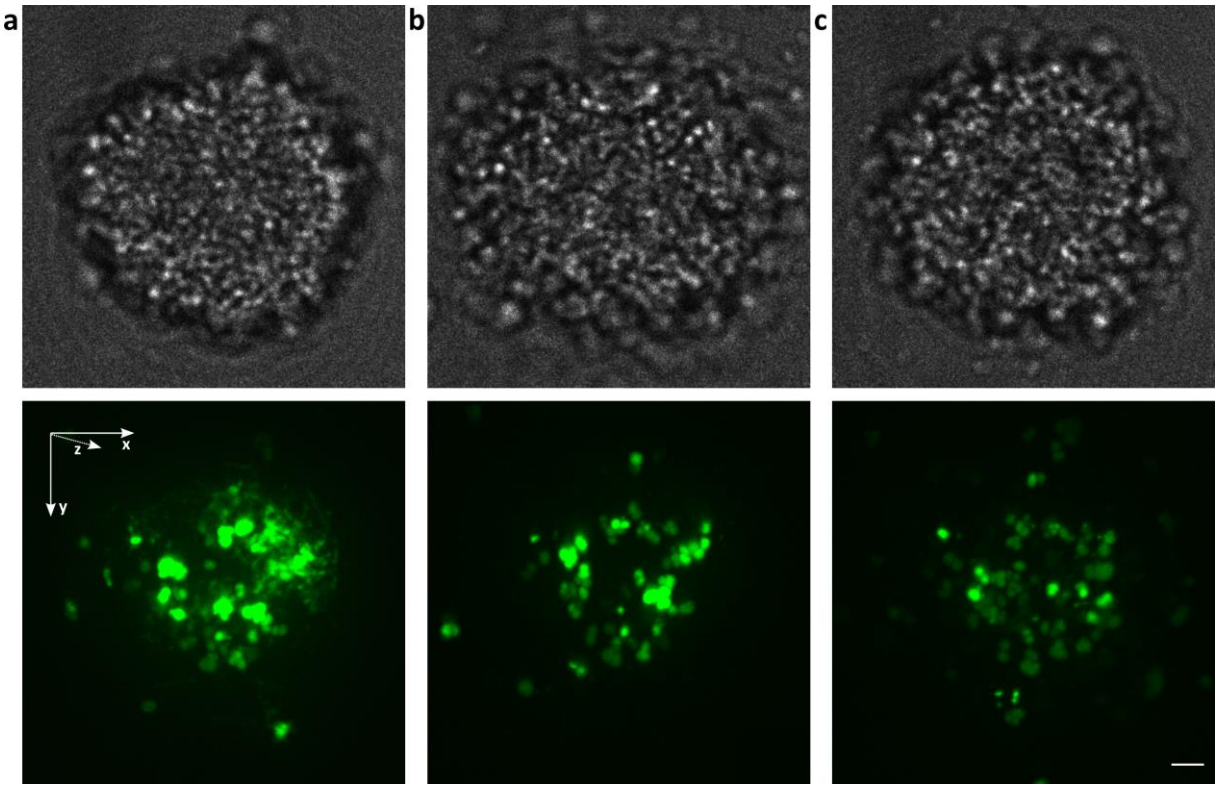

Figure 3.15: Removal of external DNA affects colony structure.

Typical YOYO-1 fluorescence within a single colony of *N. gonorrhoeae* formed by strain *ΔG4* (NG150), after 4 hours of growth **(a)**, immediately after addition of DNase **(b)** and 10 min after addition of DNase **(c)**. Upper row: brightfield images. Lower row: volume projections of YOYO-1 fluorescence intensities represented in aerial 3D view. Scale bars: 2.5 µm.

To conclude, we find that colonies which are deprived of DNA adapt a rough and bloated morphology, suggesting that removal of the DNA lattice negatively affects the structural integrity of gonococcal cell aggregates.

3.4.3. DNA filaments form in the absence of the DNA-binding minor pilin ComP, but the network structure is affected

The matrix of gonococcal biofilms and colonies is known to contain large amounts of type IV pili (see Fig. 1.5). T4P can interact with DNA via the minor pilin ComP, which is integrated into the pilus fiber during T4P assembly. Furthermore, ComP is known to prefer interaction to *Neisseria*-specific DNA bearing DNA uptake sequences [Cehovin *et al*., 2013]. The presence of DNA-binding pilus filaments within the matrix of gonococcal colonies raises the question, whether T4P are also involved in the assembly of DNA filaments or, more specifically, in the formation of the DNA lattice.

To address this question, we repeated the experiments described in section 3.4.1 with a *ΔcomP* strain. Given that ComP is the only T4P component to be known to interact with DNA, we hypothesized that deletion of *comP* abrogates the formation of the DNA network.

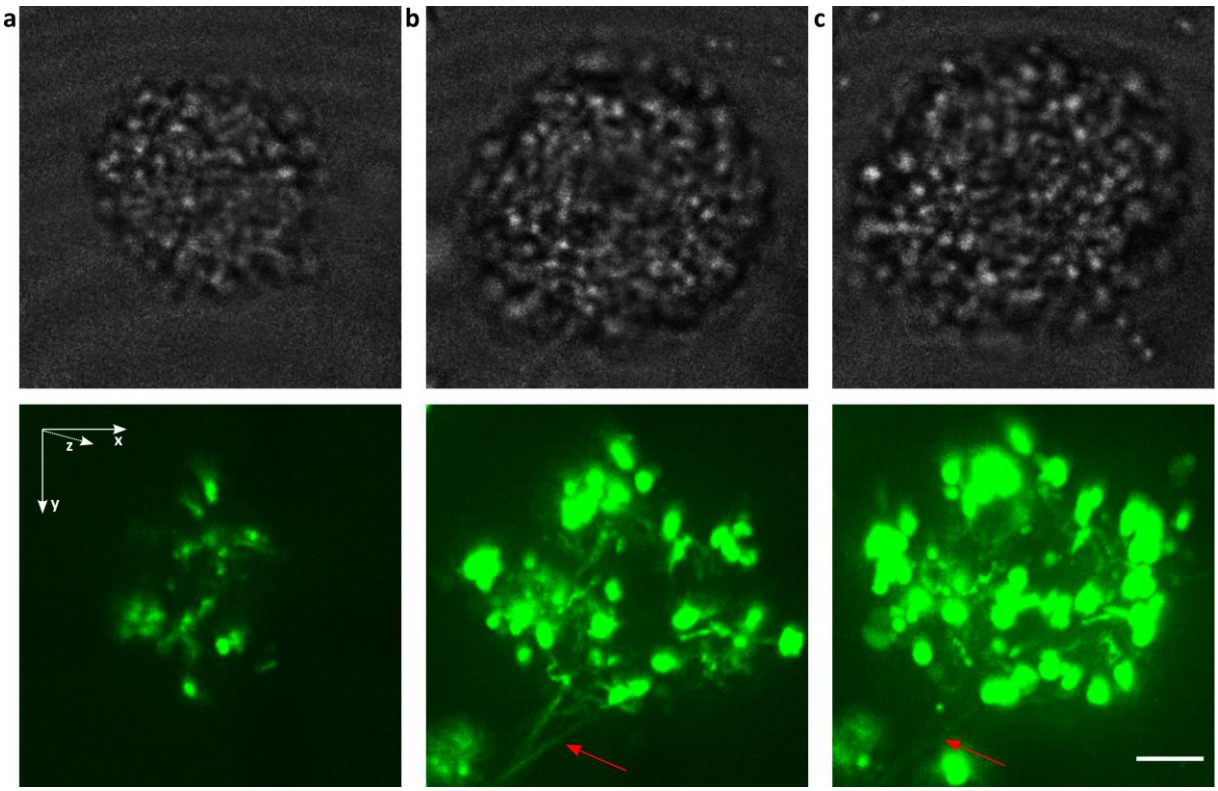

Figure 3.16: DNA filaments form independent of ComP-mediated DNA-binding.

Typical YOYO-1 fluorescence within a single colony of a *comP* deletion strain (NG236) of *N. gonorrhoeae*, immediately after colony formation **(a)**, after 2 h **(b)** and 4 hours of incubation **(c)**; highlighting that DNA filaments (red arrows) are still formed in a *ΔcomP* background. Upper row: brightfield images. Lower row: volume projections of YOYO-1 fluorescence intensities represented in aerial 3D view. Scale bar: 2.5 µm.

Surprisingly, we find that *ΔcomP* colonies exhibit DNA filaments (Fig. 3.16), indicating that the DNA mesh is formed independently from T4P or ComP-mediated DNA-binding. However, while the formation of DNA filaments is retained in a *comP*-deletion background, we note that the DNA mesh penetrating the colonies appears to be stunted compared to *wt** colonies (compare Fig. 3.12 & Fig. 3.13), as DNA fibers are not as pronounced, less numerous and seem to be truncated, which implies that deletion of *comP* affects DNA processing in gonococcal colonies. Furthermore, we could no longer detect a noticeable DNA cocoon surrounding colonies after 4 hours of incubation.

Therefore, we conclude that while deletion of *comP* does not abrogate the formation of DNA filaments and the lattice emerging from them, it affects the way that free DNA is processed in gonococcal cell aggregates, as characterized by the qualitatively different arrangement of the DNA network found in *ΔcomP* colonies.

4. Discussion

4.1. Penetration efficiencies of eDNA in early gonococcal biofilms

4.1.1. Retention of DUS$^-$ DNA increases with the length of DNA fragments

Extracellular DNA is widely accepted as a critical component in the development of bacterial biofilms [Panlilio & Rice, 2021]. However, the motility of DNA molecules within bacterial biofilms it is still not understood. In this study we investigated the dynamics of extracellular DNA penetrating early gonococcal microcolonies.

We found that the penetration dynamics of (DUS$^-$) DNA and its retention depend on the length of the nucleotide chain. Short 300 bp DUS$^-$ DNA fragments show no significant increase in fluorescence intensity compared to the background over the time course of 1.5 hours. If there was no DNA penetration during this period of time, then the fluorescence intensity within the colony should be significantly lower compared to the background because of the presence of the cell bodies. From this observation, we conclude that short DNA rapidly penetrates the entire colony. After 2 hours, the fluorescence intensity was significantly higher than the background, indicating that even in the absence of the DUS, DNA is retained within colonies. Larger DNA fragments showed a much stronger fluorescence signal, indicating that long DNA fragments are retained efficiently within the cell aggregates. In the following, we will discuss both diffusion and retention of DNA within gonococcal colonies.

Studies that characterized dispersion of molecules in dependance of molecular weight, the equivalent to DNA length-scale, conceptualize bacterial biofilms as molecular sieves, which restrict and hinder the penetration of macromolecules larger than a given pore size. Small solutes can, thus, enter the biofilm unhindered, whereas large molecules are likely prevented from penetration due to entanglement within the materials of the extracellular matrix (ECM) [Yeon *et al*., 2008; Wöll, 2014; Sankaran *et al*., 2019]. Yet, if small molecules, e.g., 300 bp DNA, can enter a cellular aggregate freely, then why is it so weekly retained compared to larger DNA fragments (3 kb, *E. coli* gDNA) which penetrate cellular aggregates way less efficient?

In general, the diffusion coefficients of DNA in the absence of a polymer network decrease as the nucleotide length increases [Robertson *et al*., 2006]. In the presence of a network (the ECM in this case), the length effect on diffusion is further strengthened by entanglement. 300 bp fragments have a length of ~ 100 nm, which is comparable to the Kuhn segment length of DNA. Therefore, they are not entangled within the polymer network of the extracellular matrix. Large DNA molecules (gDNA), by contrast, slowly enter the colony because they become

entangled within the extracellular matrix and entanglement reduces the diffusion constant of the center of mass of the DNA molecule [Doi & Edwards, 1986]. This is also in agreement with the radial profile; gDNA continuously enters at the edge of the colony and then diffuses slowly within the colony. As a consequence, a concentration gradient forms whereby the gDNA concentration is highest at the periphery of the colony.

Previous studies showed that diffusion of soluble molecules within bacterial biofilms might not only be defined by polymer length but also due to the physiochemical properties of the solute, including charge, hydrophobicity, or the rigidity of the structure [Floury *et al*., 2015]. Thus, attractive or repulsive forces may affect the penetration dynamics of DNA and, thus, contribute to the capturing of nucleotides within biofilms; although it remains difficult to assess the extent of those contributions. It is also conceivable that DNA is trapped by cytosolic proteins released and incorporated into the extracellular matrix due to autolysis, as previously reported for *S. aureus* biofilms [Kavanaugh *et al*., 2019] Gonococci are usually associated with extensive autolysis, however cell death is limited in young gonococcal colonies, thereby limiting the availability of any putative DNA capturing proteins in the extracellular space [Elmros et al., 1976; Welker *et al*., 2021]. All of these mechanisms are likely to affect diffusion of DNA, but they are also important for retention of nucleotides within the colonies. As DNA is bound to the ECM, it becomes less likely to diffuse away from the colony and, thus, accumulates within the cell aggregate.

Why do long DNA molecules accumulate more strongly within colonies than short molecules? We except that the integration of DNA into the ECM network is a slow process. Since long DNA molecules are more stationary than short DNA molecules, they are likely to be integrated in a more efficient way. This may explain why gDNA from *E. coli* is retained to a higher level than short DNA fragments. We note that the presence of truncated DUS in gDNA of *E. coli* is likely to affect DNA-binding as discussed in section 4.1.3.

In conclusion, diffusion and retention of DNA within cell aggregates of *N. gonorrhoeae* likely relies on an interplay between molecular length and attractive/repulsive forces that define the permeability of colonies and biofilms for nucleotides of various sizes. Diffusion in cellular aggregates is fast and unhindered for small DNA molecules but results in week retention in the absence of a dedicated DNA-binding mechanism. Large molecules, on the other hand, feature slowed, perturbed diffusion but are retained more strongly within the molecular sieve of a bacterial cell aggregate.

4.1.2. Specific binding of DUS$^+$ DNA slows down penetration of extracellular DNA

Next, we investigated penetration of gonococcal colonies by DNA molecules which carried DNA uptake sequences (DUS$^+$). The DUS increases the likelihood of specific DNA-binding by several orders of magnitude [Cehovin *et al*., 2013]. Indeed, we observed increased fluorescence intensities for both 300 bp and 3 kb fragments, indicating remarkedly increased retention of DNA within colonies in the presence of a dedicated DNA-binding mechanism (see Fig. 3.2).

We already stated potential explanations for the penetration dynamics of DNA in the previous section (see section 4.1.1). As we saw, small molecules readily penetrate the colony due to unhindered diffusion, yet this limits the likelihood for these molecules to be entangled by ECM components. For larger DNA we expect an opposite effect, as they diffuse poorly and have an increased chance to be trapped by extracellular material [Yeon *et al*., 2008; Wöll, 2014; Sankaran *et al*., 2019]. Concordantly, 300 bp fragments (DUS$^+$) readily penetrate colonies with little hinderance in motility but are now efficiently captured by T4P due to specific ComP mediated DNA-binding, thereby strongly enhancing retention of DNA fragments migrating within the colony (see Fig. 3.2d) [Goodman & Scocca, 1988; Berry *et al*., 2013; Spencer-Smith *et al*., 2016]. The abundance of retained DNA correlates with the length of the nucleotide polymer, as larger 3 kb fragments are retained even more efficiently (see Fig. 3.2e). The 10-fold increase in polymer length compared to 300 bp fragments results in perturbed penetration/migration and, thus, facilitates capture by T4P [Robertson *et al*., 2006].

Gonococcal gDNA, however, is exclusively and very strongly retained within the outer layers of the colony, with little to no retention or accumulation in the colony center (see Fig. 3.2f). Isolated gDNA is much larger compared to 300 bp or 3 kb samples and, based on our isolation method, contains fragments of ~ 30 kb on average (see section 2.3.1). Consequently, gonococcal gDNA should feature highly perturbed penetration of colonies. Moreover, the genome of *N. gonorrhoeae* contains hundreds of DUS; on average one per kilobase [Marri *et al*., 2010]. Hence, the odds for gDNA to be captured by T4P are significantly increasing compared to 300 bp and 3 kb DNA samples, which only featured one DUS each. This suggests that cells in the outer periphery quickly capture penetrating gDNA; thus, preventing it from reaching the inner layers of the cell aggregate in large quantities. Even so, we found that isolated gDNA of gonococci was highly fragmented, with many smaller fragments in the range of 1 kb to 3 kb (see Fig. S14). Therefore, one should expect more efficient penetration of gDNA into gonococcal colonies by these smaller fragments, similar to the one observed for *E. coli* gDNA (see Fig. 3.1f). However, the abundance of DUS potentially found on sheered fragments of

gonococcal gDNA could prevent efficient penetration of these fragments as well due to specific binding by ComP.

Interestingly, we find that the overall abundance of retained gDNA is reduced compared to 3 kb fragments (see Fig. 3.2e, f); which is a curious finding since it might indicate that even though gDNA is efficiently captured by T4P, its poor penetration and inaccessibility to a large fraction of colony dwelling cells prevents a more efficient accumulation within colonies. However, this might partially be mediated by the nuclease Nuc, which, as we will discuss in a separate section (see section 4.1.4), degrades gDNA within gonococcal colonies [Steichen *et al*., 2011].

In summary, we showed that the motility of DNA molecules within gonococcal colonies and biofilms is affected by DNA-binding mechanisms. DNA featuring DUS is retained stronger compared to DNA lacking them. Larger fragments (3 kb) are retained more strongly than shorter ones (300 bp); however, gonococcal gDNA is retained poorly. As gDNA has a larger quantity of target sites for DNA-binding (DUS), we propose that migration and penetration of DNA depends on a trade-off between molecule length-scale and the quantity of potential binding sites found on the molecule.

4.1.3. Potential causes for strong retention of *E. coli* gDNA within gonococcal colonies

A significant fraction of *E. coli* gDNA efficiently penetrated gonococcal colonies and resulted in strong and abundant retention of genetically distinct DNA in the deepest layers of the cell aggregates (see Fig. 3.1c, f). Even at the periphery of the colonies, the concentration of gDNA from *E. coli* was higher compared to the concentration of gDNA from *N. gonorrhoeae*. This unexpected finding will be discussed in the following.

First and foremost, it should be clarified that while we treat *E. coli* gDNA as *Neisseria*-unspecific DNA (DUS^-), it contains multiple truncated DUS. We identified twelve 10 bp DNA uptake sequences (5'-GCCGTCTGAA-3') in the genome of strain *NEB 5-alpha*, which is a suitable reference genome for strain *DH5α* we used in the study presented here [Anton & Raleigh, 2016]. While we could not identify any 12 bp DUS, it is possible that the genome contains additional "dialect"-DUS sequences [Frye *et al*., 2013]. Therefore, DNA derived from *E. coli* is likely to show low level binding to the minor pilin ComP, which is known to bind DNA in a DUS-specific fashion [Cehovin *et al*., 2013]. Second, based on the isolation method we applied (see section 2.3.1), we assume that the length-scale of isolated *E. coli* gDNA molecules is on average ~ 30 kb. Combined, one could expect penetration dynamics comparable

to gDNA derived from gonococci, yet this is not the case (see Fig. 3.2c, f). Here, we will speculate why *E. coli* gDNA is so strongly retained compared to the other DNA samples we screened in our assay.

During the isolation process, DNA is shred due to mechanical sheering [Abdel-Latif & Osman, 2017]. Consequently, isolated *E. coli* DNA resembles an assortment of fragments with rather undefined size, ranging from small (~ 100 bp) to large (> 30 kb), as we confirmed with agarose gel electrophoresis (see Fig. S14). As such, smaller fragments could penetrate the colony easily and reach the inner regions of the cell aggregate, where they are subsequently trapped due to DNA-binding or entanglement. Still, given that the number of DUS within the ~ 4.5 Mb *E. coli* genome is low, it is unlikely that small fragments in the length-scale of few hundred base pairs bear any DUS, which prevents efficient binding in the colony as discussed earlier [Anton & Raleigh, 2016]. Without binding, however, small fragments should not be retained efficiently in colonies, as we showed for 300 bp fragments (see section 4.1.1).

Past studies highlight that macromolecules of high molecular weight (> 100 kDa) readily accessed oral biofilms with a diameter of 100 to 200 micrometers in roughly 3 minutes, indicating that migration of molecules within bacterial aggregates is a highly diverse process which not necessarily resembles a simple molecular sieve [Takenaka *et al*., 2009; Sankaran *et al*., 2019]. This, in turn, could indicate that the dynamics of DNA depend on factors other than molecule length and active DNA-binding mechanisms. For instance, we already discussed physiochemical factors of solved molecules as potential factors affecting the migration dynamics of particles within cellular aggregates [Floury *et al*., 2015]. It is conceivable that these add to the strong retention of *E. coli* DNA within gonococcal colonies.

It is tempting to speculate that attractive, e.g., electrostatic, forces actively guide and detain genus-unspecific DNA in bacterial aggregates to use those nucleotides for intrinsic biofilm processes like horizontal gene transfer.

4.1.4. The nuclease Nuc controls the amount of DNA within gonococcal colonies

We found evidence that the nuclease Nuc adjusts the amount of eDNA in gonococcal colonies. We observed increased amounts of gonococcal gDNA within colonies formed by *nuc*-deficient *N. gonorrhoeae* (*Δnuc*), indicating that Nuc degrades gDNA in wildtype colonies. By contrast, we found a decrease in DNA abundance for 300 bp and 3 kb fragments in the *Δnuc* background, suggesting that these DNA samples are maintained by Nuc, rather than degraded. Intuitively, this finding is difficult to explain.

Information about Nuc in *N. gonorrhoeae* is rather limited. The most comprehensive study regarding Nuc is based on work by Steichen *et al*., published in 2011. They propose that Nuc is likely involved in the remodeling of eDNA in gonococcal biofilms, and that the nuclease can degrade multiple sources of DNA, including ssDNA, dsDNA and gDNA of *H. influenzae*, *Gardnerella vaginalis*, *E. coli* and *N. gonorrhoeae*; yet degradation was less efficient for DNA of gonococci compared to gDNA of the other species [Steichen *et al*., 2011]. However, we still lack detailed knowledge about Nuc's mode of action, and its activity on a molecular level, to understand how DNA is processed by the enzyme.

At least one study showed that the *S. aureus* homologue of Nuc has differential activity based on the constituent bases of the processed nucleotides [Cuatrecasas *et al*., 1967]. This could suggest a putative sequence specificity for Nuc-mediated cleavage. If so, the likelihood for short 300 bp and 3 kb to randomly carry this very cleavage site would be low compared to longer gDNA fragments; thus, preventing short fragments from being processed by Nuc.

Cleavage could also be guided by post-transcriptional modifications. Gonococcal gDNA is known to be highly methylated and methylation of DNA is known to confer resistance to restriction by nucleases [Haberman *et al*., 1972; Gunn *et al*., 1992]. Then again, nucleases such as DpnI specifically target only methylated DNA for cleavage [Lacks & Greenberg, 1975]. Thus, epigenetics seems to be critical in defining the target DNA for nucleases. This could, at least to some degree, explain the differential processing of DNA fragments, given that gDNA is derived from cells and is, thus, methylated, whereas 300 bp/3 kb fragments were generated by PCR and, therefore, lack methylation or similar modifications.

Even so, none of the aforementioned points all-out explains how, or rather, why a DNA degrading enzyme (Nuc) degrades gDNA but, simultaneously, maintains short 300 bp and 3 kb fragments in gonococcal colonies. Further investigation is required to uncover the exact molecular mechanisms of Nuc to obtain a deeper understanding of the nuclease's role in gonococcal colonies and biofilms. Still, based on our findings, we assume that the enzyme has differential processing activity for DNAs of varying length, potentially mediated by sequence specificity and post-transcriptional methylation.

4.1.5. DNA-binding is heterogenous in gonococcal colonies

We found evidence that DNA-binding is non-uniform in gonococcal cell aggregates. First, we observed that Cy3-labeled DNA fragments formed fluorescent foci, which were previously reported to indicate DNA uptake in isolated single cells of *N. gonorrhoeae* [Gangel *et al*., 2014]. However, as stated earlier, foci might indicate either intracellular or extracellular DNA in the context of gonococcal cell aggregates (see section 3.1.4). In case ComE foci signaled DNA uptake, we expected the spatial distributions of foci and fluorescence intensities to differ between DUS^+ DNA (which can be taken up) and DUS^- DNA (which cannot be taken up), yet we did not observe any noteworthy differences in spatial distributions (see Fig. S6 - S8). Thus, it is likely, that these foci indicate binding or entanglement of extracellular DNA, rather than intracellular DNA. Interestingly, we found that the highest abundance of fluorescent foci was obtained when colonies were treated with *E. coli* gDNA (see Fig. S9). Since, *E. coli* DNA has only few DUS (see section 4.1.3) binding should be inefficient [Cehovin *et al*., 2013]. Therefore, the high number of foci found for this DNA further strengthens the interpretation that there is excessive retention of unspecific DNA in gonococcal cell aggregates. We already discussed potential reasons for this finding in a previous section (see section 4.1.1), yet it is conceivable that extracellular DNA-binding proteins are involved in retaining extracellular DNA within cellular aggregates [Kavanaugh *et al*., 2019].

Strikingly, we found that a small fraction of cells showed much stronger interaction with Cy3-labeled DNA compared to the majority of cells dwelling within colonies (see Fig. 3.5a, b, c). This observation was independent of DNA sample, time of recording or even the gonococcal strain we used and, thus, their appearance had an almost random characteristic. We tested whether the strong retention of Cy3-DNA at the cell envelope was caused by cell death; yet this was not the case (see Fig. 3.5d, e, f).

There is reason to speculate that the strong retention of Cy3-DNA is the result of unspecific binding at the cell envelope, as we also observe this phenomenon in the presence of DNA samples lacking DUS, which cannot be taken up or specifically interacted with by gonococci [Cehovin *et al*., 2013]. Furthermore, we find that these cells often appeared in small clusters of few cells, which could indicate a heritable cause, i.e., phase variations of outer membrane proteins passed on to the progeny, as an explanation for this phenomenon [refer Makino *et al*., 1991]. However, colony dwelling gonococci have a generation time of ~ 1.5 hours [Welker *et al*., 2021]. Since we did not screen colonies for longer than 2 hours, it is unlikely that cell division explains cluster formation in this particular case.

4.2. DNA uptake and ComE foci formation in cellular aggregates

In this study, we investigated the spatio-temporal dynamics of ComE foci formation. ComE foci have been reported to indicate DNA uptake in isolated gonococci since ComE binds to DNA taken up into the periplasm [Gangel *et al*., 2014]. We intended to use ComE foci as an indicator for uptake in gonococcal colonies and characterized their formation under different conditions. We found that in young colonies DNA uptake correlates with ComE focus formation (see section 4.2.1), but our data also reveals that uptake of DNA from the environment cannot fully explain the phenomenon of ComE aggregation and focus formation in gonococcal colonies (see section 4.2.2).

4.2.1. External DNA is primarily taken up by cells in the periphery of colonies

For untreated colonies we found an initial ComE foci density profile with a noticeable slope towards the colony center (see Fig. 3.7a, blue curve), implying that uptake is more abundant in the inner layers of the colony in the absence of external DNA. Since DNA uptake is a prerequisite for transformation, this might indicate that gene transfer is primarily limited to the inner regions of colonies in the absence of (transformable) external DNA [Chen & Dubnau, 2004]. Yet, cells in the deeper layers of colonies and biofilms are known to have inhibited growth rates, which might limit their ability to transform DNA efficiently [Madsen *et al*., 2012; Stalder & Top, 2016; Welker *et al*., 2021].

We established that gonococcal gDNA is very strongly retained in the outer periphery of colonies in previous experiments (see Fig. 3.2c, f); thus, we expected more abundant uptake (i.e., foci formation) around the colony contour when this DNA is added into the growth medium of colonies. Indeed, we found an elevated foci density profile in the peripheral regions compared to untreated colonies, indicating that uptake of external gDNA was limited to the cells in the periphery (see Fig. 3.7). This finding can serve as a first hint that external DNA, penetrating a colony from the surrounding medium or environment, is more efficiently transformed by cells in the periphery; an assumption that is very much in line with previous reports, which highlight that transformation is more efficient in outer cell layers of biofilms [Stalder & Top, 2016].

However, we found that external DNA elevated not just the density of ComE foci in the periphery, but throughout the entire extend of colonies (see Fig. 3.7a, red curve). This finding requires furthers contemplating, since it does not match the strong retention in the periphery we observed for gonococcal gDNA based on detection of fluorescence intensities. We previously

discussed the circumstance that isolation of gonococcal gDNA from cells results in heavily fragmented DNA due to mechanical sheering (see Fig. S14). Hence, smaller fragments could readily penetrate colonies upon which they trigger ComE foci due to uptake [Abdel-Latif & Osman, 2017]. This strong increase is limited to the initial stages of the experiment, as foci density profiles in colonies treated with DNA and untreated control colonies tend to converge for later time points (see Fig. 3.7). This could suggest that DNA uptake is highly efficient in gonococcal colonies, as added eDNA is quickly ridded from the growth medium due to rapid uptake.

We propose that external DNA, which is penetrating gonococcal colonies, is primarily taken up by cells in the outer periphery of colonies, thereby drastically reducing the number of potential transformation targets within the cell aggregate.

4.2.2. Evidence for alternative mechanisms of ComE focus formation in gonococcal colonies

We found evidence that ComE foci in gonococcal colonies might be formed independently of eDNA. First, in the absence of external DNA, we noted that ComE foci are formed extensively in the center colonies. This is not necessarily unexpected, since gonococci can release ample amounts of extracellular DNA due to cell death and autolysis, or secretion of ssDNA by the type IV secretion system (T4SS) and, thus, provide enough DNA as a potential target for ComE to form foci during uptake [Elmros *et al*., 1976; Hamilton *et al*., 2005]. However, the fraction of dead cells in gonococcal colonies is usually below 5 % in the first 4 hours of microcolony formation [Welker *et al*., 2021]. Therefore, DNA release by means of cell death or lysis should be relatively low in early, 1 to 2-hour old colonies composed of few cells. This leaves ssDNA secretion as an alternate mean for DNA release, yet, assessing the contribution of the T4SS to the total amount of extracellular DNA available in colonies is difficult. However, multiple studies have shown that secreted DNA affects initial biofilm formation; thus, one could speculate that the contribution of T4SS-mediated DNA release is substantial [Zweig *et al*., 2014; Callaghan *et al*., 2017]. Nonetheless, the observation that ComE foci formation is extensive in early colonies, even in the absence of externally added DNA, served as a first hint that ComE foci might form independent of any DNA.

To further characterize this observation, we treated colonies with DNase in order to degrade any DNA in the growth medium. Treatment of isolated gonococci with DNase effectively abolishes foci formation, or uptake (see Fig. 3.6) [Gangel *et al*., 2014]; however, this is, surprisingly, not the case in colonies. While foci formation is diminished in the presence of DNase, it does not completely abolish foci formation. This finding was unexpected, since it indicates that DNA uptake is maintained even in the absence of all extracellular DNA in the growth medium.

The foci density profile of DNase treated colonies indicates that foci formation was primarily affected in the outer periphery but maintained in the center of colonies (see Fig. 3.7d, black curve). Therefore, we initially proposed that DNase is maybe hindered from penetrating the colony efficiently, thus preventing the enzyme from degrading DNA in the deeper layers of colonies. This enables sustained foci formation even in the presence of DNase. However, additional experiments utilizing the DNA stain YOYO-1 later revealed that DNase essentially rids all extracellular DNA from colonies (see Fig. 3.14 & Fig. 3.15), thereby disqualifying this hypothesis. Combined, these findings might suggest that ComE forms foci independently of the presence of any extracellular or external DNA.

Recent studies highlight that bacteria can form tubular protrusions, called nanotubes, that bridge neighboring cells. These nanotube-bridges are subsequently used to shuttle cellular components, including DNA, between individual cells, while simultaneously bypassing the extracellular space [Dubey & Ben-Yehuda, 2011]. Furthermore, gonococci are also known to create extracellular outer membrane vesicles, which could act as an alternate pathway for exchange of genetic material while avoiding the extracellular space [Ficht, 2011; Deo *et al*., 2018]. Both mechanisms of DNA exchange would allow gonococci to maintain foci formation and uptake, in the presence of nucleases. Whether or not *N. gonorrhoeae* forms nanotubes remains to be shown, however.

Finally, we cannot rule out that ComE forms foci by a mechanism that is completely independent of DNA. It was shown previously that the DNA uptake systems in bacteria are involved in biofilm formation [Petersen *et al*., 2005]. As ComE is one of the central proteins in the uptake machinery of *N. gonorrhoeae*, it is intriguing to picture that ComE is somehow involved in aiding gonococci to aggregate into colonies and biofilms. If so, ComE foci formation could, in fact, be triggered by colony formation and might not necessarily serve solely as an indicator for DNA uptake in aggregates of *N. gonorrhoeae*.

4.3. Transformation efficiencies in gonococcal colonies

4.3.1. Transformation by external DNA depends on DNA length, cellular growth rates, and the position of transforming cells within colonies

Bacterial biofilms are often described as environments that facilitate highly efficient exchange of genetic material [Li *et al*., 2001; Hendrickx *et al*., 2003; Madsen *et al*., 2012]. However, this assumption is oftentimes not critically questioned and many of the processes regarding gene transfer in cellular aggregates and communities remain unknown [Stalder & Top, 2016]. In this study, we investigated the dynamics of transformation of extracellular DNA penetrating gonococcal colonies with spatial and temporal resolution.

We found that transformation with 3 kb DNA fragments (DUS^+) was limited to the outer periphery of colonies, with very limited transformation in the inner layers of gonococcal cell aggregates (see Fig. 3.9). This observation is in agreement with previous reports, which highlight that gene transfer might be confined to the outer layers of bacterial aggregates and biofilms [Haagensen *et al*., 2002; Stalder & Top, 2016]. It has been proposed that this is likely caused by a large fraction of recipient cells not receiving transformable DNA due to gradients formed within the cell aggregate, which hinder availability of DNA [Molin & Tolker-Nielsen, 2003]. However, this concept is not applicable here, as we showed that Cy3-labelled 3 kb fragments readily reach the inner core of colonies (see Fig. 3.2). Thus, we can exclude a lack of transformable DNA as a reason for limited transformation in the center of gonococcal colonies.

The prerequisite for transformation is DNA uptake, which is mediated by the DNA-binding protein ComE [Chen & Dubnau, 2004]. Indeed, we find evidence that cells in the periphery are more active in taking up external DNA from the growth medium compared to cells in the colony center (see Fig. 3.7). Hence, limited DNA uptake in the presence of ample amounts of transformable DNA could indicate, that uptake and/or transformation of cells in the inner layers is inhibited. This assumption is supported by studies that characterized growth within gonococcal colonies, which was shown to be spatially heterogenous. To be more specific, growth is limited to the outer layers of colonies while cells in the core show signs of growth arrest [Welker *et al*., 2021]. Growth arrested cells might prioritize maintenance and survival functions and, thus, inhibit transformation (and DNA uptake) in favor of cell viability, resulting in poor transformability of cells within the colony core [Bergkessel *et al*., 2016; Stalder & Top, 2016]. However, it should be noted that growth arrest is also known to trigger the exact opposite

effect, as specific bacteria, e.g., *B. subtilis*, are known to induce competence and gene transfer specifically in a growth arrested state [Yüksel *et al*., 2016].

The number of transformants in colonies should increase continuously throughout the experiment assuming we reach saturating levels of transformable DNA. Yet, amounts of DNA in the range of few femtogram are sufficient to obtain detectable transformation frequencies, which is much lower compared to the concentration of 5 ng/µl of DNA we used in our experiments [Molin & Tolker-Nielsen, 2003]. Even so, we find that the average number of transformants in colonies saturates after ~2 hours (see Fig. 3.9b). As we normalized this average with respect to colony size, this finding could serve as evidence that growth rates within gonococcal colonies outcompete transformation rates. Moreover, gonococci organized into cell aggregates are known to move radially from the center towards the periphery of the colony due to cell division and growth [Welker *et al*., 2021. Combined, this indicates that only cells in the periphery of colonies are active and able to transform, whereas cells in the center are arrested for transformation.

Aside from 3 kb DNA fragments we also investigated the transformation efficiencies of 300 bp fragments and gonococcal gDNA; however, none of those samples resulted in transformants after 4 hours of incubation. We established that gonococcal gDNA is very strongly retained in the periphery of colonies (see Fig. 3.2), thereby, drastically limiting the number of recipient cells for this particular nucleotide sample. Even so, given the high density of DNA uptake sequences present within the genome of *N. gonorrhoeae*, uptake of gonococcal gDNA within colonies should be efficient (see also Fig. 3.7). Still, emergence of transformants was not detectable. However, our approach of detecting transformation is based on the replacement of a single nucleotide, yet the genome of *N. gonorrhoeae* is ~ 2.2 Mb [Chung *et al*., 2008]. The bulk of gDNA, thus, represents "junk", at least in the context of our experimental design. Therefore, the likelihood for replacement of the introduced point mutation (*sfgfp*$_{nf}$) by means of gene exchange is significantly reduced compared to 3 kb and 300 bp fragments, as these were generated by PCR and exposed the genetic region of interest on every single molecule. The most likely explanation for the poor transformability of gonococcal gDNA is that the size of the genome significantly decreases the odds to efficiently replace a single point mutation, which is partially mediated by strong retention at the periphery and, thus, a limited number of potential recipient cells.

There is reason to believe that an opposite effect explains the poor transformation of 300 bp fragments: We showed that 300 bp fragments readily penetrate gonococcal colonies, therefore we can exclude a lack of DNA for poor gene transfer (see Fig. 3.2). Furthermore, uptake of 300 bp fragments in gonococci was previously shown to be rapid, occurring on a timescale of few minutes [Gangel *et al*., 2014]. Given that the 300 bp fragments we applied in our experiments contained a DUS, we can expect efficient uptake in colonies, thereby excluding DNA uptake as a limiting factor for poor transformability as well. All things considered, 300 bp fragments are, most likely, simply too short to allow recombination into the genome of *N. gonorrhoeae* due to limited homologous flanking regions [Fujitani *et al*., 1995]. Even so, this highlights that the transformability of aggregated gonococci critically depends on the length-scale of the transforming DNA.

4.4. Free DNA is an important connective linker in bacterial colonies but not an essential one

4.4.1. DNA forms a supporting, stabilizing mesh in gonococcal colonies

We visualized free extracellular DNA within gonococcal colonies utilizing the DNA-intercalating dye YOYO-1. In doing so we could show that extracellular DNA is processed and woven into a lattice of DNA filaments that elongate through the entire cellular aggregate. After 4 hours of growth, the DNA network contained a combination of thin and thick filaments of variable sizes coupled with areas of aggregation, thus creating an intricate 3D structure within the colony (see Fig. 3.12 & Fig. 3.13). Aggregation was particularly abundant in the outer periphery, were the lattice formed a cocooning shell (see Fig. 3.12), and close to lysed cells, indicating that DNA is mainly released by cell death (see Fig. 3.13).

Formation of interwoven eDNA lattices was shown previously within biofilms formed by a variety of bacteria, including *Burkholderia cenocepacia* and *H. influenzae*, indicating that mesh-like arrangement of eDNA is a more universal characteristic of bacteria that aggregate into biofilms [Jurcisek & Bakaletz, 2007; Novotny *et al*., 2013; Devaraj *et al*., 2019]. This suggests that the arrangement of eDNA in biofilms is likely not random, and, in addition, might serve as an indicator that the infrastructure provided by eDNA likely affects the structural integrity of the biofilm [Goodman *et al*., 2011]. For instance, it was proposed that eDNA forms an electrostatic net, which interconnects cells in cellular aggregates [Dengler *et al*., 2015]. Gonococci lack genes to produce exopolysaccharides as potential ECM components [Steichen *et al*., 2011]. Thus, eDNA is, most likely, of more significance in maintaining coherence in gonococcal cell aggregates compared to other bacterial species that produce those ECM components or polymers. Multiple studies have previously reported that DNase treatment had severe effects on gonococcal colonies, such as diminished initial attachment efficiencies or decreased relative biomass [Steichen *et al*., 2011; Zweig *et al*., 2014]. The fact that eDNA forms a cocooning shell around the cell aggregate might indicate that eDNA acts as a peripherical scaffold, potentially providing a framework for crosslinking interactions between cells [Das *et al*., 2013].

Indeed, we found evidence for DNAs significance when treating 4-hour old colonies with DNase. The DNA lattice was dissolved instantly, upon which colonies adopted a bloated morphology as cells dissociated from the colony at the outer periphery (see Fig. 3.15a, b), highlighting that eDNA is an important connective linker in gonococcal colonies. Interestingly

though, we find that colonies do not fall apart completely. Instead, they quickly adapt within few minutes and rearrange (see Fig. 3.15c), suggesting that cells within the colony rapidly meet the challenge of losing crosslinking eDNA. In gonococci T4P are known to affect colony structuring and cohesion by forming an intricate mesh of connective linkers as well [Giltner *et al*., 2012; Hockenberry *et al*., 2016; Pönisch *et al*., 2017; Pönisch *et al*., 2018; Welker *et al*., 2018].

Together, we find strong evidence that eDNA is, indeed, an important structural component in gonococcal colonies; however, it is not an essential one as colonies remain intact even in the absence of eDNA.

4.4.2. On the formation of eDNA filaments in bacterial biofilms

One of the most obvious questions regarding the eDNA lattice found in bacterial biofilms is how and why DNA is specifically processed into a filamentous mesh. It is known that DNA-binding T4P form a similar mesh within gonococcal colonies [Hockenberry *et al*., 2016; Piepenbrink, 2019]. Moreover, fluorescent labeling of elongated T4P reveals filamentous structures very much reminiscent to those we observed for YOYO-1-stained DNA [Ellison *et al*., 2017; Ellison *et al*., 2018]. Thus, we proposed that the formation of eDNA filaments in gonococci is related to the generation of T4P. To test this assumption, we imaged eDNA in colonies formed by a *comP*-knockout strain, which lacks the only DNA-binding pilin subunit of T4P [Cehovin *et al*., 2013].

Interestingly, we find that formation of DNA filaments is not abrogated in a *ΔcomP* background (see Fig. 3.16), indicating that DNA fiber and lattice formation is independent from T4P. However, the DNA lattice is remarkedly less pronounced compared to wildtype colonies, with seemingly truncated and less filaments overall (see Fig. 3.12 & Fig. 3.13), indicating that suppression of the DNA-binding mechanism (*ΔcomP*) affects the arrangement of eDNA in colonies. It is likely that other extracellular DNA-binding proteins are involved in the formation of DNA meshes, as was shown in biofilms of Nontypeable *H. influenzae*, *E. coli* and *S. epidermidis* [Jurcisek & Bakaletz, 2007; Goodman *et al*., 2011; Deveraj *et al*., 2019]. The DNABII family of proteins is a particularly strong candidate in this regard. DNABII have strong structural influence on intracellular DNA, however, seem to be critical in forming a DNA lattice within the ECM of biofilms [Goodman *et al*., 2011]. DNABII binds nicked Holliday Junction DNA with high-affinity and links them within the ECM of bacterial biofilms, thereby forming an integral part of the DNA mesh [Devaraj *et al*., 2019]. Holliday Junctions are DNA-

intermediates of homologous recombination [Punatar *et al*., 2017]. As such, they are formed in the cytosol, but are presumably released into the extracellular space by cell death and lysis, likely together with DNABII [Goodman *et al*., 2011]. However, studies have shown that both are secreted independent of cell lysis by a T4SS and T4P-like system in Nontypeable *H. influenzae*, a species which is closely related to *Neisseria* [Jurcisek *et al*., 2017].

This strongly suggests a similar mechanism for DNA filament formation in gonococci. Secretion of DNABII was not shown for *N. gonorrhoeae*, however gonococci are highly autolytic [Elmros *et al*., 1976]. Thus, DNABII proteins could be released in large quantities due to lysis, together with abundant eDNA. This hypothesis is in good agreement with our finding that DNA filaments tend to aggregate in close proximity to dead cells (see Fig. 3.13). Moreover, the involvement of a T4SS-like system in the formation of the DNA lattice in *H. influenzae* biofilms might highlight ssDNA as a potentially important factor in the formation of the DNA mesh in gonococci, given that they apply the T4SS to secret ssDNA during biofilm formation [Hamilton *et al*. 2005, Zweig *et al*., 2014]. However, YOYO-1 is a poor dye to stain single stranded DNA as it causes extensive DNA nicking, which may lead to breaking of ssDNA [Gibb *et al*., 2012]. It is therefore likely that we did not properly visualize ssDNA in our recordings due to YOYO-1 induced DNA cleavage. Still, a more robust and specific staining method for ssDNA might yield deeper insight into the extent of ssDNA's contribution to the formation of DNA lattices in gonococcal colonies and might provide a better understanding on how eDNA is arranged in bacterial cell aggregates.

Taken together, we propose that T4P mediate gonococcal aggregation, while DNA networks fine-tune the mechanical properties of the colony.

5. Outlook

In this work, we characterized the dynamics of penetration, uptake, and transformation of externally added DNA within cellular aggregates formed by *N. gonorrhoeae* with spatial and temporal resolution. The characterization of these processes and their underlying mechanisms is of significance, given that only few reports have previously focused on their proceedings in cellular aggregates with great detail. Given that cellular aggregates, or biofilms, are usually described as hot spots for gene transfer processes, our findings might add critical pieces of information to obtain a better understanding of genetic exchange within bacterial biofilms [Abe *et al*. 2020]. Moreover, we elucidated DNAs role as a structural component of cellular aggregates by staining free, extracellular DNA within gonococcal colonies; thereby adding additional insight into DNA processing in biofilms as a whole. However, many questions regarding these processes still remain unanswered.

For instance, we found evidence that the nuclease Nuc controls the abundance of DNA with varying length-scales within bacterial colonies, likely in a sequence or methylation dependent manner. One could further pinpoint the mode of action of the enzyme by screening DNA fragments with a given, defined size, yet with random sequences. Differential cleavage could indicate whether or not sequence specificity might be involved in Nuc-mediated DNA cleavage. Similarly, one could generate and screen DNA fragments using targeted methylation or demethylation tools to further characterize the impact of post-transcriptional modifications on the activity of Nuc [Lei *et al*., 2018].

Likewise, methylation could also be involved in the retention of DNA in gonococcal colonies. We found that (*E. coli*) DNA is very strongly retained within colonies even when specific binding is abrogated or hindered. It would be interesting to obtain a better understanding on the exact retention mechanisms and how DNA is trapped, or entangled, within cellular aggregates. Currently, a particular focus lies on cytosolic DNA-binding proteins that crosslink DNA within the biofilm matrix once they are released into the extracellular space [Jurcisek *et al*., 2017; Dengler *et al*., 2015; Deveraj *et al*., 2019]. Several antibodies have since been developed that allow their immunofluorescent visualization in biofilms or, alternatively, target their functional domains, thereby triggering biofilm collapse due to loss of function [Goodman *et al*., 2011; Novotny *et al*., 2016]. Applying said antibodies in colonies and biofilms formed by *N. gonorrhoeae* could potentially uncover the putative role of DNA-binding proteins in gonococcal cell aggregates in greater detail. These proteins are also likely involved in the

formation of DNA lattices in bacterial biofilms, thus adding additional incentives to determine their functions more thoroughly [Deveraj *et al*., 2019].

DNA lattices or meshes are likely also affected by secretion of ssDNA into the extracellular space, which is mediated by the Type IV secretion system (T4SS) [Hamilton *et al*., 2005]. However, when we imaged the formation of DNA meshes within gonococcal colonies, it is likely that we omitted staining of ssDNA due to YOYO-1 induced photocleavage and breakage [Åkermann & Tuite, 1996; Gibb *et al*., 2012]. Future studies could, thus, focus on utilizing a better suited dye or a ssDNA-specific staining method to better highlight the contributions of ssDNA to the formation on DNA filaments [Zweig *et al*., 2014]. It is known that the T4SS is encoded within a region called the gonococcal genetic island (GGI); thus, an alternate approach to further characterize the role of the T4SS in the formation of DNA meshes would include the creation of GGI-mutant strains [Ramsey *et al*., 2011].

Finally, we found evidence that transformation and gene transfer of externally added DNA is limited to the outer periphery of gonococcal colonies, putatively due to growth arrest in the inner layers of cell aggregates. Suppression of the stringent response has previously been reported to trigger premature growth arrest for gonococci [Welker *et al*., 2021]. Thus, additional experiments with a stringent response deficient strain might add further knowledge into whether transformation is really hindered due to growth arrest [Fisher *et al*., 2005]. Our experiments were limited to 4-hour old colonies and we focused on gene exchange in the early stages of biofilm formation. However, transformation is known to have drastic shifts in efficiency over the course of biofilm development [Kouzel *et al*., 2015]. Our experiments could therefore be complemented by additional assays utilizing flow chambers, which allow the investigation of gene transfer processes over prolonged periods. Thereby, these assays could add additional insights into the efficiencies of transformation and the underlying mechanisms of the process in gonococcal and bacterial cell aggregates.

6. Appendix

6.1. Supplementary data and figures

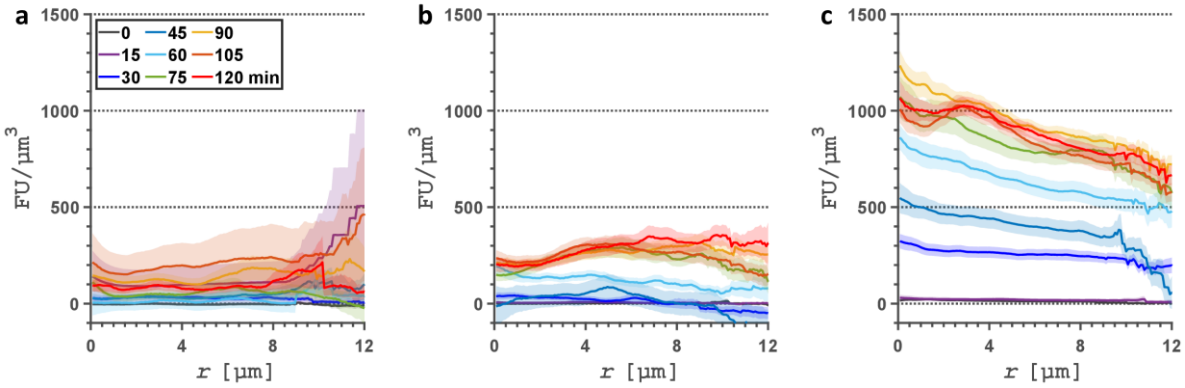

Figure S1: Intensity profiles for Cy3-labelled DUS⁻ DNA in colonies formed by strain *wt (NG194).**
Mean radial fluorescence intensities (FU, in arbitrary units) of Cy3-DNA as a function of the distance (*r*) to the colony contour for all analyzed timepoints. **(a)** 300 bp fragments, **(b)** 3 kb fragments, **(c)** gDNA of *E. coli*. Shaded areas represent standard errors of 26 - 38 colonies.

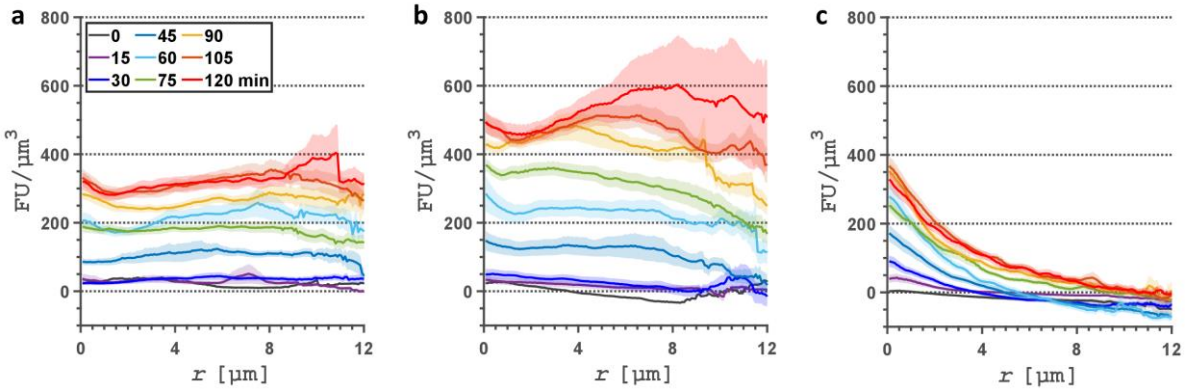

Figure S2: Intensity profiles for Cy3-labelled DUS⁺ DNA in colonies formed by strain *wt (NG194).**
Mean radial fluorescence intensities (FU, in arbitrary units) of Cy3-DNA as a function of the distance (*r*) to the colony contour for all analyzed timepoints. **(a)** 300 bp fragments, **(b)** 3 kb fragments, **(c)** gDNA of *N. gonorrhoeae*. Shaded areas represent standard errors of 30 - 40 colonies.

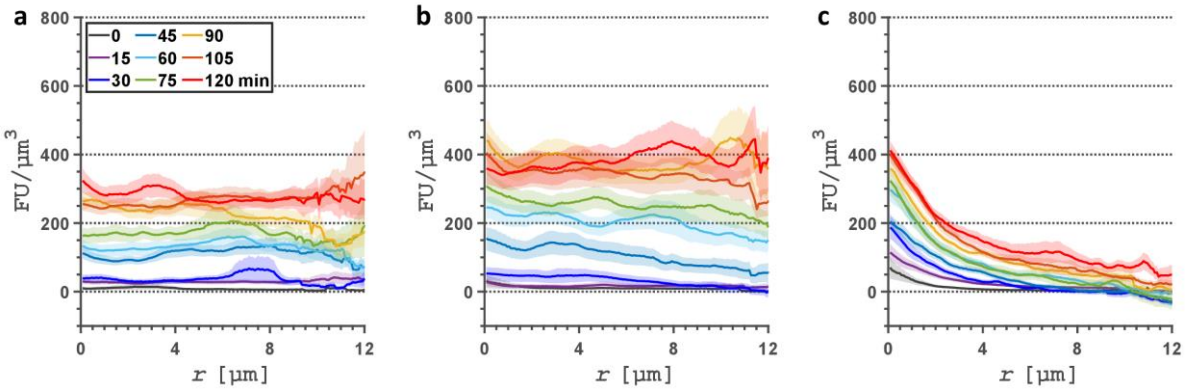

Figure S3: Intensity profiles for Cy3-labelled DUS⁺ DNA in colonies formed by strain *Δnuc* (NG235).
Mean radial fluorescence intensities (FU, in arbitrary units) of Cy3-DNA as a function of the distance (*r*) to the colony contour for all analyzed timepoints. **(a)** 300 bp fragments, **(b)** 3 kb fragments, **(c)** gDNA of *N. gonorrhoeae*. Shaded areas represent standard errors of 30 - 40 colonies.

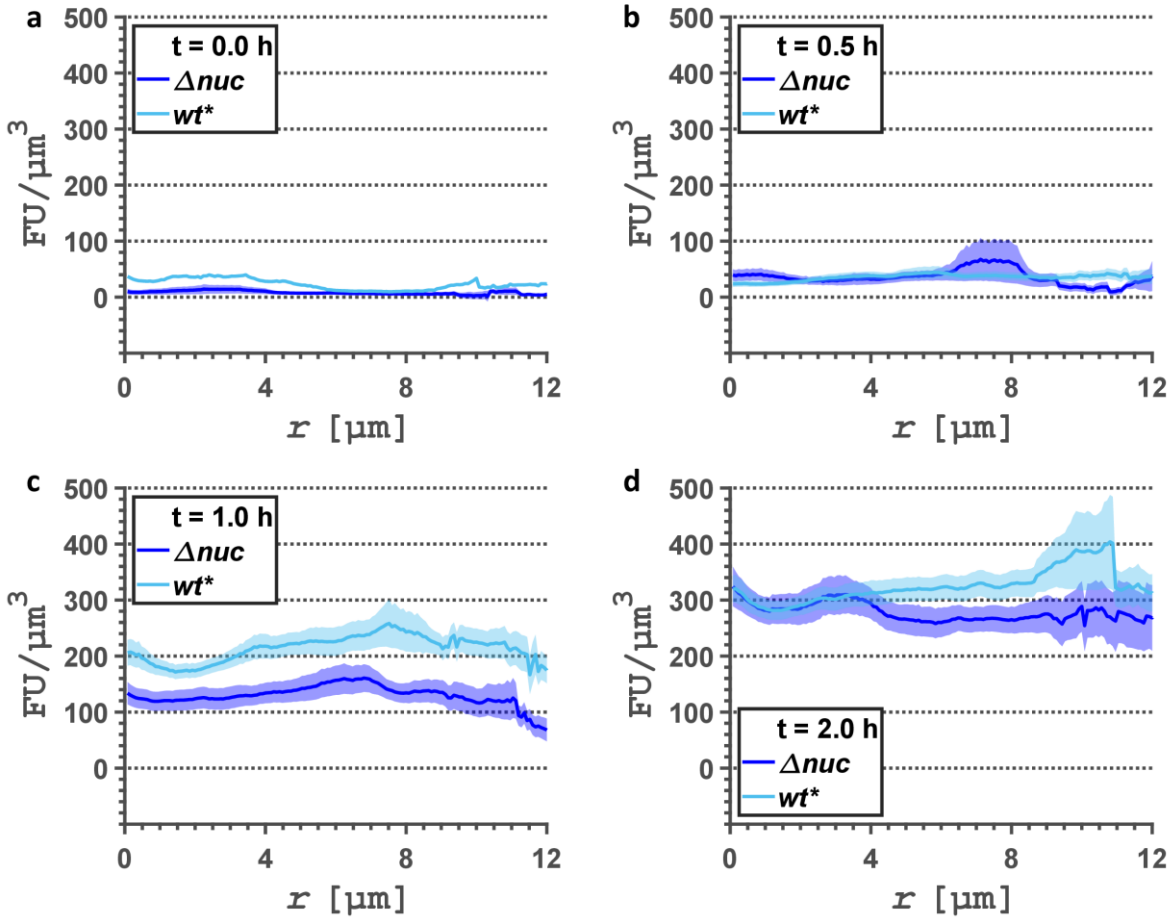

Figure S4: Effect of *nuc*-deletion on abundance of DUS⁺ 300 bp DNA within gonococcal colonies.
Mean radial fluorescence intensities (FU, in arbitrary units) of 300 bp Cy3-DNA as a function of the distance (*r*) to the colony contour immediately after addition to the medium **(a)**, and after 0.5 h **(b)**, 1 h **(c)** and 2 hours **(d)**, for colonies formed by wildtype (*wt**, NG194) and *nuc*-deletion strains (*Δnuc*, NG235). Shaded areas represent standard errors of 32 - 40 colonies.

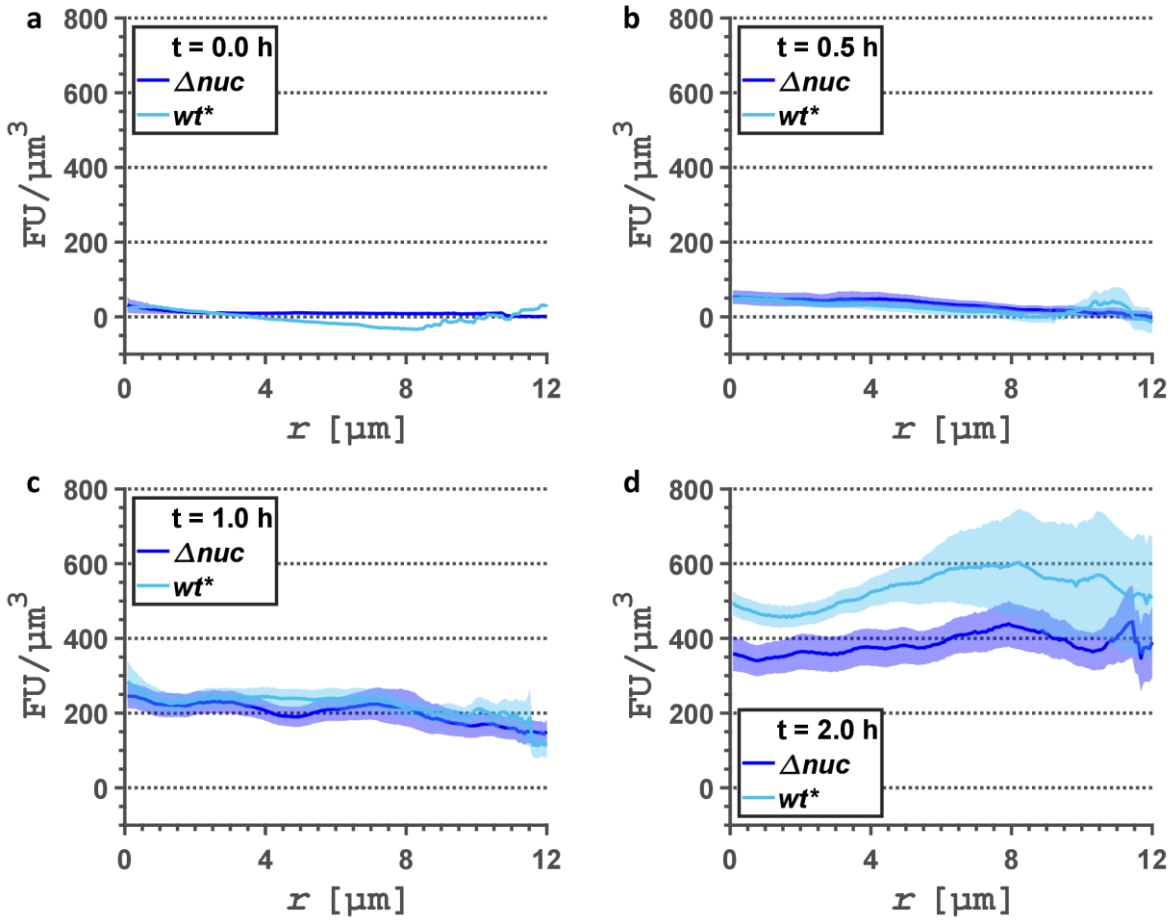

Figure S5: Effect of *nuc*-deletion on abundance of DUS$^+$ 3 kb DNA within gonococcal colonies.

Mean radial fluorescence intensities (FU, in arbitrary units) of 3 kb Cy3-DNA as a function of the distance (*r*) to the colony contour immediately after addition to the medium **(a)**, and after 0.5 h **(b)**, 1 h **(c)** and 2 hours **(d)**, for colonies formed by wildtype (*wt**, NG194) and *nuc*-deletion strains (*Δnuc*, NG235). Shaded areas represent standard errors of 32 - 35 colonies.

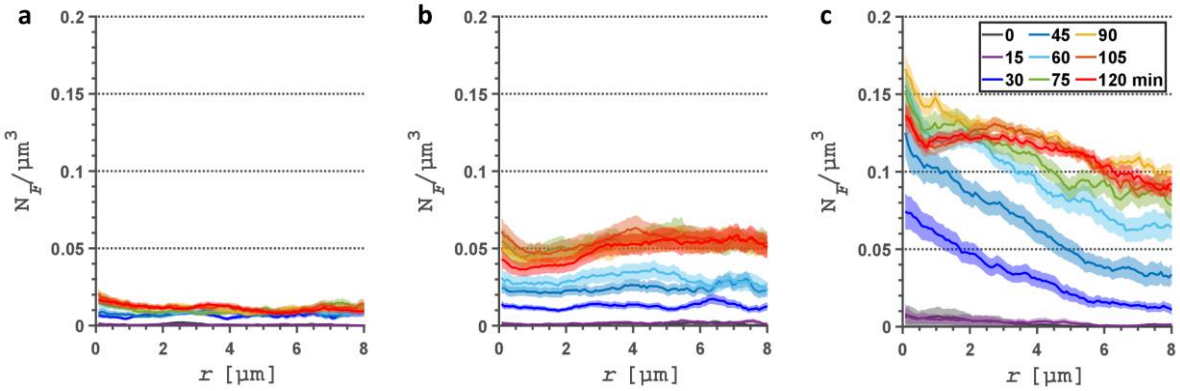

Figure S6: Fluorescence foci profile for Cy3-labelled DUS$^-$ DNA in colonies formed by strain *wt (NG194).**

Density (N_F) of Cy3-DNA foci within colonies as a function of the distance (*r*) to the colony contour for all analyzed timepoints. **(a)** 300 bp fragments, **(b)** 3 kb fragments, **(c)** gDNA of *E. coli*. Shaded areas represent standard errors of 26 - 38 colonies.

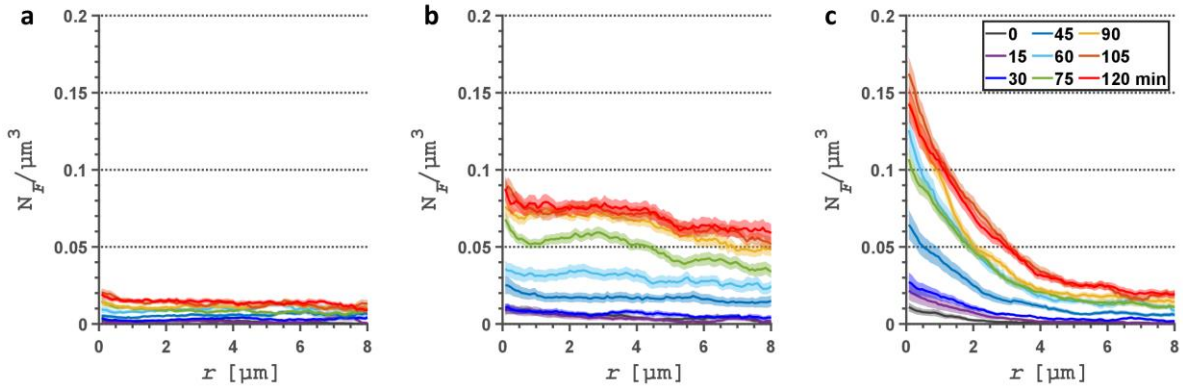

Figure S7: Fluorescence foci profile for Cy3-labelled DUS$^+$ DNA in colonies formed by strain *wt (NG194).** Density (N_F) of Cy3-DNA foci within colonies as a function of the distance (*r*) to the colony contour for all analyzed timepoints. **(a)** 300 bp fragments, **(b)** 3 kb fragments, **(c)** gDNA of *N. gonorrhoeae*. Shaded areas represent standard errors of 30 - 40 colonies.

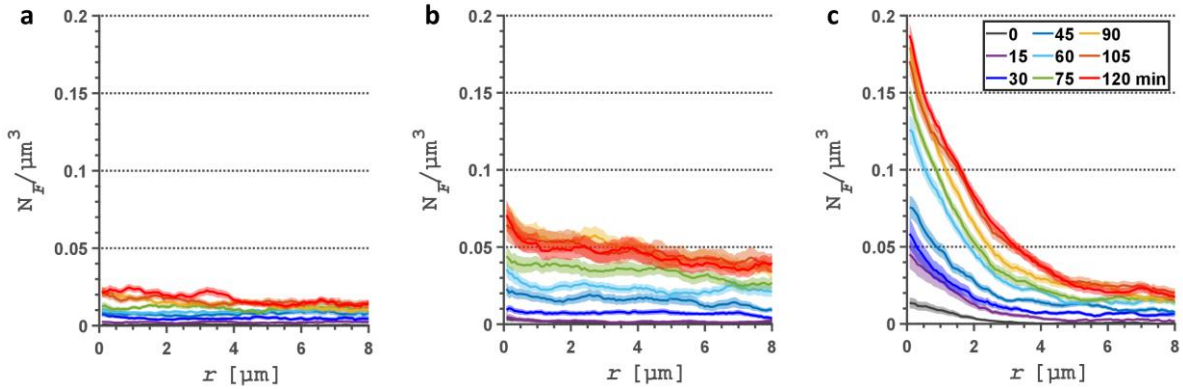

Figure S8: Fluorescence foci profile for Cy3-labelled DUS$^+$ DNA in colonies formed by strain *Δnuc* (NG235). Density (N_F) of Cy3-DNA foci within colonies as a function as a function of the distance (*r*) to the colony contour for all analyzed timepoints. **(a)** 300 bp fragments, **(b)** 3 kb fragments, **(c)** gDNA of *N. gonorrhoeae*. Shaded areas represent standard errors of 30 - 40 colonies.

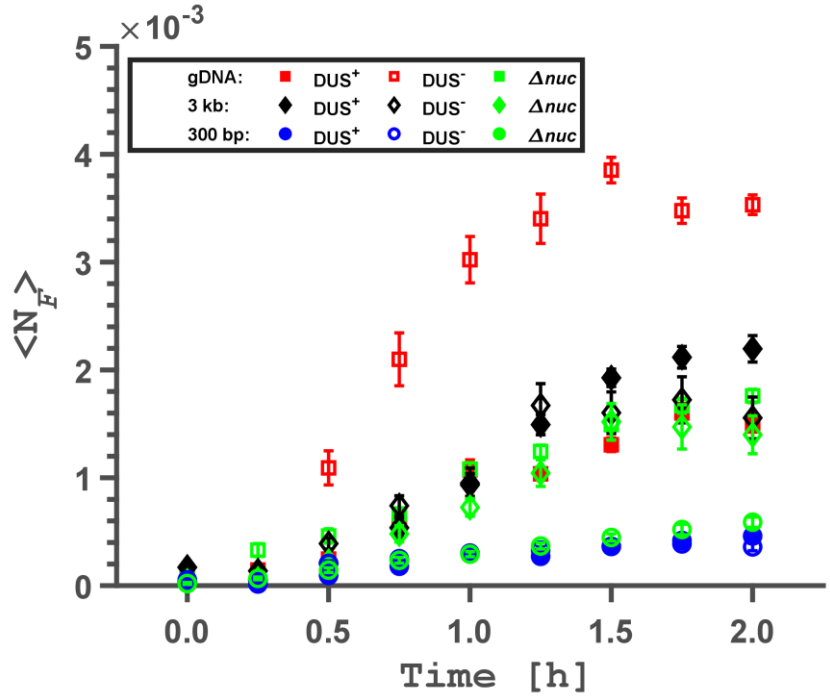

Figure S9: Nuc regulates the amount of DNA that penetrates gonococcal colonies.

Average number of Cy3-DNA foci in colonies formed by *wt** (NG194) and *Δnuc* (NG235) strains, averaged over an area of one pixel (80 x 80 nm) for both DUS^+ and DUS^- DNA samples. *Δnuc* was tested with DUS^+ only. Error bars represent standard errors of 27 – 40 colonies.

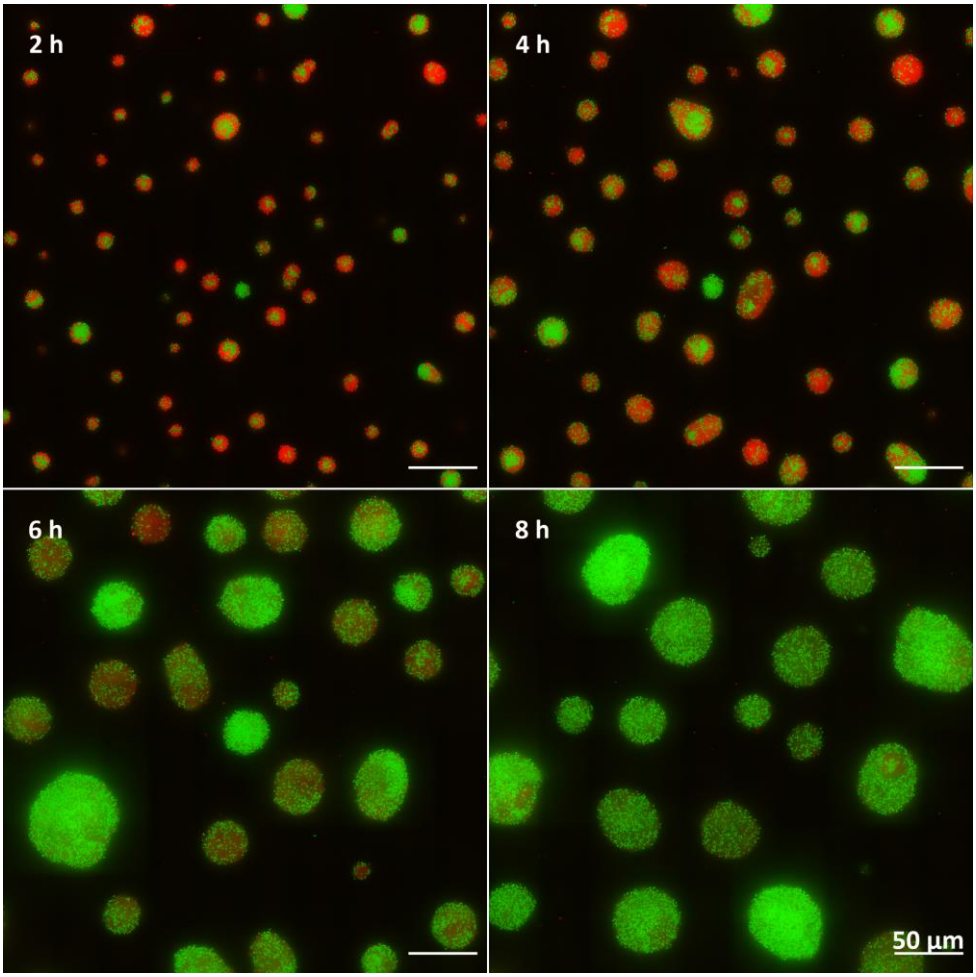

Figure S10: mCherry fluorescence quickly deteriorates within the first few hours of the experiment.
Red-fluorescent strain *wt* sfgfp*$_{nf}$ (strain 1, NG233) and green-fluorescent stain *wt** (strain 2, NG194) were cocultured in a flow chamber and imaged at the indicated time points. Cells expressing mCherry (strain 1), are nicely visible for the first 4 hours of the experiment. However, we observe a drastic decline in fluorescence intensities between 4 - 6 hours. After 8 hours of colony growth, mCherry becomes barely detectable. Scale bars: 50 µm.

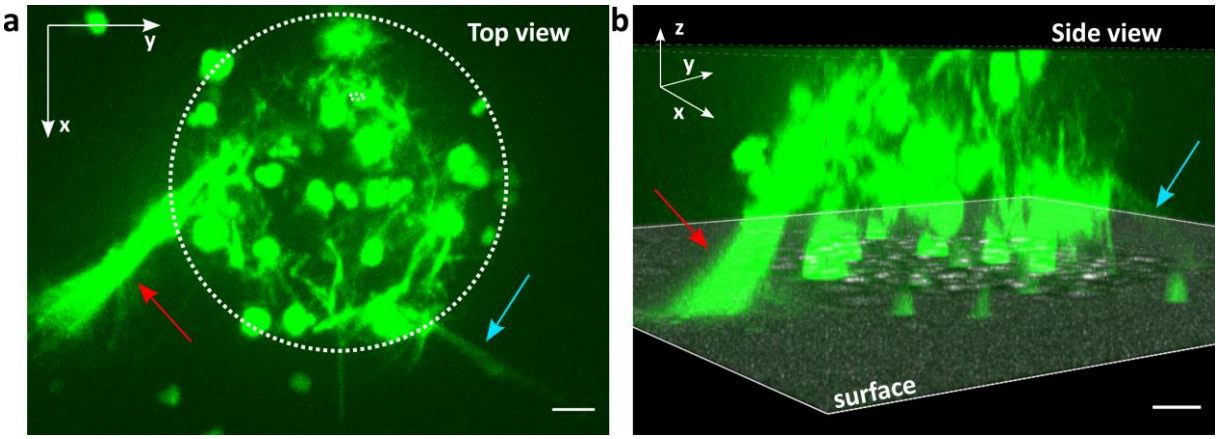

Figure S11: DNA filaments are surface associated, presumably fixing the colony to the surface.
3D volume projection of YOYO-1 fluorescence intensities within a 4-hour old colony of *N. gonorrhoeae* strain *ΔG4* (NG150). **(a)** Aerial 3D view onto the colony, revealing that DNA bundles and filaments are extended into the extracellular space beyond the colony (colored arrows). **(b)** Lateral 3D viewing angle on the same colony. It reveals that the filaments are surface associated, potentially fixating the colony onto the surface. Scale bars: 2.5 µm.

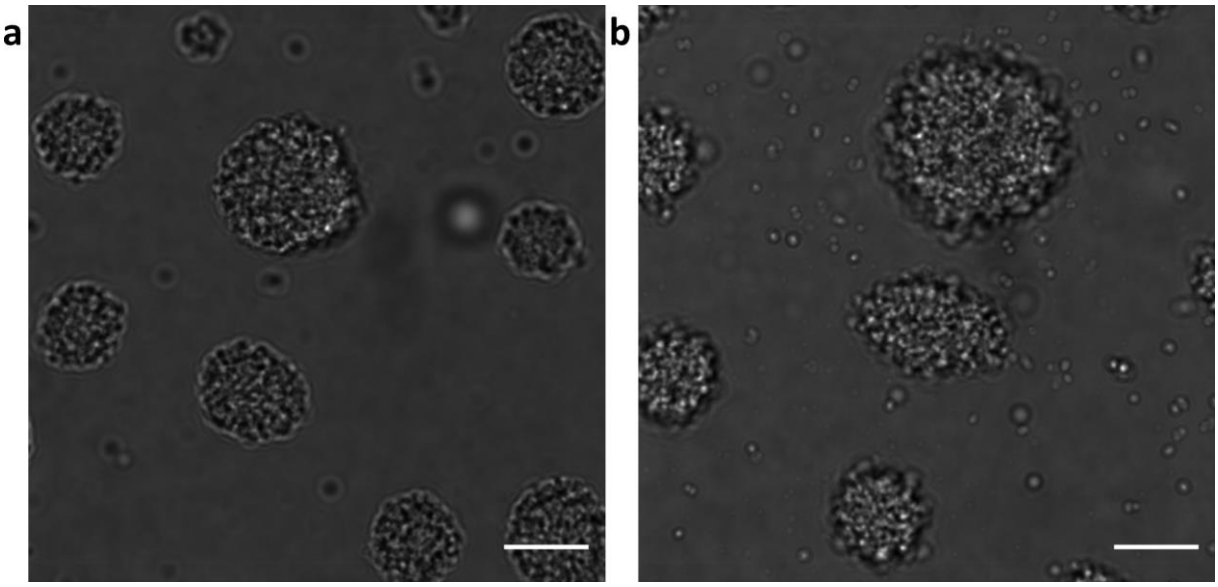

Figure S12: Colonies grown in the presence of DNase show rough and bloated surface morphologies.
Typical brightfield images of 4-hour old colonies formed by *N. gonorrhoeae* strain *ΔG4* (NG150). **(a)** Untreated colonies. **(b)** Colonies grown in medium supplemented with 10 U of recombinant DNase I. Scale bars: 10 µm.

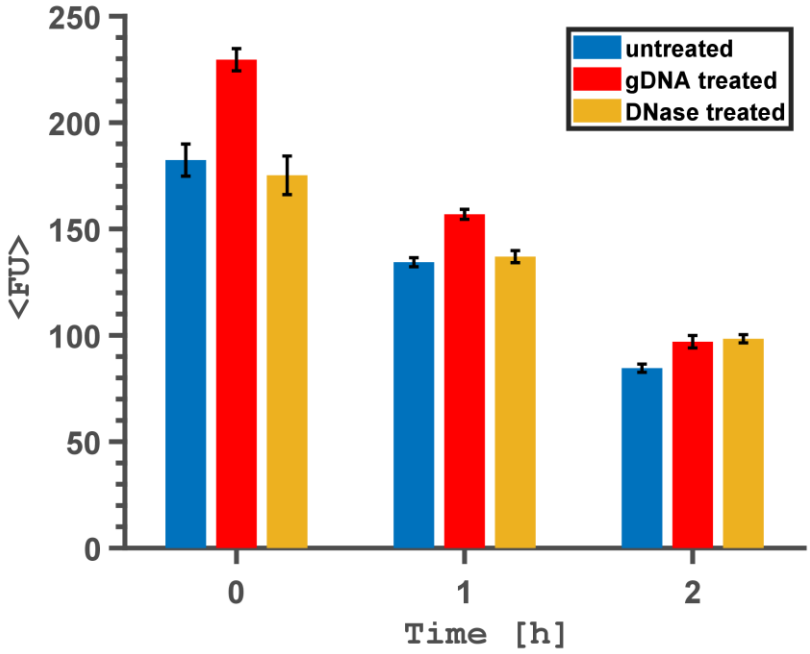

Figure S13: Average fluorescence intensity of ComE-mCherry within colonies formed by strain *comE-mcherry (NG195).**

Mean fluorescence intensities, averaged over an area of one pixel (80 x 80 nm), of ComE-mCherry within gonococcal colonies. Error bars represent standard errors of 30 colonies.

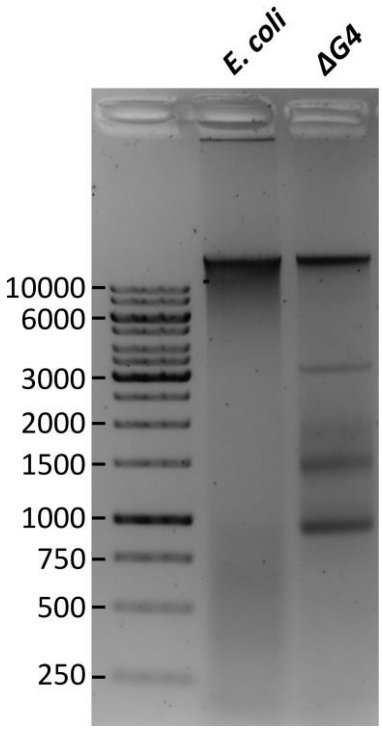

Figure S14: Genomic DNA of *E. coli* and *N. gonorrhoeae* size separated by gel electrophoresis.

1.5 µg of isolated *E. coli* DNA (left) and *N. gonorrhoeae* strain *ΔG4* (NG150, right) size separated in a 1 % agarose gel. Values indicate size marker in base pairs (bp).

6.2. Vector maps

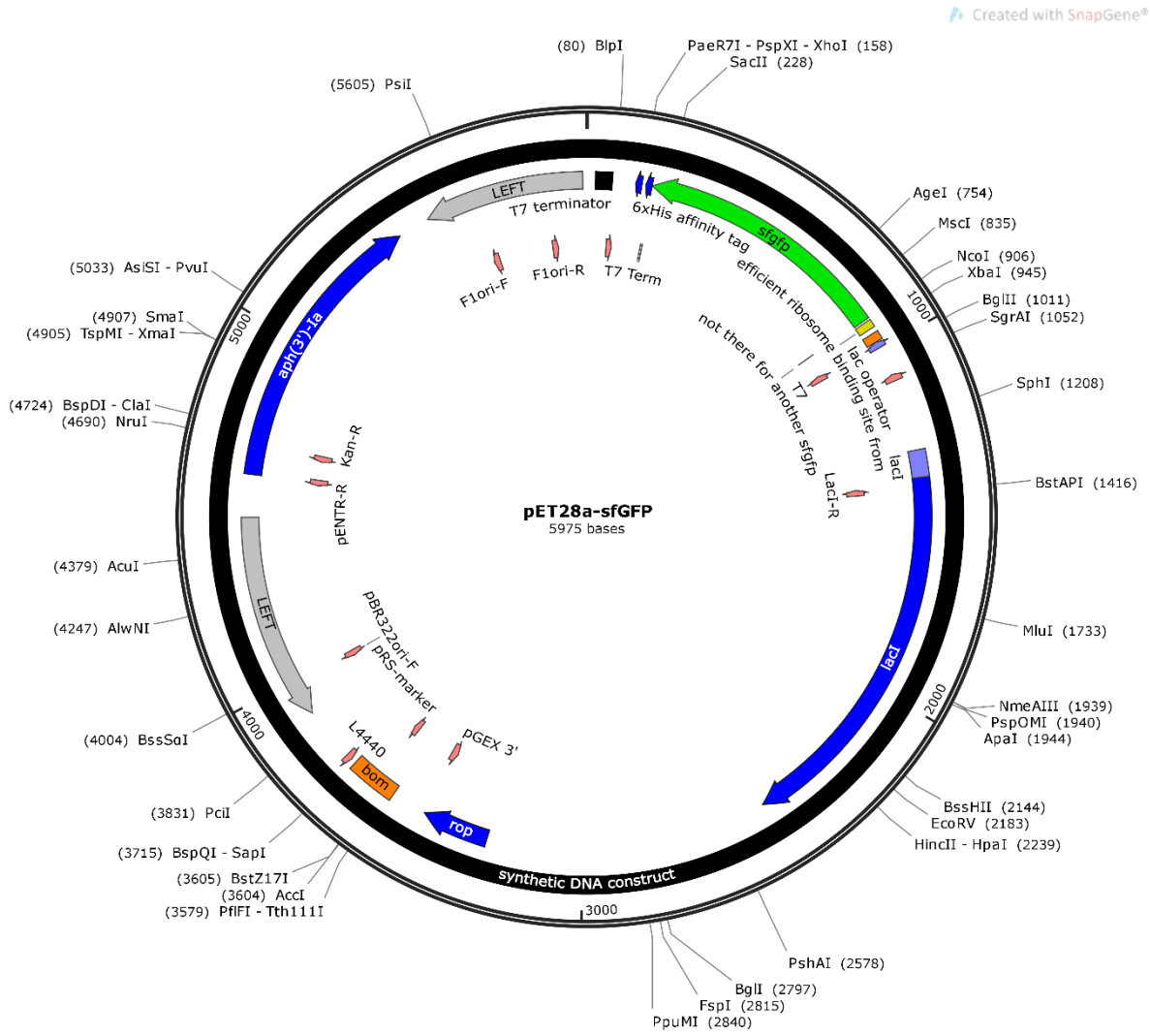


Created with SnapGene®
pLAS
7253 bases
(7058) SalI
(6871) BstXI
(6745) MluI
(6735) BsrGI
PciI (692)
NheI (875)
BmtI (879)
BstAPI (913)
(6091) BstZ17I
MscI (1443)
FspI (1463)
NcoI (1793)
BstBI (2043)
XbaI (2270)
BbvCI - Bpu10I (2293)
SexAI* (2764)
SgrAI (3001)
SspI (3285)
BmgBI (3768)
(3873) FseI
(3880) NsiI
(3886) PacI
(4265) XmnI
(4395) BsaI
(5086) BlpI
7000
1000
2000
3000
4000
5000
6000
pup6part2
DUS
ascP locus
pup6part
Promotor
nptII
SmaI / EcoRI-fragment ComE2down
Okt.-Teil des OH Primers der Resistenz
aminoglycoside-3
-35 PROMOTOR REGION
omega element from R100.1 plasmid
Region gets cut out by insertion of
lctP locus

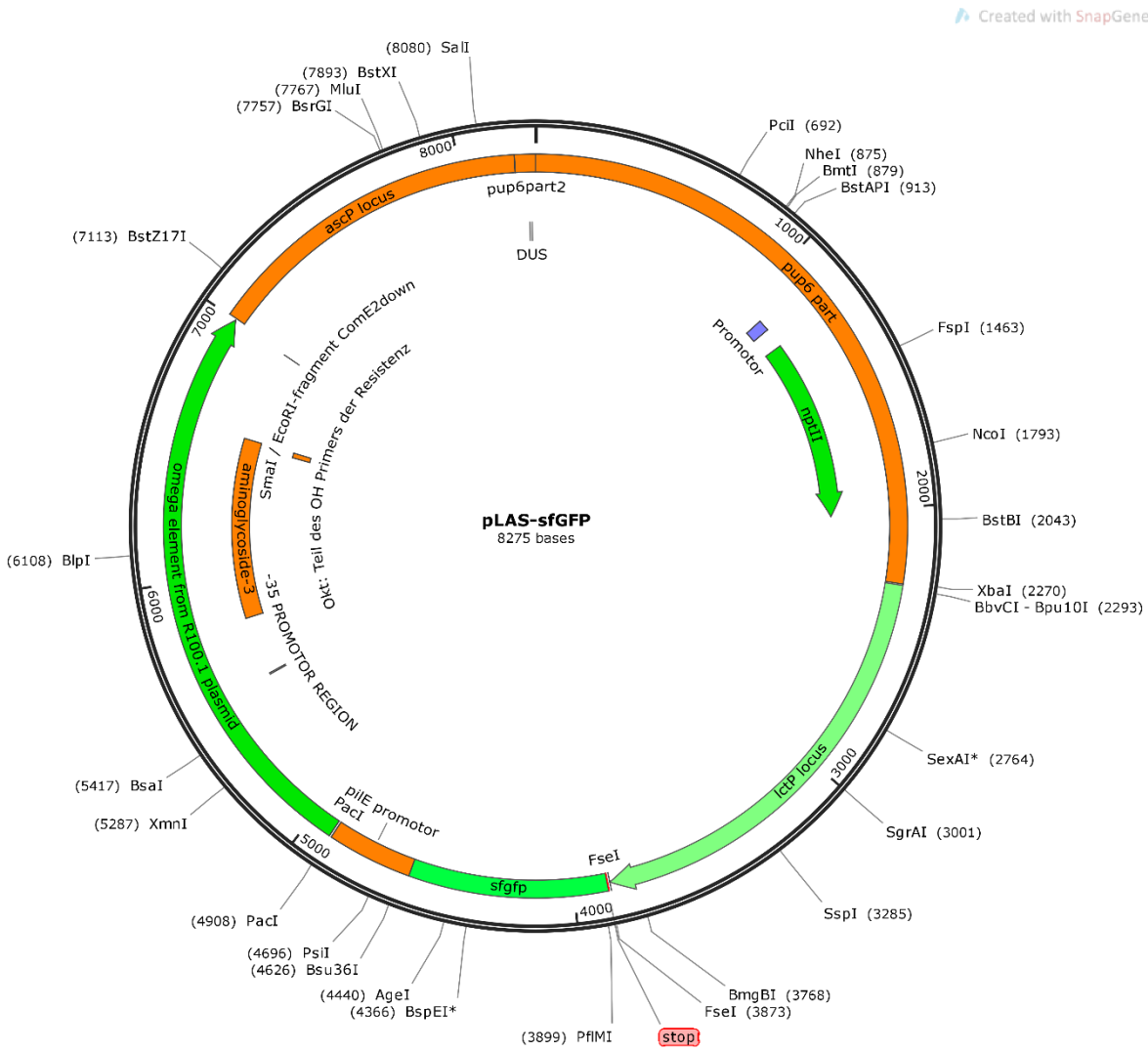
Created with SnapGene®
pLAS-sfGFP
8275 bases
(8080) SalI
(7893) BstXI
(7767) MluI
(7757) BsrGI
8000
PciI (692)
NheI (875)
BmtI (879)
BstAPI (913)
pup6part2
DUS
ascP locus
1000
pup6 part
(7113) BstZ17I
7000
FspI (1463)
Promotor
nptII
NcoI (1793)
2000
BstBI (2043)
XbaI (2270)
BbvCI - Bpu10I (2293)
SmaI / EcoRI-fragment ComE2down
OH: Teil des OH Primers der Resistenz
aminoglycoside-3
-35 PROMOTOR REGION
(6108) BlpI
6000
omega element from R100.1 plasmid
SexAI* (2764)
3000
SgrAI (3001)
(5417) BsaI
(5287) XmnI
pilE promotor
PacI
5000
fctP locus
FseI
sfgfp
4000
SspI (3285)
(4908) PacI
(4696) PsiI
(4626) Bsu36I
(4440) AgeI
(4366) BspEI*
(3899) PflMI
BmgBI (3768)
FseI (3873)
stop

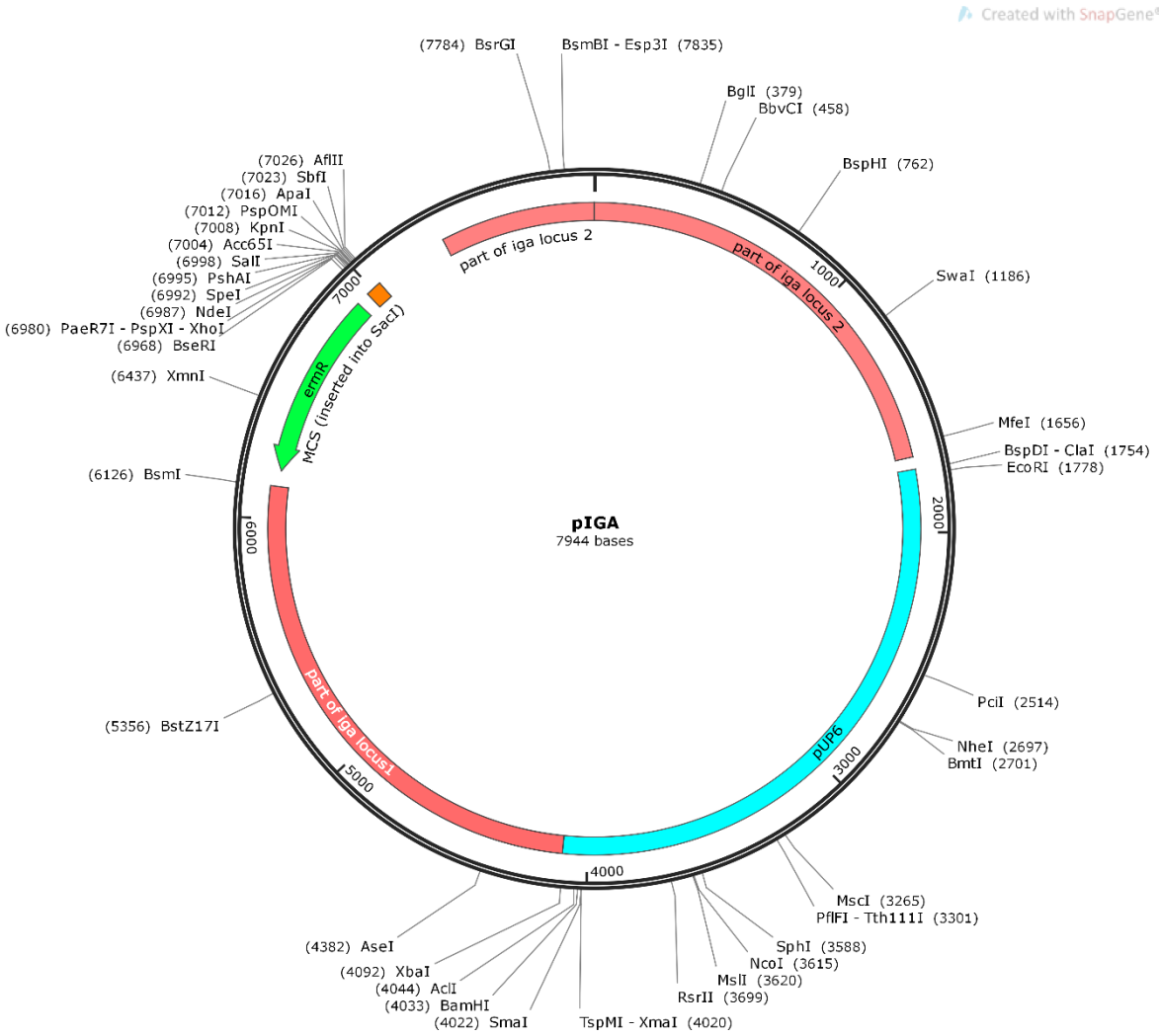
Created with SnapGene®
(7784) BsrGI
BsmBI - Esp3I (7835)
BglI (379)
BbvCI (458)
BspHI (762)
SwaI (1186)
MfeI (1656)
BspDI - ClaI (1754)
EcoRI (1778)
PciI (2514)
NheI (2697)
BmtI (2701)
MscI (3265)
PflFI - Tth111I (3301)
SphI (3588)
NcoI (3615)
MslI (3620)
RsrII (3699)
TspMI - XmaI (4020)
(4382) AseI
(4092) XbaI
(4044) AclI
(4033) BamHI
(4022) SmaI
(5356) BstZ17I
(6126) BsmI
(6437) XmnI
(6980) PaeR7I - PspXI - XhoI
(6968) BseRI
(6987) NdeI
(6992) SpeI
(6995) PshAI
(6998) SalI
(7004) Acc65I
(7008) KpnI
(7012) PspOMI
(7016) ApaI
(7023) SbfI
(7026) AflII
part of iga locus 2
part of iga locus 2
part of iga locus1
ermR
MCS (inserted into SacI)
pUP6
pIGA
7944 bases
1000
2000
3000
4000
5000
6000
7000

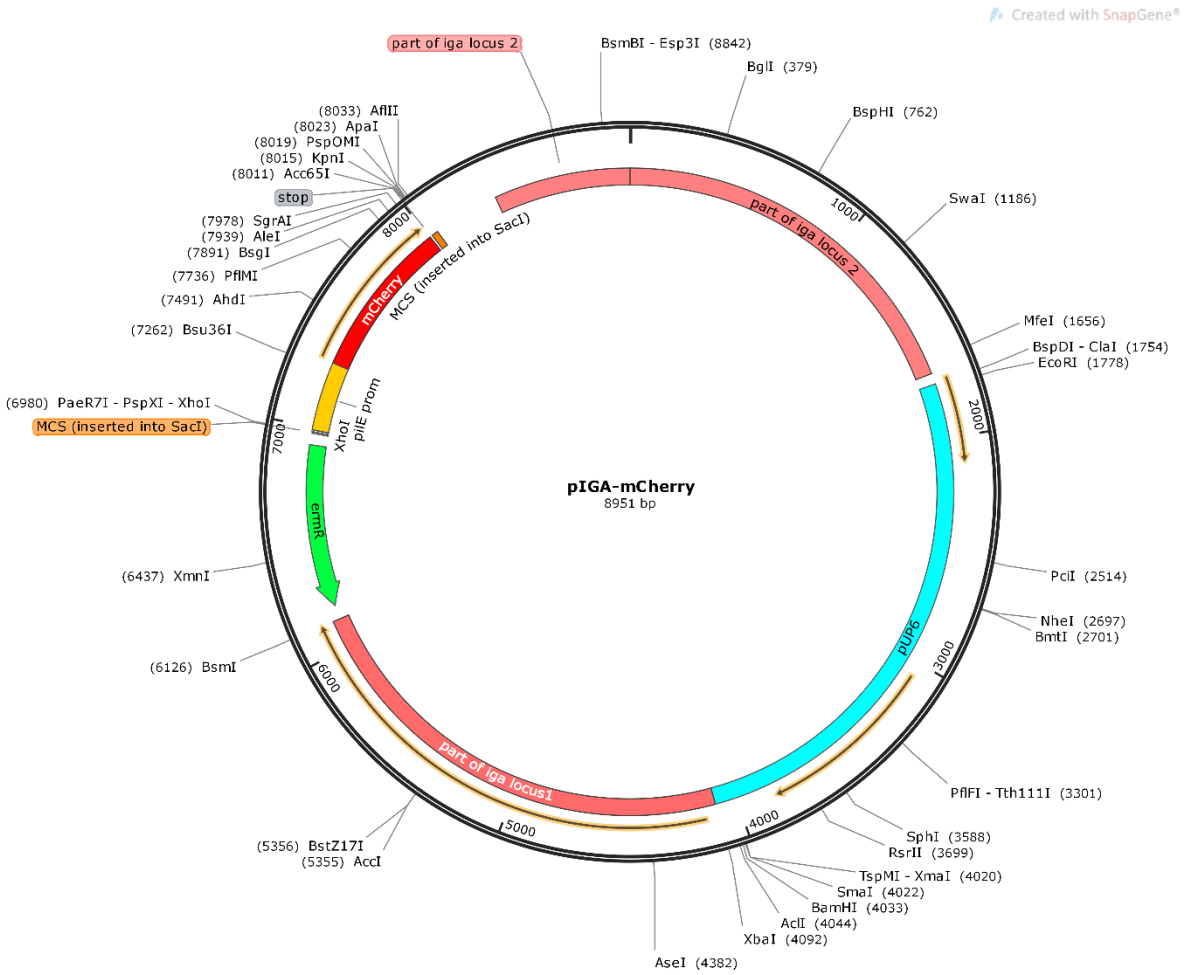
Created with SnapGene®
part of iga locus 2
BsmBI - Esp3I (8842)
BglI (379)
BspHI (762)
SwaI (1186)
MfeI (1656)
BspDI - ClaI (1754)
EcoRI (1778)
PciI (2514)
NheI (2697)
BmtI (2701)
PflFI - Tth111I (3301)
SphI (3588)
RsrII (3699)
TspMI - XmaI (4020)
SmaI (4022)
BamHI (4033)
AclI (4044)
XbaI (4092)
AseI (4382)
(5356) BstZ17I
(5355) AccI
(6126) BsmI
(6437) XmnI
(6980) PaeR7I - PspXI - XhoI
MCS (inserted into SacI)
(7262) Bsu36I
(7491) AhdI
(7736) PflMI
(7891) BsgI
(7939) AleI
(7978) SgrAI
stop
(8011) Acc65I
(8015) KpnI
(8019) PspOMI
(8023) ApaI
(8033) AflII
mCherry
MCS (inserted into SacI)
XhoI
pilE prom
ermR
part of iga locus 2
pUP6
part of iga locus1
1000
2000
3000
4000
5000
6000
7000
8000
pIGA-mCherry
8951 bp

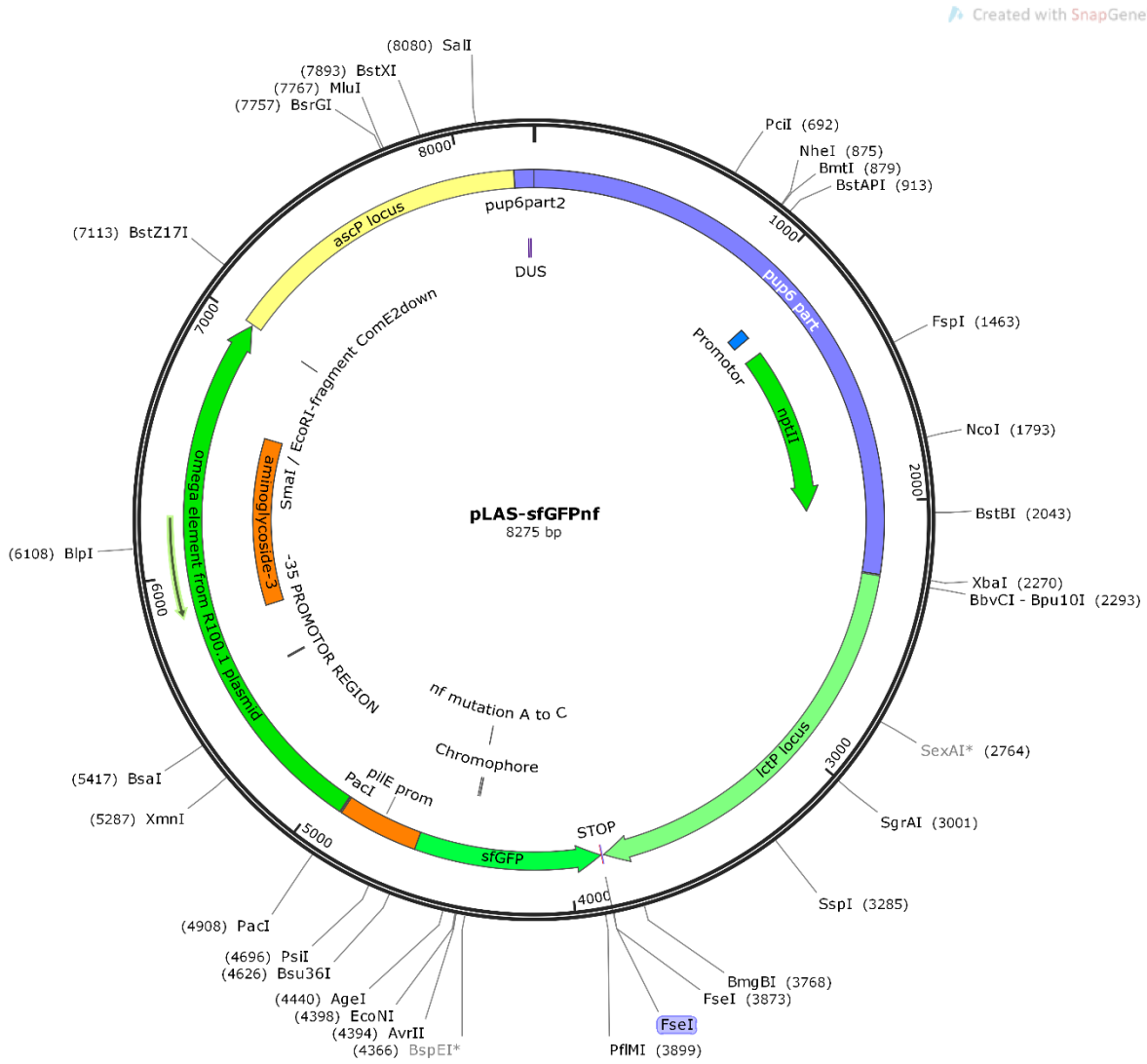
Created with SnapGene®
pLAS-sfGFPnf
8275 bp
(8080) SalI
(7893) BstXI
(7767) MluI
(7757) BsrGI
PciI (692)
NheI (875)
BmtI (879)
BstAPI (913)
(7113) BstZ17I
FspI (1463)
NcoI (1793)
BstBI (2043)
XbaI (2270)
BbvCI - Bpu10I (2293)
(6108) BlpI
SexAI* (2764)
SgrAI (3001)
SspI (3285)
(5417) BsaI
(5287) XmnI
(4908) PacI
(4696) PsiI
(4626) Bsu36I
(4440) AgeI
(4398) EcoNI
(4394) AvrII
(4366) BspEI*
BmgBI (3768)
FseI (3873)
FseI
PflMI (3899)
8000
1000
2000
3000
4000
5000
6000
7000
ascP locus
pup6part2
DUS
pup6 part
Promotor
nptII
SmaI / EcoRI-fragment ComE2down
aminoglycoside-3
-35 PROMOTOR REGION
omega element from R100.1 plasmid
nf mutation A to C
Chromophore
PacI
pilE prom
sfGFP
STOP
ictP locus

List of Figures

List of Tables

Bibliography

Aas F.E., Wolfgang M., Frye S., Dunham S., Løvold C., Koomey M., (2002); Competence for natural transformation in Neisseria gonorrhoeae: components of DNA binding and uptake linked to type IV pilus expression. Molecular Microbiology, 46(3), 749-760

Abdel-Latif A., Osman G., (2017); Comparison of three genomic DNA extraction methods to obtain high DNA quality from maize. Plant Methods, 13(1), doi: 10.1186/s13007-0160152-4

Abe K., Nomura N., Suzuki S., (2020); Biofilms: hot spots of horizontal gene transfer (HGT) in aquatic environments, with focus on a new HGT mechanism. FEMS Microbiology Ecology, 96(5)

Åkermann B., Tuite E., (1996); Single- and Double-Strand Photocleavage of DNA by YO, YOYO and TOTO. Nucleic Acids Research, 24(6), 1080-1090

Allesen-Holm M., Barken K.B., Yang L., Klausen M., Webb J.S., Kjelleberg S., Molin S., Givshov M., Tolker-Nielsen T., (2006); A characterization of DNA release in *Pseudomonas aeruginosa* cultures and biofilm. Molecular Microbiology, 59(4), 1114-1128

Aminov R.I., (2011); Horizontal gene exchange in environmental microbiota. Frontiers in Microbiology, 2, 158, doi: 10.3389/fmicb.2011.00158

Anton B.P., Raleigh E.A., (2016); Complete Genome Sequence of NEB 5-alpha, a Derivative of *Escherichia coli* K-12 DH5α. Genome Announcements, 4(6), e01245-16

Assalkhou R., Balasingham S., Collins R.F., Frye S.A., Davidsen T., Benam A.V., Bjørås M., Derrick J.P., Tønjum T., (2007); The outer membrane secretin PilQ from *Neisseria meningitidis* binds DNA. Microbiology, 153, 1593-1603

Beloin C., Roux A., Ghigo J.M., (2010); *Escherichia coli* biofilms. Current topics in Microbiology and Immunology, 322, 249-289

Bergkessel M., Basta D.W., Newman D.K., (2016); The physiology of growth arrest: uniting molecular and environmental microbiology. Nature Reviews Microbiology, 14, 549-562

Berne C., Kysela D.T., Brun Y.V., (2010); A bacterial extracellular DNA inhibits settling of motile progeny cells within a biofilm. Molecular Microbiology, 77(4), 815-829

Berry J.L., Cehovin A., McDowell M.A., Lea S.M., Pelicic V., (2013); Functional Analysis of the Interdependence between DNA Uptake Sequence and Its Cognate ComP Receptor during Natural Transformation in *Neisseria* Species. PLOS Genetics, 9(12), e1004014

Betzig E., Patterson G.H., Sougrat R., Lindwasser O.W., Olenych S., Bonifacio J.S., Davidson M.W., Lippincott-Schwartz J., Hess H.F., (2006); Imaging Intracellular Fluorescent Proteins at Nanometer Resolution. Science, 313(5793), 1642-1645

Bieber D., Ramer S.W., Wu C.Y., Murray W.J., Tobe T., Fernandez R., Schoolnik G.K., (1998); Type IV Pili, Transient Bacterial Aggregates, and Virulence of Enteropathogenic *Escherichia coli*. Science, 280, 2114-2118

Brendel V., Brocchieri L., Sandler S.J., Clark A.J., Karlin S., (1996); Evolutionary Comparisons of RecA-Like Proteins Across All Major Kingdoms of Living Organisms. Journal of Molecular Evolution, 44, 528-541

Britigan B.E., Cohen M.S., Sparling P.F., (1985); Gonococcal infection: a model of molecular pathogenesis. The New England Journal of Medicine, 312(26), 1683-1694

Broszat M., Grohmann E., (2014); In: Antibiofilm Agents, Horizontal Gene Transfer in Planktonic and Biofilm Modes. Part of the Springer Series on Biofilms book series, BIOFILMS, Vol. 8, pp 67-95

Callaghan M.M., Heilers J.H., van der Does C., Dillard J.P., (2017); Secretion of chromosomal DNA by the Neisseria gonorrhoeae type IV secretion system. Current Topics in Microbiology and Immunology, 413, 323-345

Cehovin A., Simpson P.J., McDowell M.A., Brwon D.R., Noschese R., Pallett M., Brady J., Baldwin G.S. Lea S.M., Matthews S.J., Pelicic V., (2013); Specific DNA recognition mediated by a type IV pilin. Proceedings of the National Academy of Sciences of the United States of America, 110(8), 3065-3070

Ceri H., Olson M.E., Stremick C., Read R.R., Morck D., Buret A., (1999); The Calgary Biofilm Device: new technology for rapid determination of antibiotic susceptibilities of bacterial biofilms. Journal of Clinical Microbiology, 37(6), 1771-1776

Chang Y.W., Rettberg L.A., Treuer-Lange A., Iwasa J., Søgaard-Andersen L., Jensen G.J., (2016); Architecture of the type IV pilus machine. Science, 351(6278)

Chaussee M.S., Hill S.A., (1998); Formation of single-stranded DNA during DNA transformation of *Neisseria gonorrhoeae*. Journal of Bacteriology, 180(19), 5117-5122

Chen I., Gotschlich E.C., (2001); ComE, a Competence Protein from *Neisseria gonorrhoeae* with DNA-Binding Activity. Journal of Bacteriology, 183(10), 3160-3168

Chen I., Dubnau D., (2004); DNA uptake during bacterial transformation. Nature Reviews Microbiology, 2, 241-244

Chew S.C., Kundukad B., Seviour T., van der Maarel J.R.C., Yang L., Rice S.A., Doyle P., Kjelleberg S., (2014); Dynamic Remodeling of Microbial Biofilms by Functionally Distinct Exopolysaccharides. mBio, 5(4), e01536-14

Chiang P., Habash M., Burrows L.L., (2004); Disparate Subcellular Localization Patterns of Pseudomonas aeruginosa Type IV Pilus ATPases Involved in Twitching Motility. Journal of Bacteriology, 187(3), 829-839

Cho C., Chande A., Gakhar L., Bakaletz L.O., Jurcisek J.A., Ketterer M., Shao J., Gotoh K., Foster E., Hunt J., O'Brien E., Apicella M.A., (2015); Role of the Nuclease of Nontypeable *Haemophilus influenzae* in Dispersal of Organisms from Biofilms. Infection and Immunity, 83(3), 950-957

Christensen B.B., Sternberg C., Andersen J.B., Eberl L., Moller S., Givskov M., Molin S., (1998); Establishment of new genetic traits in microbial biofilm community. Applied and Environmental Microbiology, 64(6), 2247-2255

Chung T.C., Yoo J.S., Oh H.B., Lee Y.S., Cha S.H., Kim S.J., Yoo C.K., (2008); Complete Genome Sequence of *Neisseria gonorrhoeae* NCCP11945. Journal of Bacteriology, 190(17), 6035-6036

Clark A.J., (1973); Recombination-deficient mutants of *E. coli* and other bacteria. Annual Review of Genetics, 7, 67-86

Clausen M., Jakovljevic V., Søgaard-Andersen L., Maier B., (2009); High-Force generation Is a Conserved Property of type IV Pilus Systems. Journal of Bacteriology, 191(14), 4633-4638

Collins R.F., Frye S.A., Kitmitto A., Ford R.C., Tønjum T., Derrick J.P., (2004); Structure of the *Neisseria meningitidis* Outer Membrane PilQ secretin complex at 12 Å Resolution. Journal of Biological Chemistry, 279(38), 39750-39756

Costerton J.W., (1995); Overview of microbial biofilms. Journal of Industrial Microbiology, 15(3), 137-140

Cox M.M., (2003); The Bacterial RecA Protein as a Motor Protein. Annual reviews of Microbiology, 57, 551-557

Cox M.M., (2007); Regulation of Bacterial RecA Protein Function. Critical Reviews in Biochemistry and Molecular Biology, 42, 41-63

Craig L., Pique M.E., Tainer J.A., (2004); Type IV pilus structure and bacterial pathogenicity. Nature Reviews Microbiology, 2, 363-378

Craig L., Volkmann N., Arvai A.S., Pique M.E., Yeager M., Egelman E.H., Tainer J.A., (2006); Type IV Pilus Structure by Cryo-Electron Microscopy and Crystallography: Implications for Pilus Assembly and Functions. Molecular Cell, 23(5), 651-662

Craig L., Li J., (2008); Type IV pili: paradoxes in form and function. Current Opinion in Structural Biology, 18(2), 267-277

Craig L., Forest K.T., Maier B. (2019); Type IV pili: dynamics, biophysics and functional consequences. Nature Reviews Microbiology, 17, 429-440

Cuatrecasas P., Fuchs S., Anfinsen C.B., (1967); Catalytic Properties and Specificity of the Extracellular Nuclease of *Staphylococcus aureus*. Journal of Biological Chemistry, 242(7), 1541-1547

Cugini C., Shanmugam M., Landge N., Ramasubbu N., (2019); The Role of Exopolysaccharides in Oral Biofilms. Journal of Dental Research, 98(7), 739-745

Das T., Sehar S., Manefield M., (2013); The roles of extracellular DNA in the structural integrity of extracellular polymeric substance and bacterial biofilm development. Environmental Microbiology Reports, 5(6), 778-786

Davey M.E., O'Toole G.A., (2000); Microbial Biofilms: from Ecology to Molecular Genetics. Microbiology and Molecular Biology Reviews., 64(4), 847-867

Davidsen T., Rødland E.A., Lagesen K., Seeberg E., Rognes T., Tønjum T., (2004); Biased distribution of DNA uptake sequences towards genome maintenance genes. Nucleic Acids Research, 32(3), 1050-1058

Davies D.G., Chakrabarty A.M., Geesey G.G., (1993); Exopolysaccharide production in biofilms: substratum activation of alginate gene expression by *Pseudomonas aeruginosa*. Applied and Environmental Microbiology, 59(4), 1181-1186

de Carvalho C.C.C.R., (2007); Biofilms: Recent Developments on an Old Battle. Recent Patents on Biotechnology, 1, 49-57

Dengler V., Foulston L., DeFrancesco A.S., Losick R., (2015); An Electrostatic Net Model for the Role of Extracellular DNA in Biofilm Formation by *Staphylococcus aureus*. Journal of Bacteriology, 197(24), 3779-3787

Deo P., Chow S.H., Hay I.D., Kleifeld O., Costin A., Elgass K.D., Jiang J.H., Ramm G., Gabriel K., Dougan G., Lithgow T., Heinz E., Naderer T., (2018); Outer membrane vesicles from *Neisseria gonorrhoeae* target ProB to mitochondria and induce apoptosis. PLOS Pathogens, 14(3), e1006945

Devaraj A., Buzzo J.R., Mashburn-Warren L., Gloag E.S., Novotny L.A., Stoodley P., Bakaletz L.O., Goodman S.D., (2019); The extracellular DNA lattice of bacterial biofilms is structurally related to Holliday junction recombination intermediates. Proceedings of the National Academy of Sciences of the United States of America, 116(50), 25068-25077

Di Martino P., (2018); Extracellular polymeric substances, a key element in understanding biofilm phenotype. AIMS Microbiology, 4(2), 274-288

Doi M., Edwards S.F., (1986); The Theory of Polymer Dynamics. In: The International Series of Monographs on Physics, Oxford Science Publications

Doherty A.J., Serpell L.C., Ponting C.P., (1996); The helix-hairpin-helix DNA-binding motif: a structural basis for non-sequence-specific recognition of DNA. Nucleic Acids Research, 24(13), 2488-2497

Domka J., Lee J., Bansal T., Wood T.K., (2007); Temporal gene-expression in *Escherichia coli* K-12 biofilms. Environmental Microbiology, 9(2), 332-346

Donlan R.M., (2001); Biofilm Formation: A Clinically Relevant Microbiological Process. Clinical Infectious Diseases, 33(8), 1387-1392

Donlan R.M., (2002); Biofilms: Microbial Life on Surfaces. Emerging Infectious Diseases, 8(9), 881-890

Donlan R.M., Costerton W.J., (2002); Biofilms: Survival Mechanisms of Clinically Relevant Microorganisms. Clinical Microbiology Reviews, 15(2), 167-193

Donlan R.M., (2008); Biofilms on central venous catheters: is eradication possible? In: Current Topics in Microbiology and Immunology, Bacterial Biofilms 322, 133-61

Dragoš A., Kovács Á.T., (2017); The Peculiar Functions of the Bacterial Extracellular Matrix. Trends in Microbiology, 25(4), 257-266

Dragoš A., Kiesewalter H., Martin M., Hsu C.Y., Hartmann R., Wechsler T., Eriksen C., Brix S., Drescher K., Stanley-Wall N., Kümmerli R., Kovács A.T., (2018); Division of Labor during Biofilm Matrix Production. Current Biology, 28(12), 1903-1913.e5

Driffield K., Miller K., Bostock J.M., O'Neill A.J., Chopra I., (2008); Increased mutability of *Pseudomonas aeruginosa* in biofilms. Journal of Antimicrobial Chemotherapy, 61(5), 1053-1056

Dubey G.P., Ben-Yehuda S., (2011); Intercellular Nanotubes Mediate Bacterial Communication. Cell, 144(4), 590-600

Dubnau D., (1999); DNA Uptake in Bacteria. Annual Review of Microbiology, 53, 217-244

Dunne W.M., (2002); Bacterial adhesion: seen any good biofilms lately? Clinical Microbiology Reviews, 15(2), 155-166

Dutta C., Pan A., (2002); Horizontal gene transfer and bacterial diversity. Journal of Biosciences, 27(1), 27-33

El-Khoury N., Bennaceur I., Verplaetse E., Aymerich S., Lereclus D., Kallassy M., Gohar M., (2021); Massive Integration of Planktonic Cells within a Developing Biofilm. Microorganisms, 9, 298

Elkins C., Thomas C.E., Seifert H.S., Sparling P.F., (1991); Species-specific uptake of DNA by gonococci is mediated by a 10-base-pair sequence. Journal of Bacteriology, 173(12), 3911-3913

Ellison C.K., Kan J., Dillard R.S., Kysela D.T., Ducret A., Berne C., Hampton C.M., Ke Z., Wright E.R., Biais N., Dalia A.B., Brun Y.V., (2017); Obstruction of pilus retraction stimulates bacterial surface sensing. Science, 358(6362), 535-538

Ellison C.K., Dalia T.N., Ceballos A.V., Wang J.C.Y., Biais N., Brun Y.V., Dalia A.B., (2018); Retraction of DNA-bound type IV competence pili initiates DNA uptake during natural transformation in *Vibrio cholerae*. Nature Microbiology, 3, 773-780

Elmros T., Burman L.G., Bloom G.D., (1976); Autolysis of Neisseria Gonorrhoeae. Journal of Bacteriology, 126(2), 969-976

Emamalipour M., Seidi K., Vahed S.Z., Jahanban-Esfahlan A., Jaymand M., Majdi H., Amoozgar Z., Chitkushev L.T., Javaheri T., Jahanban-Esfahlan R., Zare P., (2020); Horizontal Gene Transfer: From Evolutionary Flexibility to Disease Progression. Frontiers in Cell and Developmental Biology. Doi: 10.3389/fcell.2020.00229

Evans K.J., Lambert C., Sockett R.E., (2007); Predation by *Bdellovibrio bacteriovorus* HD100 Requires Type IV Pili. Journal of Bacteriology, 189(13), 4850-4859

Facius D., Meyer T.F., (1993); A novel determinant (*comA*) essential for natural transformation competence in *Neisseria gonorrhoeae* and the effect of a *comA* defect on pilin variation. Molecular Microbiology, 10(4), 699-712

Facius D., Fussenegger M., Meyer T.F., (1996); Sequential action of factors involved in natural competence for transformation of Neisseria gonorrhoeae. FEMS Microbiology Letters, 137(2-3), 159-164

Ficht T.A., (2011); Bacterial Exchange via Nanotubes: Lessons Learned from the History of Molecular Biology. Frontiers in Microbiology, 2(179), doi: 10.3389/fmicb.2011.00179

Fiore M.A., Raisman J.C., Wong N.H., Hudson A.O., Wadsworth C.B., (2020); Exploration of the Neisseria Resistome Reveals Resistance Mechanisms in Commensals That May Be Acquired by *N. gonorrhoeae* through Horizontal Gene Transfer. Antibiotics, 9, 656, doi: 10.3390/antibiotics9100656

Fisher S.D., Reger A.D., Baum A., Hill S.A., (2005); RelA alone appears essential for (p)ppGpp production when *Neisseria gonorrhoeae* encounters nutritional stress. FEMS Microbiology Letters, 248(1), 1-8

Flemming H.C., Neu T.R., Wozniak D.J., (2007); The EPS Matrix: The "House of Biofilm Cells". Journal of Bacteriology, 189(22); 7945-7947

Flemming H.C., Wingender J., (2010); The biofilm matrix. Nature Reviews Microbiology, 8, 623-633

Flemming H.C., Wingender J., Szewzyk U., Steinberg P., Rice S.A., Kjelleberg S., (2016); Biofilms: an emergent form of bacterial life. Nature Reviews Microbiology, 14, 563-575

Floury J., Mourdi I.E., Silva J.V.C., Lortal S., Thierry A., Jeanson S., (2015); Diffusion of solutes inside bacterial colonies immobilized in model cheese depends on their physiochemical properties: a time-lapse microscopy study. Frontiers in Microbiology, 6, 366, doi: 10.3389/fmicb.2015.00366

Friedrich C., Bulyha I., Søgaard-Andersen L., (2014); Outside-In Assembly Pathway of the Type IV Pilus System in *Myxococcus xanthus*. Journal of Bacteriology, 196(2), 378-390

Frye S.A., Nilsen M., Tønjum T., Ambur O.H., (2013); Dialects of the DNA Uptake Sequence in *Neisseriaceae*. PLOS Genetics, 9(4), e1003458

Fujitani Y., Yamamoto K., Kobayashi I., (1995); Dependence of frequency of homologous recombination on the homology length. Genetics, 140(2), 797-809

Gangel H., Hepp C., Müller S., Oldewurtel E.R., Aas F.E., Koomey M., Maier B., (2014); Concerted Spatio-Temporal Dynamics of Imported DNA and ComE DNA Uptake Protein during Gonococcal Transformation. PLOS Pathogens, 10(4), e1004043

Garcia D.L., Dillard J.P., (2006); AmiC Functions as an *N*-Acetylmuramyl-L-Alanine Amidase Necessary for Cell Separation and Can Promote Autolysis in *Neisseria gonorrhoeae*. Journal of Bacteriology, 188(20), 7211-7221

Gibb B., Silverstein T.D., Finkenstein I.J., Greene E.C., (2012); Single-Stranded DNA Curtains for Real-Time Single-Molecule Visualization of Protein-Nucleic Acid Interactions. Analytical Chemistry, 84(18), 7607-7612

Giltner C.L., Nguyen Y., Burrows L.L. (2012); Type IV Pilin Proteins: Versatile Molecular Modules. Microbiology and Molecular Biology Reviews, 76(4), 740-772

Gloag E.S., Turnbull L., Huang A., Vallotton P., Wang H., Nolan L.M., Mililli L., Hunt C., Lu J., Osvath S.R., Monahan L.G., Cavaliere R., Charles I.G., Wand M.P., Gee M.L., Prabhakar R., Whitchurch C.B., (2013); Self-organization of bacterial biofilms is facilitated by extracellular DNA. Proceedings of the National Academy of Sciences of the United States of America, 110(28), 11541-11546

Goldenfeld N., Woese C., (2007); Biology's next revolution. Nature, 445, 369

Goodman S.D., Scocca J.J., (1988); Identification and arrangement of the DNA sequence recognized in specific transformation of Neisseria gonorrhoeae. Proceedings of the National Academy of Sciences of the United States of America, 85(18), 6982-6986

Goodman S.D., Obergfell K.P., Jurcisek J.A., Downey L.A., Ayala E.A., Tjokro N., Li B., Justice S.S., Bakaletz L.O., (2011); Biofilms can be dispersed by focusing the immune system on a common family of bacterial nucleoid-associated proteins. Mucosal Immunology, 4, 625-637

Greiner L.L., Edwards J.L., Shao J., Rabinak C., Entz D., Apicella M.A., (2005); Biofilm Formation by *Neisseria gonorrhoeae*. Infection and Immunity, 73(4), 1964-1970

Gunn J.S., Piekarowicz A., Chien R., Stein D.C., (1992); Cloning and Linkage Analysis of *Neisseria gonorrhoeae* DNA Methyltransferases. Journal of Bacteriology, 174(17), 5654-5660

Gyles C., Boerlin P., (2014); Horizontally Transferred Genetic Elements and Their Role in Pathogenesis of Bacterial Disease. Veterinary Pathology, 51(2), 328-340

Haagensen J.A.J., Hansen S.K., Molin J.S., (2002); In situ detection of horizontal transfer of mobile genetic elements. FEMS Microbiology Ecology, 42(2), 261-268

Haberman A., Heywood J., Meselson M., (1972); DANN Modification Methylase Activity of *Escherichia coli* Restriction Endonucleases K and P. Proceedings of the National Academy of Sciences of the United States of America, 69(11), 3138-3141

Hall-Stoodley L., Costerton W.J., Stoodley P., (2004); Bacterial biofilms: from the Natural environment to infectious diseases. Nature Reviews Microbiology, 2, 95-108

Hamilton H.L., Dominguez N.M., Schwartz K.J., Hackett K.T., Dillard J.P., (2005); *Neisseria gonorrhoeae* secretes chromosomal DNA via a novel type IV secretion system. Molecular Microbiology, 55(6), 1704-1721

Hamilton H.L., Dillard J.P., (2005); Natural transformation of *Neisseria gonorrhoeae*: from DNA donation to homologous recombination. Molecular Microbiology, 59(2), 376-385

Hara T., Ueda S., (1981); A Study on the Mechanism of DNA Excretion from *P. aeruginosa* KYU-1 – Effect of Mitomycin C on Extracellular DNA Production -. Agricultural and Biological Chemistry, 45(11), 2457-2461

Harmsen M., Lappann M., Knøchel S., Molin S., (2010); Role of Extracellular DNA during Biofilm Formation by *Listeria monocytogenes*. Applied and Environmental Microbiology, 76(7), 2271-2279

Hasegawa H., Suzuki E., Maeda S., (2018); Horizontal Plasmid Transfer by Transformation in *Escherichia coli*: Environmental Factors and Possible Mechanisms. Frontiers in Microbiology, doi: 10.3389/fmicb.2018.02365

Hausner M., Wuertz S., (1999); High Rates of Conjugation in Bacterial Biofilms as Determined by Quantitative In Situ Analysis. Applied and Environmental Microbiology, 65(8), 3710-3713

Hazan Z., Zumeris J., Jacob H., Raskin H., Kratysh G., Vishnia M., Dror N., Barliya T., Mandel M., Lavie G., (2006); Effective Prevention of Microbial Biofilm Formation on Medical Devices by Low-Energy Surface Acoustic Waves. Antimicrobial Agents and Chemotherapy, 50(12), 4144-4152

Hegge F.T., Hitchen P.G., Aas F.E., Kristiansen H., Løvold C., Egge-Jacobsen W., Panico M., Leong W.Y., Bull V., Virji M., Morris H.R., Dell A., Koomey M., (2004); Unique modifications with phosphocholine and phosphoethanolamine define alternate antigenic forms of *Neisseria gonorrhoeae* type IV pili. Proceedings of the National Academy of Sciences of the United States of America, 101(29), 10798-10803

Helaine S., Dyer D.H., Nassif X., Pelicic V., Forest K.T., (2007); 3D structure/function analysis of PilX reveals how minor pilins can modulate the virulence properties of type IV pili. Proceedings of the National Academy of Sciences of the United States of America, 104(40), 15888-15893

Hendrickx L., Hausner M., Wuertz S., (2003); Natural Genetic Transformation in Monoculture *Acinetobacter sp*. Strain BD413 Biofilms. Applied and Environmental Microbiology, 69(3), 1721-1727

Hepp C., Maier B., (2016); Kinetics of DNA uptake during transformation provide evidence for a translocation ratchet mechanism. Proceedings of the National Academy of Sciences of the United States of America, 113(44), 12467-12472

Hepp C., (2017); The molecular mechanism of outer membrane DNA transport in bacterial transformation. PhD thesis, University of Cologne

Hess S.T., Girirajan T.P.K., Mason M.D., (2006); Ultra-High Resolution Imaging by Fluorescence Photoactivation Localization Microscopy, Biophysical Journal, 91(11), 4258-4272

Higashi D.L., Lee S.W., Snyder A., Weyand N.J., Bakke A., So M., (2007); Dynamics of *Neisseria gonorrhoeae* Attachment: Microcolony Development, Cortical Plaque Formation, and Cytoprotection. Infection and Immunity, 75(10), 4743-4753

Hill S.A., Masters T.L., Wachter J., (2016); Gonorrhea – am evolving disease of the new millennium. Microbial Cell, 3(9), 371-389

Hobley L., Harkins C., MacPhee C.E., Stanley-Wall N.R., (2015); Giving structure to the biofilm matrix: an overview of individual strategies and emerging common themes. FEMS Microbiology Reviews, 39(5), 649-669

Hockenberry A.M., Hutchens D.M., Agellon A., So M., (2016); Attentuation of Type IV Pilus Retraction Motor Influences Neisseria gonorrhoeae Social and Infection Behavior. mBio, 7(6), e01994-16

Høiby N., Bjarnsholt T., Givskov M., Molin S., Ciofu O., (2010); Antibiotic resistance of bacterial biofilms. International Journal of Antimicrobial Agents, 35(4), 322-332

Høiby N., Bjarnsholt T., Moser C., Bassi G.L., Coenye T., Donelli G., Hall-Stoodley L., Holá V., Imbert C., Kirketerp-Møller K., Lebeaux D., Oliver A., Ullmann A.J., Williams C., ESCMID Study Group for Biofilms and Consulting External Expert Werner Zimmerli, (2014); ESCMID guideline for the diagnosis and treatment of biofilm infections 2014. Clinical Microbiology and Infection, 21(1), S1-S25

Holz C., Opitz D., Greune L., Kurre R., Koomey M., Schmidt M.A., Maier B., (2010); Multiple Pilus Motors Cooperate for Persistent Bacterial Movement in Two Dimensions. Physical Review Letters, 104, 178104, 1-4

Horii Z., Clark A.J., (1973); Genetic analysis of the *recF* pathway to genetic recombination in *Escherichia coli* K12: isolation and characterization of mutants. Journal of Molecular Biology, 80(2), 327-328

Hospenthal M.K., Costa T.R.D., Waksman G., (2017); A comprehensive guide to pilus biogenesis in Gram-negative bacteria. Nature Reviews Microbiology, 15, 365-379

Ibánez de Aldecoa A.L., Zafra O., González-Pastor J.E., (2017); Mechanisms and Regulation of Extracellular DNA Release and Its Biological Roles in Microbial Communities. Frontiers in Microbiology, 8, 1390, doi: 10.3389/fmicb.2017.01390

Inamine G.S., Dubnau D., (1995); ComEA, a *Bacillus subtilis* Integral Membrane Protein Required for Genetic Trasnformation, Is Needed for Both DNA Binding and Transport. Journal of Bacteriology, 177(11), 3045-3051

Jacobsen T., Bardiaux B., Francetic O., Izadi-Pruneyre N., Nilges M., (2019); Structure and function of minor pilins of type IV pili. Medical Microbiology and Immunology, 209, 301-308

Johnson L., Horsman S.R., Charron-Mazenod L., Turnbull A.L., Mulcahy H., Surette M.G., Lewenza S., (2013); Extracellular DNA-induced antimicrobial peptide resistance in *Salmonella enterica* serovar Typhimurium. BMC Microbiology, 13, 115

Jones E.A., McGillivary G., Bakaletz L.O., (2013); Extracellular DNA within a Nontypeable *Haemophilus influenzae*-Induced Biofilm Binds Human Beta Defensin-3 and Reduces Its Antimicrobial Activity. Journal of Innate Immunity, 5, 24-38

Juneau R.A., Stevens J.S., Apicella M.A., Criss A.K., (2015); A Thermonuclease of *Neisseria gonorrhoeae* Enhances Bacterial Escape From Killing by Neutrophil Extracellular Traps. The Journal of Infectious Diseases, 212(2), 316-324

Jurcisek J.A., Bakaletz L.O., (2007); Biofilms Formed by Nontypeable *Haemophilus influenzae* In Vivo Contain both Double-Stranded DNA and Type IV Pilin Protein. Journal of Bacteriology, 189(10), 3868-3875

Jurcisek J.A., Brockman K.L., Novotny L.A., Goodman S.D., Bakaletz L.O., (2017); Nontypeable *Haemophilus influenzae* releases DNA and DNABII proteins via a T4SS-like complex and ComE of the type IV pilus machinery. Proceedings of the National Academy of Sciences of the United States of America, 114(32), E6632-E6641

Kaplan J.B., Ragunath C., Ramasubbu N., Fine D.H., (2003); Detachment of *Acinobacillus actinomycetemcomitans* Biofilms Cells by an Endogenous β-Hexosaminidase Activity. Journal of Bacteriology, 185(16), 4693-4698

Karygianni L., Ruf S., Follo M., Hellwig E., Bucher M., Anderson A.C., Vach K., Al-Ahmad A., (2014); Novel Broad-Spectrum Antimicrobial Photoinactivation of *In Situ* Oral Biofilms by Visible Light plus Water-Filtered Infrared A. Applied and Environmental Microbiology, 80(23), 7324-7336

Karygianni L., Ren Z., Koo H., Thurnherr T., (2020); Biofilm Matrixome: Extracellular Components in Structured Microbial Communities. Trends in Microbiology, 28(8), 668-681

Kavanaugh J.S., Flack C.E., Lister J., Ricker E.B., Ibberson C.B., Jenul C., Moormeier D.E., Delmain E.A., Bayles K.W., Horswill A.R., (2019); Identification of Extracellular DNA-Binding Proteins in the Biofilm Matrix. mBio, 10(3), e01137-19

Kidane D., Graumann P.L., (2005); Intracellular Protein and DNA Dynamics in Competent *Bacillus subtilis* Cells. Cell, 122, 73-84

Kiedrowski M.R., Kavanaugh J.S., Malone C.L., Mootz J.M., Voyich J.M., Smeltzer M.S., Bayles K.W., Horswill A.R., (2011); Nuclease Modulates Biofilm Formation in Community-Associated Methicillin-Resistant *Staphylococcus aureus*. PLOS One, 6(11), e26714

Kim M., Jeon J., Kim J., (2018); *Streptococcus mutans* extracellular DNA levels depend on the number of bacteria in a biofilm. Scientific Report,s 8:13313, DOI:10.1038/s41598-018-31275-y

Kim W., Racimo F., Schluter J., Levy S.B., Foster K.R., (2014); Importance of positioning for microbial evolution. Proceedings of the National Academy of Sciences of the United States of America, https://doi.org/10.1073/pnas.13236332111

Kirchner M., Meyer T.F., (2005); The PilC adhesin of the *Neisseria* type IV pilus-binding specificities and new insights into the nature of the host cell receptor. Molecular Microbiology, 56(4), 945-957

Klausen M., Aaes-Jørgensen A., Molin S., Tolker-Nielsen T., (2003); Involvement of bacterial migration in the development of complex multicellular structures in *Pseudomonas aeruginosa* biofilms. Molecular Microbiology, 50(1), 61-68

Koomey J.M., Falkow S. (1987); Cloning of the recA gene of *Neisseria gonorrhoeae* and construction of gonococcal recA mutants. Journal of Bacteriology, 169(2), 790-795

Kostakioti M., Hadjifrangiskou M., Hultgren S.J., (2013); Bacterial Biofilms: Development, Dispersal, and Therapeutic Strategies in the Dawn of the Postantibiotic Era. Cold Spring Harbor Perspectives in Medicine, 3(4): a010306

Kouzel N., Oldewurtel E.R., Maier B., (2015); Gene Transfer Efficiency in Gonococcal Biofilms: Role of Biofilm Age, Architecture, and Pilin Antigenic Variation. Journal of Bacteriology, 197(14), 2422-2431

Kowalczykowski S.C., Dixon D.A., Eggleston A.K., Lauder S.D., Rehrauer W.M., (1994); Biochemistry of homologous recombination in *Escherichia coli*. Microbiological Reviews, 58(3), 401-465

Kushner S.R., Nagaishi H., Templin A., Clark A.J., (1971); Genetic Recombination in *Escherichia coli*: The Role of Exonuclease I. Proceedings of the National Academy of Sciences of the United States of America, 68(4), 824-827

LaPointe C.F., Taylor R.K., (2000); The Type 4 Prepilin Peptidases Comprise a Novel Family of Aspartic Acid Proteases. Journal of Biological Chemistry, 27(2), 1502-1510

Lappann M., Claus H., van Alen T., Harmsen M., Elias J., Molin S., Vogel U., (2010); A dual role of extracellular DNA during biofilm formation of *Neisseria meningitides*. Molecular Microbiology, 75(6), 1355-1371

Lee S.F., Li Y.H., Bowden G.H., (1996); Detachment of Streptococcus mutans biofilm cells by an endogenous enzymatic activity. Infection and Immunity, 64(3), 1035-1038

Lei Y., Huang Y.H., Goodell MA., (2018); DNA methylation and de-methylation using hybrid site-targeting proteins. Genome Biology, 19(287)

Leighton T.L., Buensuceso R.N.C., Howell P.L., Burrows L.L., (2015a); Biogenesis of *Pseudomonas aeruginosa* type IV pili and regulation of their function. Environmental Microbiology, 17(11), 4148-4163

Leighton T.L., Dayalani N., Sampaleanu L.M., Howell P.L., Burrows L.L., (2015b); Novel Role for PilNO in Type IV Pilus Retraction Revealed by Alignment Subcomplex Mutations. Journal of Bacteriology, 197(13), 2229-2238

Lerminiaux N.A., Cameron A.D.S., (2018); Horizontal transfer of antibiotic resistance genes in clinical environments. Canadian Journal of Microbiology, 65, 34-44

Lerner A., Matthias T., Aminov R., (2017); Potential Effects of Horizontal Gene Exchange in the Human Gut. Frontiers in Immunology, 8, 1630, doi: 10.3389/fimmu.2017.01630

Letham S.C., Bharat T.A.M., (2020); Illuminating the dynamics of biofilms. Nature Reviews Microbiology, 18, 544

Liao S., Klein M.I., Heim K.P., Fan Y., Bitoun J.P., Ahn S.J., Burne R.A., Koo H., Brady L.J., Wen Z.T., (2014); *Streptococcus mutans* Extracellular DNA is Upregulated during Growth in Biofilms, Actively Released via Membrane Vesicles, and Influenced by Components if the Protein Secretion Machinery. Journal of Bacteriology, 196(13), 2355-2366

Li B., Qiu Y., Song Y., Lin H., Yin H., (2019); Dissecting horizontal and vertical gene transfer of antibiotic resistance plasmid in bacterial community using microfluidics. Environment International, 131, 105007

Li Y.H., Lau P.C., Lee J.H., Ellen R.P., Cvitkovich D.G., (2001); Natural Genetic Transformation of *Streptococcus mutans* Growing in Biofilms. Journal of Bacteriology, 183(3), 897-908

Londoño-Vallejo J.A., Dubnau D., (1993); comF, a *Bacillus subtilis* late competence locus, encodes a protein similar to ATP-dependent RNA/DNA helicases. Molecular Microbiology, 9(1), 119-131

Long C.D., Tobiason D.M., Lazio M.P., Kline K.A., Seifert H.S., (2003); Low-Level Pilin Expression Allows for Substantial DNA Transformation Competence in Neisseria gonorrhoeae. Infection and Immunity, 71(11), 6279-6291

López D., Vlamakis H., Kolter R., (2010); Biofilms. Cold Spring harbor Perspectives in Biology, 2(7), doi: 10.3201/eid0809.020063

Madsen J.S., Burmølle M., Hansen L.H., Sørensen S.J., (2012); The interconnection between biofilm formation and horizontal gene transfer. FEMS Immunology and Medical Microbiology, 65(2), 183-195

Maier B., Potter L., So M., Seifert H.S., Sheetz M.P. (2002); Single pilus motor forces exceed 100 pN. Proceedings of the National Academy of Sciences of the United States of America, 99(25), 16012-16017

Maier B., (2021); How Physical Interactions Shape Bacterial Biofilms. Annual Review of Biophysics., 11(33), 401-417

Makino S., van Putten J.P.M., Meyer T.F., (1991); Phase variation of the opacity outer membrane protein controls invasion by *Neisseria gonorrhoeae* into human epithelial cells. The EMBO Journal, 10(6), 1307-1315

Mann E.E., Rice K.C., Boles B.R., Endres J.L., Ranjit D., Chandramohan L., Tsang L.H., Smeltzer M.S., Horswill A.R., Bayles K.W., (2009); Modulation of eDNA Release and Degradation Affects *Staphylococcus aureus* Biofilm Maturation. PLOS One, 4(6), e5822

Marri P.R., Paniscus, Weyand N.J., Rendón M.A., Calton C.M., Hernández D.R., Higashi D.L., Sodergren E., Weinstock G.M., Rounsley S.D., So M., (2010); PLOS One, 5(7): e11835

Marsh P.D., Do T., Beighton D., Devine D.A., (2000); Influence of salvia on the oral microbiota. Periodontology, 70(1), 80-92

Mayer C., Moritz R., Kirschner C., Borchard W., Maibaum R., Wingender J., Flemming H.C., (1999); The role of intermolecular interactions: studies on model systems for bacterial biofilms. International Journal of Biological Macromolecules, 26(1), 3-16

McCallum M., Tamman S., Khan A., Burrows L.L., Howell P.L., (2017); The molecular mechanism of the type IVa pilus motors. Nature Communication, 8, DOI: 10.101038/ncomms15091

Mell J.C., Redfield R.J., (2014); Natural Competence and the Evolution of DNA Uptake Specificity, Journal of Bacteriology, 196(8), 1471-1483

Merz A.J., Enns C.A., So M., (2002); Type VI pili of pathogenic *Neisseriae* elicit cortical plaque formation in epithelial cells. Molecular Microbiology, 32(6), 1316-1332

Molin S., Tolker-Nielsen T., (2003); Gene transfer occurs with enhanced efficiency in biofilms and induces enhanced stabilization of the biofilm structure. Current Opinion in Biotechnology, 14, 255-261

Monds R.D., O'Toole G.A., (2009); The development model of microbial biofilms: ten years of a paradigm up for review. Trends in Microbiology, 17(2), 73-87

Montanaro L., Poggi A., Visai L., Ravaioli S., Campoccia D., Speziale P., Arciola C.R., (2011); Extracellular DNA in biofilms. The International Journal of Artificial Organs, 34(9), 824-831

Morici L.A., Carterson A.J., Wagner V.E., Frisk A., Schurr J.R., Höner zu Bentrup K., Hassett D.J., Iglewski B.H., Sauer K., Schurr M.J., (2007); *Pseudomonas aeruginosa* AlgR represses the Rhl quorum-sensing system in a biofilm-specific manner. Journal of Bacteriology, 189(21), 7752-7764

Motta J.P., Wallace J.L., Buret A.G., Deraison C., Vergnolle N., (2021); Gastrointestinal biofilms in health and disease. Nature Reviews Gastroenterology & Hepatology, https://doi.org/10.1038/s41575-020-00397-y

Muhammad M.H., Idris A.L., Fan X., Guo Y., Yu Y., Jin X., Qiu J., Guan X., Huang T., (2020); Beyond Risk: Bacterial Biofilms and Their Regulating Approaches. Frontiers in Microbiology, 11, 928, doi: 10.3389/fmicb.2020.00928

Mulcahy H., Charron-Mazenod L., Lewenza S., (2008); Extracellular DNA Chelates Cations and Induces Antibiotic Resistance in *Pseudomonas aeruginosa* Biofilms. PLOS Pathogens, 4(11), e1000213

Mulcahy H., Charron-Mazenod L., Lewenza S., (2010); *Pseudomonas aeruginosa* produces as extracellular deoxyribonuclease that is required for utilization of DNA as a nutrient source. Environmental Microbiology, 12(6), 1621-1629

Müller S., Strack S.N., Ryan S.E., Kearns D.B., Kirby J.R., (2015); Predation by *Myxococcus xanthus* Induces *Bacillus subtilis* To Form Spore-Filled Megastructures. Applied and Environmental Microbiology, 81(1), 203-210

Nazir R., Zaffar M.R., Amin I., (2019); In: Freshwater Microbiology, Chapter 8: Bacterial biofilms: the remarkable heterogenous biological communities and nitrogen fixing microorganisms in lakes., 307-340

Newman L.M., Moran J.S., Workowski K.A., (2007); Update on the Management of Gonorrhea in Adults in the United States. Clinical Infectious Diseases, 44 (Suppl. 3), S84-S101

Nielsen P.H., Jahn A., (1999); In: Microbial Extracellular Polymeric Substances, Chapter 3: Extraction of EPS., 49-72, Springer

Novotny L.A., Amer A.O., Brockson M.E., Goodman S.D., Bakaletz L., O., (2013); Structural Stability of *Burkholderia cenocepacia* Biofilms Is Reliant on eDNA Structure and Presence of a Bacterial Nucleic Acid Binding Protein. PLOS One, 8(6), e67629

Novotny L.A., Jurcisek J.A., Goodman S.D., Bakaletz L.O., (2016); Monoclonal antibodies against DNA-binding tips of DNABII proteins disrupt biofilms *in vitro* and induce bacterial clearance *in vivo*. EBioMedicine, 10, 33-44

Okshevsky M., Meyer R.L., (2013); The role of extracellular DNA in the establishment, maintenance and perpetuation of bacterial biofilms. Critical Reviews in Microbiology, 41(3)

Oldewurtel E.R., Kouzel N., Dewenter L., Henseler K., Maier B., (2015); Differential interaction forces govern bacterial sorting in early biofilms. eLIFE, DOI: 10.7554/eLife.10811

Oliveira P.H., Touchon M., Cury J., Rocha E.P.C., (2017); The chromosomal organization of horizontal gene transfer in bacteria. Nature Communications, 8, 841

Opitz D., Clausen M., Maier B., (2009); Dynamics of gonococcal type VI pili during infection. ChemPhysChem, 10(9-10), 1614-1618

O'Toole G.A., Kolter R., (1998); Flagellar and twitching motility are necessary for *Pseudomonas aeruginosa* biofilm development. Molecular Microbiology, 30(2), 295-304

Otto K., Silhavy T.J., (2002); Surface sensing and adhesion of *Escherichia coli* controlled by the Cpx-signalling pathway. Proceedings of the National Academy of Sciences of the United States of America, 99(4), 2287-2292

Panlilio H., Rice C.V., (2021); The role of extracellular DNA in the formation, architecture, stability, and treatment of bacterial biofilms. Biotechnology and Bioengineering, https:doi.org./10.1002/bit.27760

Paraje M.G., (2011); Antimicrobial resistance in biofilms. Science against Microbial Pathogens: Communicating Current Research and Technological Advances, 2, 693-1348

Parge H.E., Forest K.T., Hickey M.J., Christensen D.A., Getzoff E.D., Tainer J.A., (1995); Structure of the fibre-forming protein pilin at 2.6 Å resolution. Nature, 378, 32-38

Patel R., (2005); Biofilms and Antimicrobial Resistance. Clinical Orthopaedics and Related Research, 437, 41-47

Pédelacq J.-D., Cabantous S., Tran T., Terwilliger T.C., Waldo G.S. (2006); Engineering and characterization of a superfolder green fluorescent protein. Nature Biotechnology, 24, 79-88

Percival S.L., Malic S., Cruz H., Williams D.W., (2011a); In: Biofilms and Veterinary Medicine, Chapter I: Introduction to Biofilms, Part of the Springer Series on Biofilms book series, BIOFILMS, Vol. 6, pp 41-68

Percival S.L., Hill K.E., Malic S., Thomas D.W., Williams D.W., (2011b); Antimicrobial tolerance and the significance of persister cells in recalcitrant chronic wound biofilms. Wound Repair and Regeneration, 19(1), 1-9

Peskin C.S., Odell G.M., Oster G.F., (1993); Cellular Motions and Thermal Fluctuations: The Brownian Ratchet. Biophysical Journal, 65, 316-324

Petersen F.C., Tao L., Scheie A.A., (2005); DNA Binding-Uptake System: a Link between Cell-to-Cell Communication and Biofilm Formation. Journal of Bacteriology, 187(13), 4392-4400

Peterson B.W., He Y., Ren Y., Zerdoum A., Libera M.R., Sharma P.K., van Winkelhoff A.J., Neut D., Stoodley P., van der Mei H., Busscher H.J., (2015); Viscoelasticity of biofilms and their recalcitrance to mechanical and chemical challenges. FEMS Microbiology Reviews, 39(2), 234-245

Piepenbrink K.H., (2019); DNA Uptake by Type IV Filaments. Frontiers in Molecular Biosciences, 6, 1, doi: 10.3389/fmolb.2019.00001

Punatar R.S., Martin M.J., Wyatt H.D.M., Chan Y.W., West S.C., (2017); Resolution of single and double Holliday junction recombination intermediates by GEN1. Proceedings of the National Academy of Sciences of the United States of America, 114(3), 443-450

Pönisch W., Weber C.A., Juckeland G., Biais N., Zaburdaev V., (2017); Multiscale modeling of bacterial colonies: how pili mediate the dynamics of single cells and cellular aggregates. New Journal of Physics, 19, 015003

Pönisch W., Eckenrode K.B., Alzurqa K., Nasrollahi H., Weber C., Zaburdaev V., Biais N., (2018); Pili mediated intercellular forces shape heterogenous bacterial microcolonies prior to multicellular differentiation. Scientific Reports, 8, 16567

Qin Z., Ou Y., Yang L., Zhu Y., Tolker-Nielsen T., Molin S., Qu D., (2007); Role of autolysin-mediated DNA release in biofilm formation of *Staphylococcus epidermidis*. Microbiology, 153(7), 2083-2092

Rabin N., Zheng Y., Opoku-Temeng C., Du Y., Bonsu E., Sintim H.O., (2015); Biofilm formation mechanism and targets for developing antibiofilm agents. Future Medicinal Chemistry, 7(4), 493-512

Ramboarina S., Fernandes P.J., Daniell S., Islam S., Simpson P., Frankel G., Booy F., Donnenberg M.S., Matthews S., (2005); Structure of the Bundle-forming Pilus from Enteropathogenic *Escherichia coli*. Journal of Biological Chemistry, 280(48), 40252-40260

Remsay M.E., Woodhams K.L., Dillard J.P., (2011); The Gonococcal Genetic Island and Type IV Secretion in the Pathogenic *Neisseria*. Frontiers in Microbiology, 2(61), doi: 10.3389/fmicb.2011.00061

Robertson R.M., Laib S., Smith D.E., (2006); Diffusion of isolated DNA molecules: Dependence on length and topology. Proceedings of the National Academy of Sciences of the United States of America, 103(19), 7310-7314

Rudel T., Scheuerpflug I., Meyer T.F., (1995); *Neisseria* PilC protein identified as type-4 pilus tip-located adhesin. Nature, 373, 357-359

Rumbaugh K.P., Sauer K., (2020); Biofilm dispersion. Nature Reviews Microbiology, 18, 571-586

Rust M.J., Bates M., Zhuang X., (2006); Sub-diffraction-limit imaging by stochastic optical reconstruction microscopy (STORM), Nature Methods, 3, 793-796

Ryder V.J., Chopra I., O'Neill A.J., (2012); Increased Mutability of Staphylococci in Biofilms as a Consequence of Oxidative Stress, PLOS One, 7(10), e47695

Sambrook J., Russel D.W. (2001); The Inoue Method for Preparation and Transformation of Competent *E. Coli*: "Ultra-Competent" Cells. Molecular Cloning, 3rd Edition, Cold Spring Harbor Laboratory

Sankaran J., Tan N.J.H.J., But K.P., Cohen Y., Rice S.A., Wohland T., (2019); Single microscopy diffusion analysis in *Pseudomonas aeruginosa* biofilms. npj Biofilms and Microbiomes, 5(35)

SantaLucia J. (1998); A unified view of polymer, dumbbell, and oligonucleotide DNA nearest-neighbor thermodynamics. Proceedings of the National Academy of Sciences of the United States of America, 95(4), 1460-1465

Sauer K., Camper A.K., Ehrlich G.D., Costerton J.W. Davies D.G., (2002); *Pseudomonas aeruginosa* displays multiple phenotypes during development as a biofilm. Journal of Bacteriology, 184(4), 1140-1154

Sauer K., Cullen M.C., Rickard A.H., Zeef L.A.H., Davies D.G., Gilbert P. (2004); Characterization of nutrient-induced dispersion in *Pseudomonas aeruginosa* PAO1 biofilm. Journal of Bacteriology, 186(21), 7312-7326

Savage V.J., Chopra I., O'Neill A.J., (2013); *Staphylococcus aureus* Biofilms Promote Horizontal Transfer of Antibiotic Resistance, 57(4), 1968-1970

Schoen I., Ries J., Klotzsch E., Ewers H., Vogel V., (2011); Binding-Activated Localization Microscopy of DNA Structures. NANO Letters, 11, 4008-4011, dx.doi.org/10.1021/nl2025954

Seper A., Fengler V.H.I., Roier S., Wolinski H., Kohlwein S.D., Bishop A.L., Camilli A., Reidl J., Schild S., (2011); Extracellular nucleases and extracellular DNA play important roles in *Vibrio cholerae* biofilm formation. Molecular Microbiology, 82(4), 1015-1037

Sevillya G., Adato O., Snir S., (2020); Detecting horizontal gene transfer: a probabilistic approach. BMC Genomics, 21(106)

Seviour T., Winnerdy F.R., Wong L.L., Shi X., Mugunthan S., Foo Y.H., Castaing R., Adav S.S., Subramoni S., Kohli G.S., Shewan H.M., Stokes J.R., Rice S.A., Phan A.T., Kjelleberg S., (2021); The biofilm matrix scaffold of *Pseudomonas aeruginosa* contains G-quadruplex extracellular DNA structures. npj Biofilms and Microbiomes 7(27)

Sharma D., Misba L., Khan A.U., (2019); Antibiotics versus biofilm: an emerging battleground in microbial communities. Antimicrobial Resistance and Infection Control, 8(76)

Siewering K., Jain S., Friedrich C., Webber-Birungi M.T., Semchonok D.A., Binzin I., Wagner A., Huntly S., Kahnt J., Klingl A., Boekema E.J., Søgaard-Andersen L., van der Does C., (2014); Peptidoglycan-binding protein TsaP functions in surface assembly of type IV pili. Proceedings of the National Academy of Sciences of the United States of America, 111(10), E953-E961

Simon S.M., Peskin C.S., Oster G.F., (1992); What drives the translocation of proteins?. Proceedings of the National Academy of Sciences of the United States of America, 89(9), 3770-3774

Sommer M.O.A., Munck C., Toft-Kehler R.V., Andersson D.I., (2017); Prediction of antibiotic resistance: time for a new preclinical paradigm? Nature Reviews Microbiology, 15, 689-696

Spencer-Smith R., Roberts S., Gurung N., Snyder L.A.S., (2016); DNA uptake sequences in Neisseria gonorrhoeae as intrinsic transcriptional terminators and markers of horizontal gene transfer. Microbial Genomics, 2(8), e000069

Spormann A.M., (2008); Physiology of Microbes in Biofilms. Current Topics in Microbiology and Immunology, 322

Stalder T., Top E., (2016); Plasmid transfer in biofilms: a perspective on limitations and opportunities. npj Biofilms and Microbiomes, 2, 16022

Steichen C.T., Shao J.Q., Ketterer M.R., Apicella M.A., (2008); Gonococcal Cervicitis: A Role for Biofilm in Pathogenesis. The Journal of Infectious Diseases, 198(12), 1856-1861

Steichen C.T., Cho C., Shao J.Q., Apicella M.A., (2011); The *Neisseria gonorrhoeae* Biofilm Matrix Contains DNA, and an Endogenous Nuclease Controls Its Incorporation. Infection and Immunity, 79(4), 1504-1511

Steinberger R.E., Holden P.A., Extracellular DNA in Single- and Multiple-Species Unsaturated Biofilms. Applied and Environmental Microbiology, 71(9), 5404-5410

Stewart P.S., Franklin M.J., (2008); Physiological heterogeneity in biofilms. Nature Reviews Microbiology, 6, 199-210

Stoodley P., Cargo R., Rupp C.J., Wilson S., Klapper I., (2002); Biofilm material properties as related to shear-induced deformation and detachment phenomena. Journal of Industrial Microbiology & Biotechnology, 29(6), 361-367

Strom M.S., Lory S., (1992); Kinetics and Sequence Specificity of Processing of Prepilin by PilD, the Type IV Leader Peptidase of *Pseudomonas aeruginosa*. Journal of Bacteriology, 174(22), 7345-7351

Strom M.S., Nunn D.N., Lory S., (1993); A single bifunctional enzyme, PilD, catalyzes cleavage and N-methylation of proteins belonging to the type IV pilin family. Proceedings of the National Academy of Sciences of the United States of America, 90(6), 2404-2408

Strom M.S., Nunn D.N., Lory S., (1994); Posttranslational processing of type IV prepilin and homologs by PilD of Pseudomonas aeruginosa. Methods in Enzymology, 235, 527-540

Subach F.V., Patterson G.H., Manley S., Gillette J.M., Lippincott-Schwartz J., Verkhusha V.V., (2009); Photoactivatable mCherry for high-resolution two-color fluorescence microscopy. Nature Methods, 6, 153-159

Sutherland I.W., (2001); The biofilm matrix – an immobilized but dynamic microbial environment. Trends in Microbiology, 9(5); 222-227

Takenaka S., Pitts B., Trivedi H.M., Stewart P.S., (2009); Diffusion of Macromolecules in Model Oral Biofilms. Applied and Environmental Microbiology, 75(6), 1750-1753

Takhar H.K., Kemp K., Kim M., Howell P.L., Burrows L.L., (2013); The Platform Protein Is Essential for Type IV Pilus Biogenesis. Journal of Biological Chemistry, 288(14), 9721-9728

Tang L., Schramm A., Neu T.R., Revsbech N.P., Meyer R.L., (2013); Extracellular DNA in adhesion and biofilms formation of four environmental isolates: a quantitative study. FEMS Microbiology Ecology, 86(3), 394-403

Thanassi D.G., Bliska J.B., Christie P.J., (2012); Surface organelles assembled by secretion systems of Gram-negative bacteria: diversity in structure and function. FEMS Microbiology Reviews, 36(6), 1046-1082

Todd W.J., Wray G.P., Hitchcock P.J., (1984); Arrangement of Pili in Colonies of *Neisseria gonorrhoeae*. Journal of Bacteriology, 159(1), 312-320

van Schaik E.J., Giltner C.L., Audette G.F., Keizer D.W., Bautista D.L., Slupsky C.M., Sykes B.D., Irvin R.T., (2005); DNA Binding: a Novel Function of *Pseudomonas aeruginosa* Type IV Pili. Journal of Bacteriology, 187(4), 1455-1464

Vorkapic D., Pressler K., Schild S., (2016); Multifaceted roles of extracellular DNA in bacterial physiology. Current Genetics, 62, 71-79

Wang H., Huang Y., Wu S., Li Y., Ye Y., Zheng Y., Huang R., (2014); Extracellular DNA Inhibits *Salmonella enterica* Serovar Typhimurium and *S. enterica* Serovar Typhi Biofilm Development on Abiotic Surfaces. Current Microbiology, 68, 262-268

Wang L.C., Litwin M., Sahiholnasab Z., Song W., Stein D.C., (2018); Neisseria gonorrhoeae Aggregation Reduces Its Ceftriaxone Susceptibility. Antibiotics, 7(48), doi: 10.3390/antibiotics7020048

Wang X., Preston III J.F., Romeo T., (2004); The pgaABCD Locus of *Escherichia coli* Promotes the Synthesis of a Polysaccharide Adhesion Required for Biofilm Formation. Journal of Bacteriology, 186(9), 2724-2734

Wang X., Stone H.A., Golestanian R., (2017); Shape of the growing front of biofilms. New Journal of Physics, 19, 125007

Welker A., Cronenberg T., Zöllner R., Meel C., Siewering K., Bender N., Hennes M., Oldewurtel E.R., Maier B. (2018); Molecular Motors Govern Liquidlike Ordering and Fusion Dynamics of Bacterial Colonies. Physical Review Letters, 121

Welker A., Hennes M., Bender N., Cronenberg T., Schneider G., Maier B., (2021); Spatiotemporal dynamics of growth and death within spherical bacterial colonies. Biophysical Journal, In press, http://doi.org/10.1016/j.bpj.2021.06.022

Whitchurch C.B., Tolker-Nielsen T., Ragas P.C., Mattick J.S., (2002); Extracellular DNA Required for Bacterial Biofilm Formation. Science, 295(5559), 1487

Wiedenbeck J., Cohan F.M., (2011); Origins of bacterial diversity through horizontal genetic transfer and adaptation to new ecological niches. FEMS Microbiology Reviews, 35(5), 957-976

Wilking J.N., Angelini T.E., Seminara A., Brenner M.P., Weitz D.A., (2011); Biofilms as complex fluids. MRS Bulletin, 36(5)

Winther-Larsen H.C., Hegge F.T., Wolfgang M., Hayes S.F., van Putten J.P.M., Koomey M., (2001); Neisseria gonorrhoeae PilV, a type IV pilus-associated protein essential to human epithelial cell adherence. Proceedings of the National Academy of Sciences of the United States of America, 98(26), 15276-15281

Wolfgang M., van Putten J.P.M., Hayes S.F., Koomey M., (1999); The *comP* locus of *Neisseria gonorrhoeae* encodes a type IV prepilin that is dispensable for pilus biogenesis but essential for natural transformation. Molecular Microbiology, 31(5), 1345-1357

Wu J., Xi C., (2009); Evaluation of Different Methods for Extracting Extracellular DNA from the Biofilm Matrix. Applied and Environmental Microbiology, 75(16), 5390-5395

Wöll D., (2014); Fluorescence correlation spectroscopy in polymer science. RSC Advances, 4, 2447

Yan J., Nadell C.D., Stone H.A., Wingreen N.S., Bassler B.L., (2017); Extracellular-matrix-mediated osmotic pressure drives *Vibrio cholerae* biofilm expansion and cheater exclusion. Nature Communications, 8(327), DOI: 10.1038/s41467-017-00401-1

Yeon W.C., Kannan B., Wohland T., Ng V., (2008); Colloidal Crystals from Surface-Tension-Assisted Self-Assembly: A novel Matrix for Single-Molecule Experiments. Langmuir, 24(21), 12142-12149

Yu W., Luo K., (2011); Chaperone-assisted translocation of a polymer through a nanopore. Journal of the American Chemical Society, 133(34), 13565-13570

Yüksel M, Power J.J., Ribbe J., Volkmann T., Maier B., (2016); Fitness Trade-Offs in Competence Differentiation of *Bacillus subtilis*. Frontiers in Microbiology, 7, 888, doi: 10.3389/fmicb.2016.00888

Zhang W., Seminara A., Suaris M., Brenner M.P., Weitz D.A., Angelini T.E., (2014); Nutrient depletion in *Bacillus subtilis* biofilms triggers matrix production. New Journal of Physics, 16, 015028

Zhang X., Bishop P.L., Kupferle M.J., (1998); Measurement of polysaccharides and proteins in biofilm extracellular polymers. Water Science and Technology, 37(4-5), 345-348

Zöllner R., Oldewurtel E.R., Kouzel N., Maier B. (2017); Phase and antigenic variation govern competition dynamics through positioning in bacterial colonies. Scientific Reports, 7, 12151

Zweig M., Schork S., Koerdt A., Siewering K., Sternberg C., Thormann K., Albers S.V., Molin S., van der Does C., (2014); Secreted single-stranded DNA is involved in the initial phase of biofilm formation by *Neisseria gonorrhoeae*. Environmental Microbiology, 16(4), 1040-1052

Danksagung

An dieser Stelle möchte ich mich noch ganz herzlich bei allen Personen bedanken, die mich auf dem Weg zu dieser Arbeit begleitet haben.

An erster Stelle gebührt mein Dank dabei **Prof. Dr. Berenike Maier**, die es mir ermöglicht hat fast 5 Jahre lang in ihrer AG zu forschen, mir dabei zahlreiche Freiheiten zum Austesten verschiedenster Ideen gelassen und mich immer hervorragend betreut hat. Du hast Dir wo immer es möglich war Zeit genommen und warst mit Rat und Tat zur Stelle. Vielen, vielen Dank für die tolle Zeit!

Des Weiteren möchte ich mich bei **Prof. Dr. Tobias Bollenbach** und **Prof. Dr. Ines Neundorf** für das Interesse an meiner Arbeit bedanken und dafür, dass sie das zweite Gutachten bzw. den Vorsitz der Prüfungskommission übernommen haben. Vielen lieben Dank dafür.

Ein besonderer Dank gilt außerdem allen Mitgliedern der AG Maier; sowohl aktuelle als auch ehemalige. Im Einzelnen danke ich:

Marc Hennes; für das Korrekturlesen weiter Teile meiner Arbeit, aber insbesondere auch für die große Hilfe bei der Datenauswertung und das viele gemeinsame Fachsimpeln bei einem Feierabendbier (oder auch zwei).

Tom Cronenberg, ebenfalls für das gewissenhafte Korrekturlesen von weiten Teilen meiner Arbeit, die zahlreichen wissenschaftlichen Diskussionen, deine starken Motivationsreden und die vielen lustigen Abende die wir in Irish Pubs oder auf diversen Weihnachtsmärkten verbracht haben.

Christof Hepp für die super Einführung in Alles was mit Gonokokken zu tun hat, deine generelle Hilfestellung bei der Einarbeitung in ein neues (Forschungs-)Umfeld und deine nette und sympathische Art.

The Artist formerly known as JJP, **Jeffrey Power**, für die lange und lustige gemeinsame Zeit im Büro, dein weitreichendes Vokabular („Jabroni“) und Matlab Fachwissen, die Besuche der „Weltstadt“ Tübingen und den gemeinsamen Sommerurlaub 2019.

Robert Zöllner, dafür, dass du immer eine Idee für ein Nachfolge-Experiment oder Tipps für die Datenauswertung hattest, für die gemeinsamen Besuche von Festivals und Konzerten; und für deinen Eifer beim Verteilen von Hopfenschorle.

Melih Yüksel, für deinen Einsatz den Gruppenzusammenhalt zu bewahren, den Kaffeevollautomaten (!) und für deine nie endende gute Laune und positive Einstellung.

Sebastian Kraus, dafür dass ich mich bei dir als gleichgestelltem Team-*Neisseria*-Biologen-Leidensgenossen beraten konnte, wenn die Experimente mal wieder nicht so wollten wie ich mir das vorgestellt hatte.

Mona Förster und **Isabel Rathmann** für die angenehme Büro/Laboratmosphäre, die ihr verbreitet und dafür, dass ihr verhindert habt, dass wir alle in einem Strudel der Entropie untergehen.

Isabelle Wielert und **Anton Welker**, für die gute Zusammenarbeit, die wissenschaftlichen Diskussionen und die gemeinsame Zeit bei den BioSoft Kurstagen.

Thorsten Volkmann, für deine unglaubliche Hilfsbereitschaft und unsere gemeinsame Begeisterung für schlechte Schwer-Metall-Musik; sowie **Gabriele Schneider**, ebenfalls für deine Hilfsbereitschaft und deine Unterstützung beim Klonieren.

An dieser Stelle möchte ich auch noch **Dr. Thorsten Auth** für die interessante Gestaltung der Kurstage und die reibungslose Organisation in der BioSoft Graduierenden Schule danken.

Natürlich möchte ich mich hier aber auch noch bei allen Freunden und Bekannten, nahe und ferne, sowie bei allen Familienmitgliedern bedanken. Ihr seid zu viele, um euch alle zu nennen, aber ich danke jedem einzelnen von euch für euer Interesse an meiner Forschung (auch wenn ihr wohl wenig verstanden habt), eure mentale Unterstützung und die manchmal dringend notwendige Ablenkung. Danke!

Ein besonderer Dank gebührt dabei meiner Mutter, **Isolde Bender**, sowie meiner Freundin **Laura Hassel**, die immer für mich da waren und nie die Zuversicht verloren haben. Vielen, vielen Dank!

Erklärung

„Ich versichere, dass ich die von mir vorgelegte Dissertation selbständig angefertigt, die benutzten Quellen und Hilfsmittel vollständig angegeben und die Stellen der Arbeit - einschließlich Tabellen, Karten und Abbildungen -, die anderen Werken im Wortlaut oder dem Sinn nach entnommen sind, in jedem Einzelfall als Entlehnung kenntlich gemacht habe; dass diese Dissertation noch keiner anderen Fakultät oder Universität zur Prüfung vorgelegen hat; dass sie - abgesehen von den unten angegebenen Teilpublikationen - noch nicht veröffentlicht worden ist, sowie, dass ich eine solche Veröffentlichung vor Abschluss des Promotionsverfahrens nicht vornehmen werde. Die Bestimmungen der Promotionsordnung sind mir bekannt. Die von mir vorgelegte Dissertation ist von Prof. Dr. Berenike Maier betreut worden.“

Teilpublikationen:

Bender N., Hennes M., Maier B.; Mobility of extracellular DNA within gonococcal colonies. Manuscript submitted

X Köln, 31.01.2022

Ort, Datum

X N. Bender

Unterschrift